Activity-based protein profiling in plants

Inaugural-Dissertation

zur

Erlangung des Doktorgrades

der Mathematisch-Naturwissenschaftlichen Fakultät

der Universität zu Köln

vorgelegt von

Christian Gu

aus Peking

Köln, 2009

Diese Arbeit wurde am Max-Planck-Institut für Züchtungsforschung in Köln, in der Abteilung Molekulare Phytopathologie (Direktor: Prof. Dr. Paul Schulze-Lefert) angefertigt.

Berichterstatter: Prof. Dr. Paul Schulze-Lefert

                      Prof. Dr. Reinhard Krämer

Prüfungsvorsitzender: Prof. Dr. Ulf-Ingo Flügge

Tag der mündlichen Prüfung: 30.11.2009

ACKNOWLEDGEMENTS

ABSTRACT

Activity-based probes (ABPs) are reporter-tagged inhibitors that label enzymes in an activity-dependent manner. Using ABPs, activity-based protein profiling (ABPP) portrays active enzymes in complex proteomes. A collection of ABPs was screened and characterized for labeling of Arabidopsis leaf extracts and tomato leaf apoplastic fluids (AFs). We focused on four ABPs: epoxide probe DCG-04; fluorophosphonate probe FP; vinyl sulfone probe MV151; and β-lactone probe IS4. First, we optimized the labeling conditions and identified the labeling targets. Second, we performed comparative ABPP and detected proteins whose activities are differential during benzothiadiazole (BTH)-induced plant defenses and pathogen infections. Third, we performed competitive ABPP and identified targets of pathogen-derived and chemically-synthesized inhibitors. The major findings are as follows: (i) Using DCG-04, we labeled seven papain-like cysteine proteases (PLCPs) in tomato leaf AFs, and found that the activity of PLCP PIP1 is induced upon BTH treatment and is inhibited by *Cladosporium fulvum* effector protein AVR2. We also found that PLCP C14 is activated by 0.03% SDS in native AFs and is inhibited by *Phytophthora infestans* effector proteins EPIC1/2B. (ii) Using FP, we showed diversity of serine hydrolase activities in leaf extracts of unchallenged and *Botrytis cinerea*-infected Arabidopsis plants. We also detected differentials of serine hydrolase activities in tomato leaf AFs upon BTH treatment. (iii) Using MV151, we labeled three catalytic β subunits of the plant proteasome, and showed selective inhibition by aldehyde-based inhibitors. We also discovered a posttranslational, NPR1-dependent upregulation of proteasome activities upon BTH treatment in Arabidopsis. (iv) While characterizing IS4 profiling in Arabidopsis leaf extracts, we found that IS4 labeling occurs at N-terminus of chloroplast protein PsbP through a peptide bond and requires activity of PLCP RD21. This finding eventually led us to the discovery that RD21 acts as a peptide ligase *in vitro*. In conclusion, we demonstrated that ABPP is a powerful tool to dynamically track protein activities in plants, which facilitates the discovery and functional analysis of enzymes.

ZUSAMMENFASSUNG

Activity-based probes (ABPs) sind von Inhibitoren abgeleitet, die kovalent mit einem Reportermolekül verknüpft sind und mit aktiven Enzymen reagieren können. Der Einsatz von ABPs in activity-based protein profiling (ABPP) erlaubt es aktive Enzyme in einem komplexen Proteom sichtbar zu machen. In dieser Arbeit wurde eine Kollektion solcher ABPs durchmustert und dahingehend charakterisiert, wie sie mit Arabidopsis Blattextrakten und der apoplastischen Flüssigkeit (AFs) aus Tomatenblättern reagieren. In der Folge wurden vier ABPs genauer untersucht: die Epoxydsonde DCG-04, die Fluorophosphonatsonde FP, die Vinylsulfonsonde MV151 und die β-Lactonsonde IS4. Als erster Schritt wurden die optimalen Reaktionsbedingungen abgesteckt. Dann wurden vergleichende ABPP Experimente durchgeführt, bei denen Enzyme identifiziert wurden, deren Aktivität während Benzothiadiazole (BTH)-induzierter Pflanzenabwehr und Pathogeninfektion unterschiedlich waren. In einem dritten Schritt wurden kompetitive ABPPs durchgeführt, deren Ziel es war Zielproteine von Pathogen abgeleiteten und synthetischen Inhibitoren zu identifizieren. Folgende Erkenntnisse wurden gewonnen: (i) Durch den Einsatz von DCG-04 gelang es in den AFs von Tomatenblättern sieben Papain-ähnliche Cysteinproteasen (PLCPs) zu identifizieren. Die Aktivität einer dieser PLCPs, PIP1 war während BTH-Behandlung signifikant erhöht, wurde aber inhibiert durch das Effektorprotein Avr2 aus *Cladosporium fulvum*. Es wurde außerdem gezeigt, dass das PLCP C14 durch 0,03% SDS im sonst unbehandelten AF aktiviert wird und dass die Effektorproteine EPIC1/2B aus *Phytophthora infestans* diese Aktivität inhibieren. (ii) Durch den Einsatz von FP wurde gezeigt, wie verschieden die Aktivität von Serinhydrolasen in Blattextrakten von unbehandelten und *Botrytis cinerea*-infizierten Arabidopsispflanzen ist. Unterschiede in der Serinhydrolaseaktivität konnten auch in BTH-behandelten und -unbehandelten Tomaten AFs gezeigt werden. (iii) Mit der Sonde MV151 wurden die katalytischen Untereinheiten des Pflanzenproteasoms markiert und die Selektivität von Aldehyd-Inhibitoren gezeigt. Außerdem wurde die Beobachtung gemacht, dass BTH-Behandlung in Arabidopsis zu einer posttranslationalen, NPR1-abhängigen Hochregulierung der Proteasomaktivität führt. (iv) Während der Charakterisierung von IS4 in Arabidopsis Blattextrakten wurde beobachtet, dass IS4 über eine Peptidbindung mit dem N-Terminus des Chloroplastenproteins PsbP verknüpft wird und dass diese Reaktion die Anwesenheit der PLCP RD21 voraussetzt. Diese Beobachtung führte schließlich zur Entdeckung, dass RD21 *in vitro* als Peptidligase fungiert. Insgesamt wurde gezeigt, dass ABPP eine sehr potente Methode ist die Aktivität von Proteinen in Pflanzen dynamisch zu verfolgen und dass diese Methode die Entdeckung und funktionelle Analyse von Enzymen erheblich erleichtert.

TABLE OF CONTENTS

V

INDEX OF FIGURES

LIST OF ABBREVIATIONS

1D	one-dimensional
1DE	one-dimensional gel electrophoresis
2D	two-dimensional
2DE	two-dimensional gel electrophoresis
aa	amino acid
ABP	activity-based probe
ABPP	activity-based protein profiling
AF	apoplastic fluid
ATP	adenosine-5'-triphosphate
Bio	biotin
BODIPY	boron-dipyrromethene
BSA	bovine serum albumin
BTH	benzothiadiazole
C	carboxyl
cDNA	complementary DNA
CFU	colony-forming unit
CP	core protease
DFP	diisopropylfluorophosphonate
DMSO	dimethyl sulfoxide
DNA	deoxyribonucleic acid
dpi	day-post-infection
dpt	day-post-treatment
DTT	dithiothreitol
EDTA	ethylenediaminetetraacetic acid
ER	endoplasmic reticulum
FP	fluorophosphonate
GUS	β-glucuronidase
hr	hour
HR	hypersensitive response
HRP	horseradish peroxidase
ICAT	isotope coded affinity tagging
IEF	isoelectric focusing
kDa	kilo Dalton
LB	Luria-Bertani
LC	liquid chromatography
LE	leaf extract

MES	4-morpholineethansulfonic acid monohydrate
min	minute
mRNA	messenger RNA
MS	mass spectrometry
MudPIT	multiple dimensional protein identification technology
MW	molecular weight
N	amino
NAD	nicotinamide adenine dinucleotide
NE	nucleus-enriched
ND	nucleus-depleted
NHS	N-hydroxysuccinimide
NPC	no-probe control
OD	optical density
PAGE	polyacrylamide gel electrophoresis
PBS	phosphate buffered-saline
PCD	programmed cell death
PEG	polyethylene glycol
PLCP	papain-like cysteine protease
PR	pathogenesis-related
Pst	*Pseudomonas syringae* pv *tomato*
PMF	peptide-mass fingerprint
qRT-PCR	quantitative reverse-transcriptase polymerase chain reaction
Rh	rhodamine
RNA	ribonucleic acid
RP	regulatory particle
rpm	round per minute
RuBisCO	ribulose-1,5-bisphosphate carboxylase/oxygenase
SA	salicylic acid
SDS	sodium dodecyl sulfate
SP	signal peptide
TBS	Tris-buffered saline
TEV	tobacco etch virus
UV	ultraviolet
V	volt
VPE	vacuolar processing enzyme
VS	vinyl sulfone
wt	wild-type

CHAPTER 1: INTRODUCTION

1.1   Activity-based protein profiling

Proteins act at the front end of nearly all biological processes. One of the ultimate goals of biological research is to decipher their functions and networks. Therefore, detection and quantification of protein expression becomes very important for functional analysis of proteins. Due to a significant positive correlation between messenger RNA (mRNA) and protein expression, quantification of mRNA or its complementary DNA (cDNA) commonly works as an indicator for estimating protein levels (Fu *et al.*, 2007). Such methods include northern blotting, quantitative reverse-transcriptase polymerase chain reaction (qRT-PCR) and microarray analysis. Compared to protein measurements, mRNA measurements are less laborious and expensive, but may sometimes be less precise e.g. because of post-transcriptional modifications of mRNA and/or differentially controlled protein turnover (Gygi *et al.*, 2000). Western blotting with specific antibodies is a conventional and direct measurement to detect and quantify a protein of interest, and is more reliable than analytic methods on protein transcripts. Two-dimensional gel electrophoresis (2DE) plus mass spectrometry (MS) and isotope coded affinity tagging (ICAT) were recently-developed methods to detect and quantify proteins on a proteomic scale (Adam *et al.*, 2002a).

Proteins function only in active forms. The activities of proteins such as enzymes can be post-translationally regulated. For example, the pseudosubstrate sequence in the prodomain of a protease can autoinhibit proteolysis activity of the protease and the activation of the protease requires removal of the prodomain. Another example is that endogenous inhibitors residing in the active site of the target protease can also inhibit the proteolytic activity of the protease (Walsh *et al.*, 2005). Post-translational modification may regulate the protein functions other than changing the protein quantities, leading to an impaired correlation between protein activity and quantity. For this reason, the techniques determining protein levels may fail to reflect levels of the *active* proteins and, thereby, misinform functional analysis of the proteins. Furthermore, classical enzyme activity readout methods using fluorogenic substrates

usually do not apply to the individual enzymes in a complex proteome (Harris *et al.*, 2000).

To complement the protein measurements, activity-based protein profiling (ABPP) was introduced as an analytic technique for proteins in the complex proteomes. ABPP makes use of reporter-tagged inhibitor molecules named activity-based probes (ABPs). In native proteomes, ABPs bind to the active site of the target proteins with the inhibitor moiety (so-called reactive group) through a stable covalent bond. Therefore, ABPs label only functionally active proteins whose catalytic sites are available (Cravatt *et al.*, 2008). Since active site accessibility and reactivity is an important indication for protein activity (Kobe and Kemp, 1999), mechanism-dependent chemical probes read out protein activities on the basis of function rather than abundance.

1.2 Activity-based probe

ABPs are the workhorses for ABPP. A typical ABP contains three major functional elements: a reactive group (also named warhead) for covalent binding to the active-site residue of the target proteins, a reporter tag for detection and purification of the labeled proteins, and a linker as a spacer to keep reactive group and reporter tag spatially apart (Baruch *et al.*, 2004).

1.2.1 Reactive group

In an ABP, the reactive group provides the covalent interaction to the target protein and desired target specificity. The reactive group is usually derived from a covalent irreversible inhibitor. Based on the nature of the prototype inhibitors, ABPs are generally classified into two types: *directed ABP* and *non-directed ABP*. In some ABPs, incorporation of a *binding group* into the reactive group may modify the specificity of the probe. In case that the prototype inhibitor is a noncovalent reversible one, integration of a *photocrosslinker* will provide the obligatory covalent interaction for the probe.

Directed ABP

For directed ABP, the reactive group usually derives from a well-characterized irreversible enzyme inhibitor. This mechanism-based inhibitor holds an electrophile which can selectively and covalently react with the active-site nucleophilic residue of a family of enzymes. Based on the inhibitor, it is conceptually straightforward to design a directed ABP by incorporating the inhibitor moiety with a linker and a reporter tag. This type of ABPs includes fluorophosphonate probes derived from serine protease inhibitor diisopropylfluorophosphonate (DFP) for serine hydrolases, and epoxide probes derived from papain-like cysteine protease (PLCP) inhibitor E-64 for PLCPs (Liu *et al.*, 1999; Greenbaum *et al.*, 2000). All directed ABPs have excellent target selectivity within a family of enzymes sharing cognate mechanism and function, and minimal interfamily cross-reactivity. For example, epoxide probe DCG-04 derived from E-64 only targets papain subfamily but not other cysteine protease subfamilies, or serine proteases or metalloproteases (Greenbaum *et al.*, 2002a).

Non-directed ABP

Due to a limited number of dedicated irreversible inhibitors, directed ABPs only cover a small fraction of the active proteomes. Many enzymes including proteases, esterases and phosphatases catalyze hydrolytic reactions by acting on the substrates through a nucleophilic attack mechanism. Therefore, theoretically an ABP carrying a moderately reactive electrophile can covalently react with the nucleophile of the enzymes. Carbon electrophiles, including those present in reactive natural products, become the resource of choice as reactive groups of non-directed ABPs. Examples are sulfonate ester probes, and the spiroepoxide probes derived from the bioactive natural compounds fumagillin and luminacin D (Adam *et al.*, 2001; Evans *et al.*, 2005). Interestingly, the identified labeling targets of non-directed probes belong to mechanistically distinct enzyme classes.

Binding group

In many cases, the specificity for targeting one particular subset of proteins is an intrinsic feature of the electrophile of an ABP (Thornberry *et al.*, 1994). However, the target selectivity can be manipulated by embedding a binding group into the reactive group of an ABP. The binding group has a defined chemical structure, varying from

short peptides to alkyl, aryl or amine-derived chemical groups, which presumably docks the probe into the active site of certain proteins and, consequently, alters or enhances the target selectivity of the probe. For directed ABPs for proteases, probe designers exploit the knowledge on the substrates of the target proteases, and incorporate a small substrate-mimicking peptide of 2-4 amino acids as the binding group beside the reactive electrophile (Greenbaum *et al.*, 2002a). In non-directed ABPs, aliphatic or aromatic substitutions are usually integrated and determine specific targets whose binding pocket of the active site is seemingly complementary (Böttcher and Sieber, 2008). For diverse reactivity and target selectivity, ABPs are often synthesized and screened on a library scale ("cocktails") with reshuffled amino acid sequences or diverse structure-modifying chemical groups in the binding group (Barglow and Cravatt, 2004).

Photocrosslinker

ABPs require a stable covalent bond for bridging the probes to the target proteins. If an enzyme class does not exploit a nucleophilic amino acid for catalysis and only has reversible inhibitors or non-covalent affinity molecules, photocrosslinkers can be attached to the inhibitor moieties or the affinity molecules, resulting in photocrosslinking ABPs. Adding a photocrosslinker is a universal strategy to convert reversible inhibitors into covalent ABPs (Saghatelian *et al.*, 2004). When the ABP is tightly anchored into the active site of the target enzymes, ultraviolet (UV) irradiation can activate the photocrosslinker to form a covalent bond to the proximal regions in the active site of the enzymes. Examples of these ABPs are hydroxamate probes derived from a zinc-chelating reversible inhibitor of metalloproteases and suberoylanilide hydroxamic acid probes derived from a zinc-chelating reversible inhibitor of histone deacetylases. Both ABPs carry a benzophenone as photocrosslinker (Sieber *et al.*, 2006; Salisbury and Cravatt, 2007).

1.2.2 Reporter tag

The reporter tag distinguishes an ABP from its prototype inhibitor, and allows quick detection and easy purification of the profiling targets. While a *biotin tag* is usually indispensible for isolation of the target proteins, a *fluorescent tag* is more advantageous in visualization and quantification of the labeling signals. While a

trifunctional probe carries both biotin and fluorescent tags, a *click-chemistry probe* does not contain either of the two tags but a small adapter ready for a chemical ligation to a reporter tag.

Biotin tag

An ABPP signal has little biological meaning until its identity is resolved. That is probably the reason why the earliest ABPs all used biotin as reporter tag, as it plays dual roles in both signal detection and identification. When an ABP carries a biotin tag, labeled proteins can be visualized with streptavidin-conjugated reporters (e.g. streptavidin-horse radish peroxidase, HRP) on protein blots, and can be enriched and purified with immobilized streptavidin (e.g. streptavidin agarose beads) for MS identification. The extremely strong and specific interaction between biotin and streptavidin guarantees the quantitative and sensitive detection and purification, even of low-abundant proteins (Solinas and Motto, 1999). While biotin remains the affinity tag of choice for target identification, for signal detection it has some disadvantages. First, western blotting-based detection is labor-intensive and time-consuming. Second, endogenously biotinylated proteins cause background that may mask the labeled proteins, so that unlabeled negative control ("no-probe control") is strictly mandatory. Third, unspecific binding of the second reporter or luminescence reagents to abundant proteins on protein blots introduce background signals and decrease sensitivity. Finally, the hydrophilic character of biotin limits the cell permeability of the ABPs during *in vivo* profiling.

Fluorescent tag

The current trend of reporter tags for ABPs is a fluorophore. Commonly used fluorophores for ABPs include rhodamine and boron-dipyrromethene (BODIPY). Labeled proteins can be easily and immediately visualized in-gel with a fluorescence scanner after gel electrophoresis, although each experimental step involving a fluorescent ABP should take place in reduced light conditions to avoid photoquenching. Detection of fluorescent signals from probe-bound protein targets is sensitive and specific, with low background signals. Furthermore, the excellent dynamic range provided by advanced fluorophores and the measurement by modern fluorescence scanners ensures reliable quantification of signal intensities. Finally, fluorescent profiling is devoid of elaborate blotting procedures, and avoids signal

variation among different gels. This makes multiple gels quantitatively comparable, and facilitates high-throughput screening. In addiction, the hydrophobic character of the fluorophores makes fluorescent ABPs more cell membrane-permeable, and enable *in vivo* profiling and imaging in living cells (Jeffery and Bogyo, 2003).

Trifunctional probe

Two versions of one ABP, one with fluorescent tag, the other with affinity tag are usually synthesized to exploit advantages of the fluorophore for signal detection and biotin for target purification. Mutual competition can be done to confirm that the fluorescent signals are identical to the biotin signals. Another option is to combine both fluorophore and biotin into one reporter tag. The resulting ABP is called a trifunctional ABP: a reactive group for activity-based labeling, and a fluorophore and a biotin for simultaneous in-gel detection and affinity purification (Adam *et al.*, 2002b). As bonus, fluorescence scanning is a lot more sensitive than protein staining to locate and select enriched targets for MS analysis, and excludes co-isolated endogenously biotinylated proteins as background. However, trifunctional ABPs can have reduced probe reactivity due to a bulkier tag causing steric hindrance, and these probes are more challenging to synthesize.

Click-chemistry probe

The function of an ABP eventually relies in the inhibitor moiety. However, the reporter tag inevitably modifies the structure and physic-chemical features of the inhibitor, leading to changes in e.g. size and hydrophobicity. This may cause reduced cellular uptake or biased subcellular distribution of the ABP, particularly hampering its application for *in vivo* profiling. The click-chemistry probe is an untagged ABP, with a small chemical adapter for the attachment of a reporter tag after labeling. This "tag-free" ABP maximally resembles the prototype inhibitor and minimally affects its target binding, especially *in vivo*. Alkyne and azide are two such adapters. Following covalent labeling of protein targets, the probe is ligated to the reporter tag *in vitro*, through Cu(I)-catalyzed cycloaddition reaction ("click chemistry"; Speers *et al.*, 2003). In aqueous solution of biological samples, either adapter molecule is inert while their coupling is quick, efficient and specific under mild conditions. This two-step labeling strategy also allows one probe to accept diverse reporter tags, and simplifies probe design and synthesis. Click-chemistry ABPs facilitate profiling

6

protein activities in living cells and even in whole animals, and have a deep impact on ABPP techniques (Speers and Cravatt, 2004).

1.2.3   Linker

A linker connects the reactive group to the reporter tag, and keeps them at an appropriate distance. Enough distance avoids steric congestion, so the reporter tag will not hinder the access of the reactive group to the active site of the target protein, and the reactive group will not hinder the access of the reporter tag to its counterpart for detection or purification. However, the linker is more than a scaffold. Commonly used linkers include the hydrophobic alkyl linkers and the hydrophilic poly ethylene glycol (PEG) linkers. The former may enhance cell membrane permeability of the probe favored by *in vivo* profiling, while the latter may enhance probe solubility in aqueous extracts favored by *in vitro* profiling. Two ABPs that only differ in the linker region may confer different profiling properties (Kidd *et al.*, 2001). Furthermore, a linker region may also contain a latent analytical handle like a click-chemistry adapter, or other functional elements like a specific cleavage site (e.g. Tobacco Etch Virus (TEV) protease recognition peptide) for mild elution of affinity-isolated targets (Weerapana *et al.*, 2007)

1.3   Target identification

To elucidate signal identities as well as labeling sites, target identification is absolutely a key step of ABPP. To this end, proteomes of interest are labeled in a large scale with biotin-tagged ABPs, and biotinylated proteins are then captured on avidin/streptavidin resins. Purified target proteins are subject either to gel-based or gel-free identification techniques, both eventually relying on mass spectrometry-based peptide sequencing and database searches for hypothetical peptide matches.

1.3.1   Gel-based techniques

Conventional proteomic techniques include the gel-based target identifications. In brief, target proteins are eluted under harsh conditions, separated by one-dimensional

gel electrophoresis (1DE) or two-dimensional gel electrophoresis (2DE) and visualized by staining. Next, gel slices containing labeling signals are excised and digested with trypsin. Tryptic peptides are extracted from the gel pieces and identified by first dimensional MS for peptide finger printing. Second dimensional MS or micro-sequencing of the selected peptides further confirms the peptide sequence, and can identify the residue label by the probe.

The gel-based target identification generates activity-based proteome reference maps, which mirror the labeling patterns of routine gel-based profiling and offer direct links between signals and their identities (Phillips and Bogyo, 2005). As reference standard, these index maps are important for comparative activity-based proteomics of, for example, abiotic and biotic stresses, and high-throughput selective inhibitor screening. The gel-based target identification is advantageous also because it retains topological information of target proteins and displays protein modifications. However, gel electrophoresis and protein staining limits protein separation and quantification. These limits are caused by the lack of resolving power for very large or small proteins, extremely hydrophobic, acidic or basic proteins and proteins in low abundance. These limitations make the high sensitivity of the MS not fully exploited.

1.3.2 Gel-free techniques

Multidimensional protein identification technology (MudPIT) is tailored for gel-free target identification of ABPP, and has greatly accelerated the development and application of ABPP. In brief, affinity-purified target proteins are digested with trypsin on-beads, and the tryptic peptides are separated by two-dimensional liquid chromatography (LC) based on charge separation (e.g. with ion exchange column) and hydrophobicity separation (e.g. with C18 reverse phase column). The difference between gel-based and gel-free methods lies in the tryptic peptides entering MS analytic platforms, which are either separated in protein by gel electrophoresis and then digested in-gel, or digested on-beads and then separated by tandem LC.

In theory, tryptic peptides from all affinity-purified target proteins can be separated by tandem LC and identified by MS sequencing even in trace quantities undetectable by protein staining. MudPIT provides an extraordinary resolution, supreme sensitivity

and maximal target coverage — three crucial parameters for target identification of ABPP, far beyond gel-based techniques (Sieber and Cravatt, 2006). For example, Cravatt and coworkers identified seven FP targets in mammalian proteomes with gel-based technique, and over fifty with gel-free technique (Kidd *et al.*, 2001; Jessani *et al.*, 2005a). However, MudPIT loses topological and modification information of analyzed proteins, and is unable to reveal the labeled residue. MudPIT also requires highly sophisticated equipment and daunting computation power, and lacks the desirable run-to-run reproducibility and reliable quantification. Thus, it is currently neither suitable for comparative ABPP nor compatible to high-throughput screening. Nevertheless, the gel-based and gel-free techniques have a complementary value, and their combination causes optimal balance between breadth and depth of analysis.

1.4   Applications of ABPP

Up to now, directed ABPs have been developed for more than a dozen enzyme classes including cysteine proteases, serine hydrolases, catalytic β-subunits of proteasome, metalloproteases, histone deacetylases, kinases and nucleotide-binding proteins, phosphotases, ubiquitin-specific proteases, glycosidases and cytochrome P450s, and non-directed ABPs for several other enzymes classes, many of which are implicated in important biological processes from normal metabolism to patho-physiology (Cravatt *et al.*, 2008). The rapidly-expanding ABP toolbox has been applied to both basic research on function and regulation of individual proteins, and medical research from pharmacological studies to clinical practices.

1.4.1   Applications in mammalian studies

Activity-based proteomics and enzyme mechanism studies
Genome-sequencing projects deciphered genetic codes on an overwhelming scale, yet left structure, function, regulation and interaction of most proteins largely untouched. Proteomics took over these challenges, and its focus gradually switches from whole proteomes to sub-proteomes for greater dynamic range of detection and more in-depth analysis. ABPs can not only be used to detect and measure activities of individual

proteins, but also be used on a proteomic scale. ABPP portraits proteomes with enzymes only in active forms, and fosters "activity-based proteomics" on a sub-proteome of active enzymes extracted from a complex proteome, which are biochemically traceable with small molecule ABPs (Phillips and Bogyo, 2005). For any ABP, disclosure of its target spectrum in a model proteome with advanced MS is of paramount importance. This establishes reference for comparative ABPP mentioned below, and entitles the ABP as an activity-readout of any its target protein for functional analysis.

Chemistry is the basis of biological processes. For this reason, ABPs as reactive chemical modifiers are undoubtedly a powerful tool to study enzyme mechanisms, including the catalytic mode, substrate selectivity and molecular function. For example, sialyl acetylesterase (SAE) had previously been reported as a protein of unannotated mechanism due to the lack of sequence homology, but was assigned by Cravatt and coworkers as a serine hydrolase through FP profiling and subsequent analyses (Jessani *et al.*, 2005b). Thus, ABPP also facilitates structure-function investigation of individual proteins.

Comparative ABPP and biomarkers/drug targets discovery

By comparing protein activity profiles of two or more proteomes under normal and disease conditions or at different pathological stages, comparative ABPP identifies proteins whose activity level differs. These differential activities may be caused by different protein accumulation levels, or by a higher order of regulation, e.g. presence of inhibitors or cofactors. Differential protein activities can serve as biomarkers for diagnosis and/or drug targets for treatment.

For example, Bogyo and coworkers profiled the life cycle of *Plasmodium falciprum*, the causative agent of human malaria, with DCG-04 and identified that a pathogen PLCP falcipain 1, but not falcipain 2 or 3, is upregulated in invasive merozoites (Greenbaum *et al.*, 2002c). This implies that falcipan-1 plays a role in host cell invasion and that it is an anti-malaria drug target. Cravatt and coworkers profiled 33 human specimen proteomes from 28 breast tumors and 5 healthy breast tissues with FP, and identified 7 membrane-associated serine hydrolases with differential activities common to breast cancer samples (Jessani *et al.*, 2005a). Notably, a cDNA microarray

on the same samples provided a direct comparison of protein transcript and activity levels, and showed a negative correlation for thrombin and KIAA1363. This reveals that KIAA1363 is a potential breast cancer biomarker and drug target that would not have been recognized by molecular profiling methods other than ABPP.

Competitive ABPP and inhibitor screening

A competitive version of ABPP allows screening of small molecule libraries and evaluation of inhibitors, since most inhibitors compete with the ABP for the same active site of a target protein. In a typical experiment, the model proteome is pretreated with candidate inhibitors, and then labeled with ABP for the remaining active, not inhibited target proteins. Inhibitory efficacy is indirectly interpreted by the decrease in ABP labeling compared to inhibitor-untreated control, and is usually quantified and clustered into a heat-map for assessment. Screening of reversible inhibitors requires kinetically controlled conditions, because the end-point readout of ABPP is determined by both the affinity of the inhibitor and the rate of the probe reactivity. For this reason, labeling time must be optimized and restricted to the period before labeling with ABP reaches saturation (Jessani and Cravatt, 2004).

Competitive ABPP facilitates the selection of potent and specific inhibitors of known drug targets to generate novel drugs, and for proteins with unknown function to carry out chemical knockout assays. It offers several advantages over conventional substrate-based inhibitor screening. First, it takes place directly in physiologically-relevant complex proteomes with no requisite for purified recombinant target protein. Second, it is "substrate-free", which makes the inhibitor selection for the target protein with unknown substrates possible. Third, the candidate inhibitors are examined against not only the target protein, but also many other family members with similar enzymatic mechanism, therefore, the selectivity of the inhibitors is evaluated simultaneously (Speers and Cravatt, 2004).

For example, using competitive ABPP with DCG-04 probe, Bogyo and coworkers screened a tripeptide epoxide library for covalent inhibitors of *Plasmodium falciprum* PLCP falcipain 1, and discovered YA29-Eps(S,S) as a specific inhibitor (Greenbaum *et al.*, 2002c). With this inhibitor, they successfully prevented parasite invasion of cultured human erythrocytes, demonstrating a role of falcipain 1 and indicating this

inhibitor as a potential lead for a new anti-malaria drug. Using competitive ABPP with FP probe, Cravatt and coworkers screened a mixed library of trifluoromethyl ketones and α-keto heterocycles for reversible inhibitors of KIAA1363, an uncharacterized membrane-associated protein with unknown substrates (Leung *et al.*, 2003). Based on and derived from the inhibitors discovered from this screening, the researchers designed and confirmed carbamate AS115 as a potent and selective inhibitor of KIAA1363 *in vivo*. Through chemical knockout using AS115, they characterized the function of KIAA1363 in ether lipid metabolism and identified that 2-acetyl monoalkylglycerol is the substrate of KIAA1363 (Chiang *et al.*, 2006).

1.4.2 Applications in plant studies

Detecting plant enzyme activities with reporter-tagged inhibitors had been performed before the concept of ABPP was formally introduced into the plant field. For example, Hara-Nishimura and coworkers infiltrated biotin-xVAD-fmk, a biotinylated irreversible inhibitor of mammalian caspases, into tobacco leaves and labeled two signals *in vivo* (Hatsugai *et al.*, 2004). Although they did not directly identify the labeled proteins with MS, they demonstrated caspase activity of the target because other caspase inhibitors could outcompete the labeling, and indirectly confirmed the targets as vacuolar processing enzyme (VPE) because a VPE-specific antibody can immuno-deplete the labeling targets. Thus, with this prototype ABPP, the researchers discovered that VPE has caspase activity as they previously postulated. Interestingly, biotin-xVAD-fmk also prevented hypersensitive response (HR) in tobacco leaves, suggesting that an ABP during *in vivo* labeling may functionally affect living experimental samples.

As a pioneer of ABPP in plants, van der Hoorn and coworkers profiled PLCP activities in leaf proteomes of the model plant *Arabidopsis thaliana* with the biotin-version of DCG-04 (Van der Hoorn *et al.*, 2004). They characterized profiling features, optimized labeling conditions and identified target proteins with gel-based separation coupled to MS analysis. Six PLCPs were identified and three were confirmed with specific antibodies. Competitive ABPP of diverse commercially-available protease inhibitors to DCG-04 labeling showed the potential of DCG-04 profiling for identification of PLCP inhibitors. De Wit and coworkers labeled tomato

apoplastic PLCP RCR3 with DCG-04, and identified the *Cladosporium fulvum-*secreted protein AVR2 as a pathogen-derived inhibitor of RCR3, because AVR2 can outcompete DCG-04 labeling of RCR3 (Rooney *et al.*, 2005). Interestingly, this inhibition only happens at pH 4.5-5.5 but not higher, consistent with the pH of apoplast, where the interaction naturally occurs. Also with DCG-04, Kamoun and coworkers labeled tomato apoplastic PLCP PIP1, and identified the *Phytophthora infestans*-secreted protein EPIC2B as a pathogen-derived inhibitor of PIP1, because EPIC2B can outcompete DCG-04 labeling of PIP1 in apoplastic proteomes (Tian *et al.*, 2007). Since EPIC2B and PIP1 interact reversibly, the researchers chose restricted labeling times. Unlike in mammalian fields, these two studies highlight competitive ABPP in the discovery of plant pathogen-secreted inhibitors, but not synthesized inhibitors.

Other applications of ABPP in plants involve DCG-04 profiling to monitor cysteine protease activity during wheat-leaf senescence; to test target specificity of cathepsin B inhibitors in *Nicotiana benthamiana*, and FP profiling to identify AtCXE12 as the major carboxyesterase in activating herbicide 2,4-D methyl in Arabidopsis (Martinez *et al.*, 2006; Gilroy *et al.*, 2007; Gershater *et al.*, 2007). Undoubtedly, ABPP in plants is just at its beginning. At the crossroad of chemistry and biology, ABPP grows with technical advances in chemical synthesis and analytical systems to address fundamental biological questions. As a powerful tool to readout protein activities from proteome mining to structure-function analysis of individual proteins, ABPP in plants offers great opportunities in future plant research. Challenges are the development of ABPs for plant-specific proteins, comparative ABPP with biotic and abiotic stimuli, and competitive ABPP to identify and study novel endogenous or pathogen-derived inhibitors.

1.5   Research objective

The objective of this project is to introduce novel ABPs in plant science, and to use these to detect differential enzyme activities during plant-pathogen interactions and immune responses, and to discover targets of pathogen-derived inhibitors. To achieve this objective, we will follow the following approaches:

First, a collection of ABPs representing different chemotypes will be screened for robust labeling in Arabidopsis leaf proteomes. The probes with strong and reproducible signals will be chosen and their labeling will be characterized in detail.

Second, labeling conditions of the best ABPs will be optimized, and their labeling targets in Arabidopsis leaf proteomes and tomato leaf apoplastic proteomes will be identified by large-scale purification and MS analysis.

Third, comparative ABPP will be performed with selected ABPs to leaf proteomes of Arabidopsis during benzothiadiazole (BTH)-induced defense, and Pseudomonas and Botrytis infections. Comparative ABPP will be performed to tomato leaf apoplastic proteomes during BTH-induced defense.

At last, competitive ABPP will be performed with selected ABPs to test putative pathogen-derived inhibitors in tomato leaf apoplastic proteomes and identify their targets.

CHAPTER 2: RESULTS

2.1 ABPP with fluorophosphonate probe FP

2.1.1 FP profiling of Arabidopsis leaf extracts

Serine hydrolases comprise a large collection of enzymes from different structural classes that fulfill diverse biochemical roles such as proteases, lipases, esterases, and transferases. The Arabidopsis genome encodes for hundreds of serine hydrolases that belong to dozens of large multigene families (The Arabidopsis Genome Initiative, 2000). Common to these enzymes is that the active site contains an activated serine residue that performs the nucleophilic attack on the substrate, resulting in a covalent intermediate.

To study the diverse roles of serine hydrolases in plants and in other organisms in detail, it is essential to display the activities of these enzymes because enzyme activities depend on various post-translational processes like phosphorylation, nitrosylation, processing, cofactors, and inhibitors, and prediction of enzyme activities from transcriptomics or proteomics data can be misleading. Serine hydrolase activities can be displayed by activity-based protein profiling. A frequently used probe for serine hydrolases is based on fluorophosphonate (FP), which is also the reactive moiety in the broad range serine hydrolase inhibitor diisopropyl fluorophosphonate. When used on mammalian extracts, FP probes display dozens of serine hydrolase activities, including proteases, lipases, and esterases (Liu *et al.*, 1999; Kidd *et al.*, 2000; Patricelli *et al.*, 2001). In plants, the roles of serine hydrolases are even more diverse because many of these enzymes act in the production of elaborate secondary metabolites. To study the role of serine hydrolases in plants further, we applied serine hydrolase profiling using FP-based probes on Arabidopsis leaf extracts.

2.1.1.1 Characterization of FP labeling

In these studies we used three FP probes that differ only in the linker and reporter tags (Figure 1-1). The linker is either a hydrophobic C_9 hydrocarbon linker or a

15

hydrophilic C_8O_4 polyethylene glycol (PEG; p) linker, which makes the probe more water-soluble (Kidd *et al.*, 2001). The reporter tag is either biotin (Bio) for affinity purification or rhodamine (Rh) for fluorescence detection.
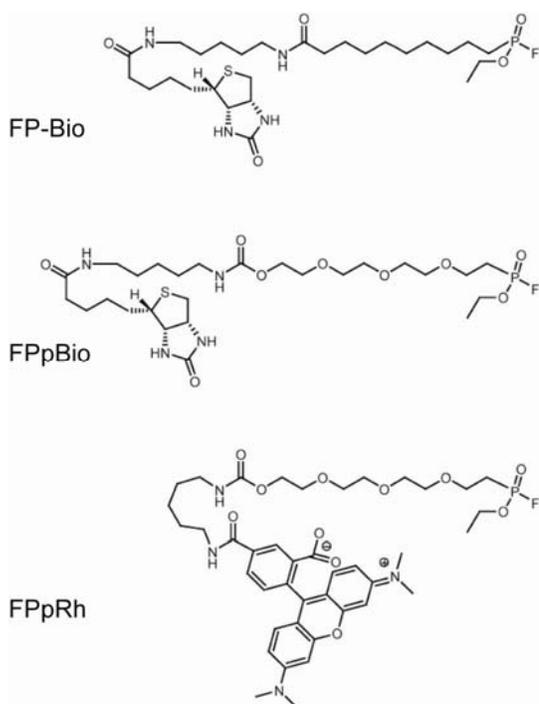
FIGURE 1-1 Structures of activity-based probes FP-Bio, FPpBio and FPpRh.
All carry the same fluorophosphonate (FP) reactive group. FP-Bio has a hydrocarbon linker and a biotin (Bio) reporter tag. FPpBio has a PEG linker and a biotin reporter tag. FPpRh has a PEG linker and a rhodamine (Rh) reporter tag.

Because protein activities depend on pH, we tested labeling of Arabidopsis leaf extracts at various pH values. This revealed that the labeling of each signal has its own pH optimum (Figure 1-2A, left panel). The pH range for labeling of each signal is illustrated with double-ended arrowheads (Figure 1-2A, right panel). For example, the 48-kDa signal was only visible at pH 4-8, whereas the 40-kDa signal was strong at pH 5-11. pH dependence is a hallmark for activity-dependent labeling because it reflects that each enzyme has its own pH-dependent activity. Because most of the FP signals can be labeled at pH 8, this cytosolic pH was used for subsequent profiling experiments. The signals at 95-kDa and 35-kDa also appear in no-probe controls (Figure 1-2C). They represent endogenously biotinylated proteins 3-methylcrotonyl-

CoA carboxylase (MCCA) and biotin carboxyl carrier protein (BCCP), respectively, and therefore are "background" signals on streptavidin-HRP-probed blots.
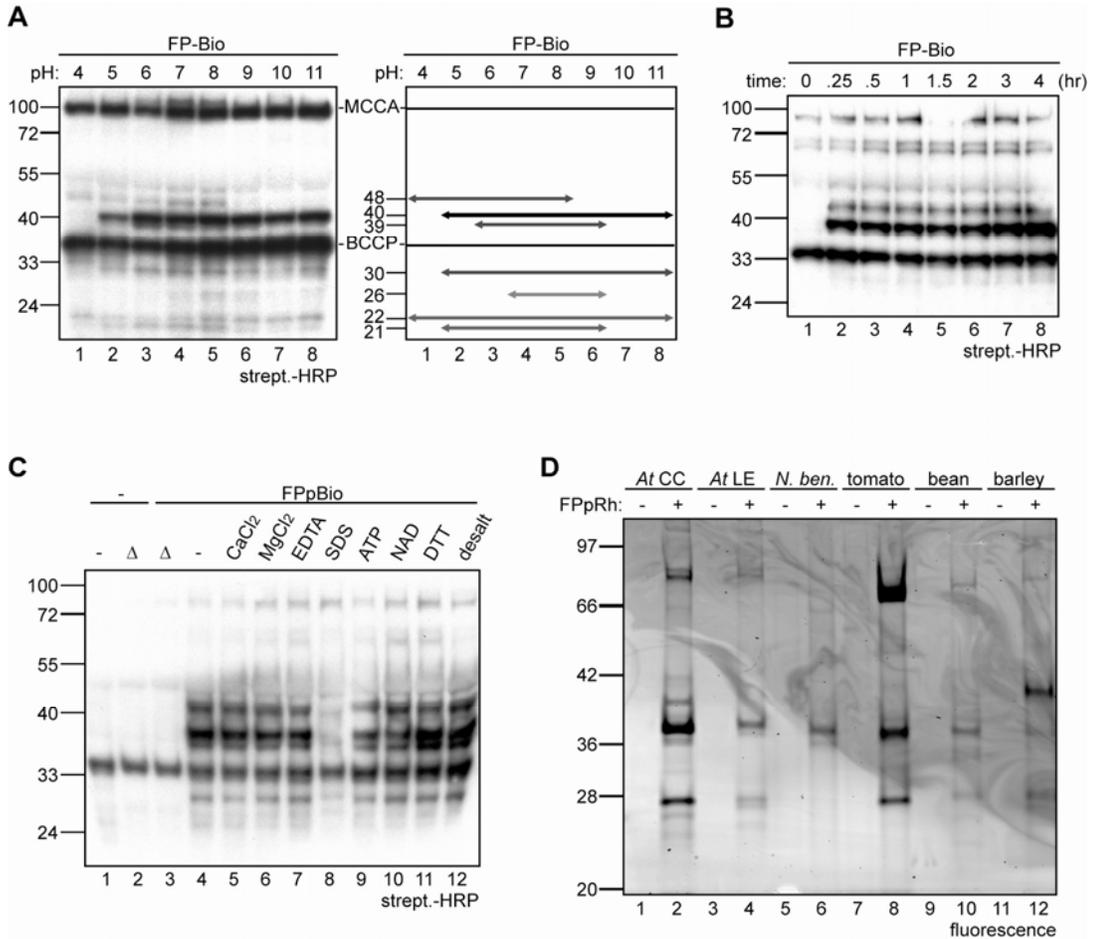
FIGURE 1-2 Characterization of FP labeling in Arabidopsis leaf extracts.
A, pH dependency of FP profiling. Leaf extracts were labeled with 0.1 µM FP-Bio at different pH values (left panel). For each specific FP-Bio signal, the labeling pH range is illustrated with double-ended arrows at its estimated MW (right panel). *B*, Time course of FP profiling. Leaf extracts were labeled with 0.1 µM FP-Bio at pH 8. Labeling reactions were terminated at various time points by adding cold acetone to a final concentration of 67%. *C*, Cofactor effects on FP profiling. Leaf extracts were heat-denatured, desalted with PD-10 size-exclusion column or mixed with cofactors CaCl₂, MgCl₂, EDTA, ATP, NAD or DTT at 1 mM, or SDS at 0.1%, and then labeled with 0.2 µM FPpBio at pH 8. *D*, FP profiling in various model plant species. 100 µg protein extracts from *Arabidopsis thaliana* cell culture, or leaves of *Arabidopsis thaliana*, *Nicotiana benthamiana*, tomato (*Solanum lycopersicon*), bean (*Vicia faba*) or barley (*Hordeum vulgare*) were labeled with 0.2 µM FPpRh. Labeled proteins were detected on protein gel (10 µg protein/lane) by fluorescence scanning.

17

To characterize the time course of FP profiling, labeling was followed over different periods. This shows that FP labeling occurs very fast, and the labeling of 48-kDa, 40-kDa and 30-kDa signals saturates within 15 minutes (Figure 1-2B).

The activities of some enzymes depend on certain cofactors. We examined the effects of enzyme cofactors and some small molecule additives on FP labeling profiles. No specific changes were caused by those cofactors, additives or the desalting condition to FP labeling profiles, except that 0.1% sodium dodecyl sulfate (SDS) globally suppresses the labeling (Figure 1-2C, lane 8). Labeling was completely prevented if the proteome was heat-inactivated (Figure 1-2C, lane 3), indicating that labeling with FPpBio is specific and dependent on protein activities.

To expand the use of FP profiling, we tested the labeling of Arabidopsis cell cultures and leaf extracts from *Nicotiana benthamiana*, tomato (*Solanum lycopersicum*), bean (*Vicia faba*) and barley (*Hordeum vulgare*) with FPpRh. Advantageous over biotin-tagged probe FPpBio, the fluorescent probe FPpRh avoids background signals including endogenously-biotinylated proteins MCCA and BCCP during visualization of the labeled targets (Figure 1-2D). The resulting labeling profiles are different but, interestingly, share some similarities (Figure 1-2D). There are three hallmark signals at 70-90-kDa, ~40-kDa and ~28-kDa for each proteome, though the relative intensity of each signal differs.

2.1.1.2 Comparative FP profiling of defense-related and pathogen-infected Arabidopsis plants

First, we applied FP profiling to investigate serine hydrolase activities in defense-related Arabidopsis leaf proteomes. Benzothiadiazole (BTH) is a functional analogue of salicylic acid (SA), and application of BTH on Arabidopsis plants can trigger SA-dependent signaling (Lawton *et al.*, 1996). We sprayed BTH to wild-type Arabidopsis plants and labeled leaf extracts with FP at 5 day-post-treatment (dpt). Signal intensity of several FP targets was higher in BTH-treated plants compared to H_2O-treated plants, and a 45-kDa signal only appeared in BTH-treated plants but not in H_2O-treated plants (Figure 1-3A).
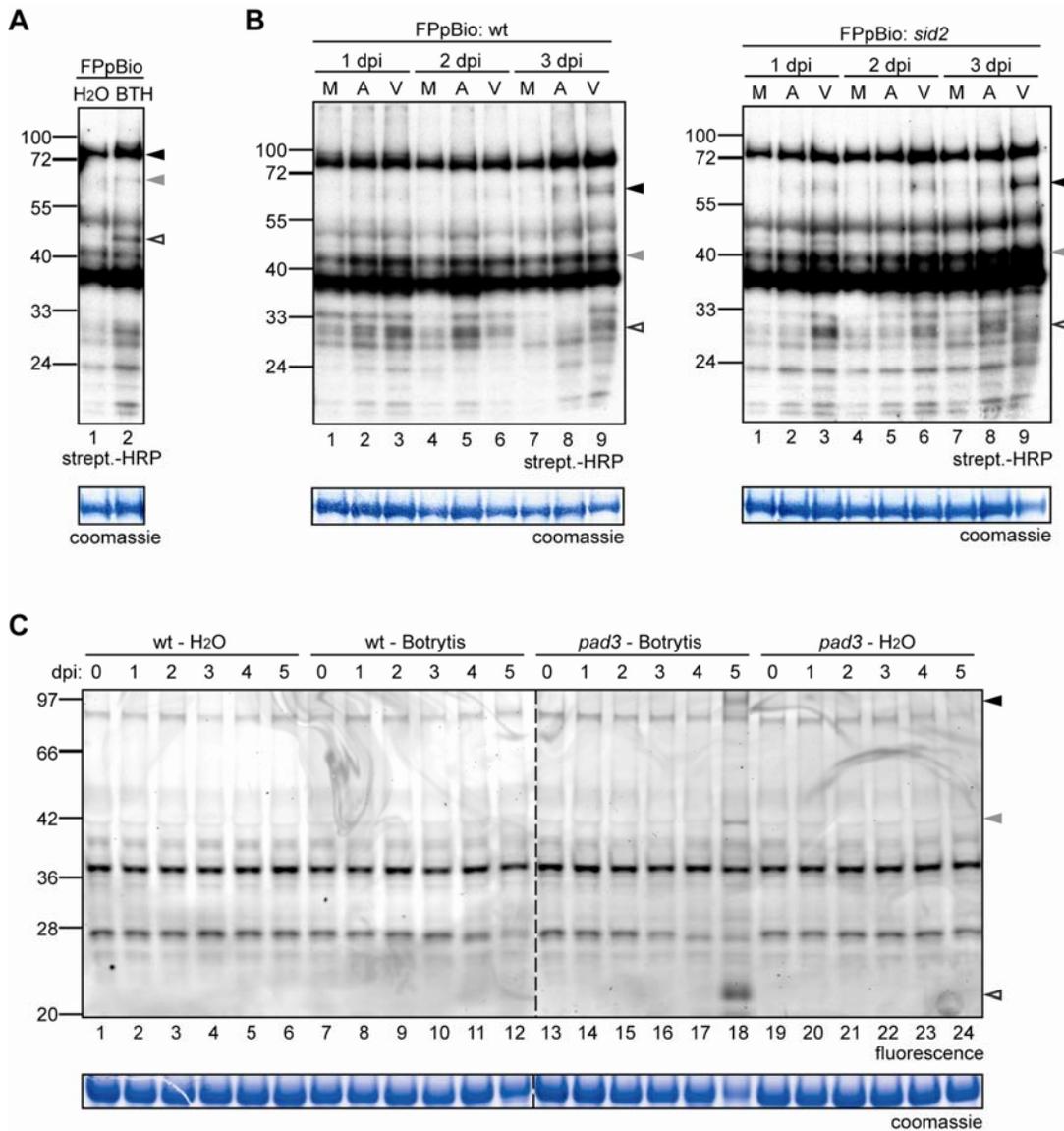
FIGURE 1-3 FP profiling of defense-related and pathogen-infected Arabidopsis plants.
A, FP profiling of leaf extracts of BTH-treated Arabidopsis plants. Four-week-old Arabidopsis plants were sprayed with H_2O or 300 μM BTH. Leaf proteins were extracted after 5 days, and equal protein quantities were labeled with 0.4 μM FPpBio. **B**, Time course of FP profiling of Pseudomonas-infected Arabidopsis leaf proteomes. Four-week-old Arabidopsis wild type (left panel) and *sid2* mutant (right panel) were sprayed with 10 mM $MgCl_2$ mock solution (M), or bacterial suspension containing 5 x 10^8 CFU/ml *Pseudomonas syringae* pv. tomato DC3000 avirulent strain AvrPphB (A) or virulent strain (V). Leaf proteins were extracted from each treatment at different dpi, and equal quantities were labeled with 0.4 μM FPpBio. **C**, Time course of FP profiling of Botrytis-infected Arabidopsis leaf proteomes. Four-week-old Arabidopsis wild type and *pad3* mutant were infected with LB droplets containing 1 x 10^6 CFU/ml *Botrytis cinerea* spores. Leaf proteins were extracted, and equal quantities were labeled with 0.2 μM FPpRh at different dpi. Arrows indicate the specific signals which are discussed in detail in the text.

Next, we applied comparative FP profiling to study the changes in serine hydrolase activities in the interaction between *A. thaliana* and hemibiotrophic bacterial pathogen *Pseudomonas syringae* pv *tomato* (*Pst*), the model patho-system for molecular genetic analysis of plant-pathogen interactions. *Pst* is a Gram-negative, rod-shaped bacterium with polar flagella, that causes foliar spots and blights on Arabidopsis (Dong *et al.*, 1991). Wild-type *A. thaliana* ecotype Columbia-0 is susceptible to *Pst* DC3000, but is resistant to *Pst* DC3000 carrying AvrPphB, a cysteine protease that elicits the hypersensitive response (HR) (Whalen *et al.*, 1991; Shao *et al.*, 2002). The salicylic acid-induction deficient mutant-2 (*sid2*) of Arabidopsis, in which biogenesis of SA is impaired, is more susceptible to both virulent and avirulent forms of *Pst* (Nawrath and Métraux, 1999).

To investigate serine hydrolase activities in the compatible interaction (susceptible plant with virulent pathogen) and the incompatible interaction (resistant plant with avirulent pathogen), we spayed *Pst* DC3000 virulent strain (V) and avirulent strain (A) carrying AvrPphB to wild-type Arabidopsis plants, and performed FP profiling on extracts taken at different day-post-infection (dpi). This analysis revealed diverse changes in the FP profile among three treatments during the first 3 days (Figure 1-3B, left panel). For example, the 65-kDa signal became upregulated in avirulent and virulent pathogen-infected leaves at 3 dpi (Figure 1-3B, left panel, black arrowhead); the 40-kDa signal became upregulated in avirulent and virulent pathogen-infected leaves after 1 dpi (Figure 1-3B, left panel, grey arrowhead); and the 30-kDa became upregulated transiently at 2 dpi in avirulent pathogen-infected leaves, while became downregulated in virulent pathogen-infected leaves after 1 dpi (Figure 1-3B, left panel, open arrowhead).

The upregulation of the 65-kDa and 40-kDa signals was faster and stronger in *sid2* mutants than in wild-type plants (Figure 1-3B, right panel, black and grey arrowheads). The 30-kDa signal showed different and more dynamic changes: it was upregulated in the infection with virulent pathogen at 1 dpi and started decreasing since 2 dpi, while it was upregulated in the infection with avirulent pathogen only at 3 dpi (Figure 1-3B, right panel, open arrowhead). In conclusion, FP profiling of leaf proteomes of *Pst*-infected Arabidopsis plants revealed miscellaneous and dynamic changes in serine hydrolase activities.

20

We also investigated changes in serine hydrolase activities during infection with the necrotrophic fungal pathogen *Botrytis cinerea*. Botrytis can penetrate healthy undamaged tissues of a wide range of plants and fruits and cause severe losses in the grape and fruit industry (Van Kan, 2006). Arabidopsis plants are well protected against Botrytis through the inducible production of phytoalexins like camalexin. Phytoalexin-deficient mutant *pad3* carries a mutation in CYP71B15, which catalyzes the last step in camalexin biosynthesis (Zhou *et al.*, 1999; Schuhegger *et al.*, 2006). The absence of camalexin production in *pad3* mutant plants explains their susceptibility for Botrytis infection (Ferrari *et al.*, 2003).

To investigate serine hydrolase activities during infection with Botrytis, we infected wild-type and *pad3* mutant Arabidopsis plants with Botrytis and performed FP profiling on extracts taken at different days post-infection (dpi). This analysis revealed no changes in the FP profile during the first 3 days, consistent with the 3-day latent period of Botrytis infection (Figure 1-3C). At 4 and 5 dpi, the 25-kDa signal became weaker in Botrytis-infected leaves (Figure 1-3C, lanes 12, 13 and 17, 18). This process was faster in *pad3* mutants than in wild-type plants. At 5 dpi a number of additional signals appeared in the *pad3* mutant. At this stage, half of the Botrytis-infected leaves of the *pad3* mutant were macerated, whereas the infection in wild-type plants did not progress beyond the site of the inoculation (data not shown).

2.1.1.3 Identification of FP targets in Botrytis-infected Arabidopsis plants

To identify the FP targets Botrytis-infected Arabidopsis plants, we labeled leaf extracts of Botrytis-infected wild-type and *pad3* mutant plants taken at 5 dpi with FP, and the biotinylated proteins were purified, separated on SDS-PAGE gel, and identified by tandem mass spectrometry (MS). Target purification and MS analysis was performed by Farnusch Kaschani at the Scripps Research Institute in San Diego, USA. The fluorescent FPpRh labeling profile (Figure 1-4) is consistent with the Coomassie blue-stained gel containing purified FP targets (data not shown), and shows that we can simultaneously detect the activities of serine hydrolases from both Arabidopsis and Botrytis. The wild-type Arabidopsis sample consists almost entirely of Arabidopsis enzymes, whereas the *pad3* mutant sample also contains several Botrytis enzymes. The activities of Arabidopsis methylesterases MES2 and MES3

decrease in *pad3* mutant plants (Figure 1-4, italic). FP profiling signals exclusively in *pad3* mutant sample were caused by Botrytis-derived enzymes including a lactamase, an SCPL-like enzyme and two cutinases (Figure 1-4, bold). Thus, FP profiling revealed a series of serine hydrolase activities that change during Botrytis infection. It is possible that these serine hydrolase activities play a role during the Botrytis-Arabidopsis interaction.
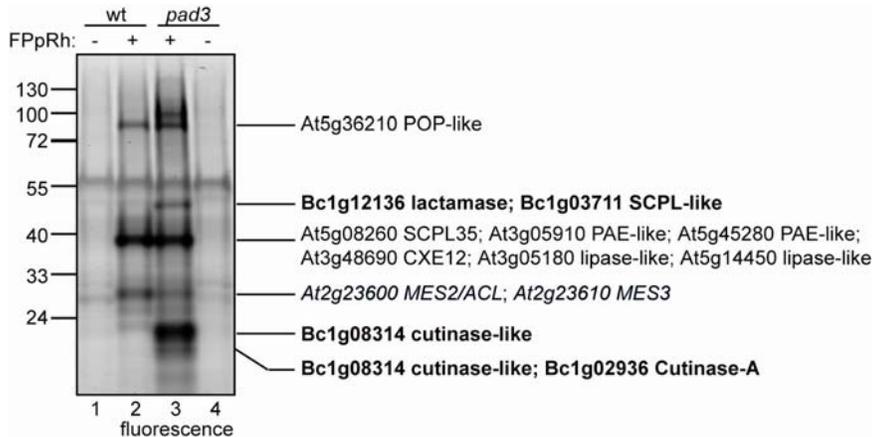
FIGURE 1-4 Identities of serine hydrolases during the Arabidopsis-Botrytis interaction.
Four-week-old Arabidopsis wild-type (wt) and *pad3* mutant were infected with LB droplets containing 1 x 10^6/ml *Botrytis cinerea* spores. Leaf proteins were extracted at 5 dpi, and equal quantities were labeled with 0.2 µM FPpRh. The fluorescent signals represent serine hydrolases identified by *in vitro* FP labeling, affinity purification and tandem MS analysis. Proteins whose activities were upregulated are bold. Proteins whose activities were downregulated are italic.

2.1.2 FP profiling of tomato apoplastic fluids

The apoplast is an important molecular frontier of plant cells to shield invading pathogens. Plant cells secret a variety of proteases into apoplastic space to build a proteolytic barrier. The functions of these proteases during plant-pathogen interactions vary from non-self recognition to direct proteolytic defenses (Van der Hoorn and Jones, 2004; Boller, 2005). Coevolving with their host plants, pathogens developed counter-defense mechanisms including the secretion of protease inhibitors into the apoplastic space to assist the colonization (Misas-Villamil and Van der Hoorn, 2008). Therefore, the plant apoplast became an appealing research model for studying the antagonistic plant-pathogen interactions in basal and *R*-gene mediated plant defenses.

To study the functions of soluble apoplastic proteins during plant defenses, apoplastic fluids (AFs) are advantageous over extracellular medium of cell suspension cultures. The AF of tomato (*Solanum lycopersicum*) can be obtained by simple vacuum-infiltration and centrifugation with minimal intracellular contaminants (De Wit and Spikman, 1982). In this study, we utilized ABPP with FP probes to study the activities of serine hydrolases in tomato AFs and the activity changes during salicylic acid-dependent defenses. Applying activity-based proteomics on tomato AFs is beneficial for the following reasons. First, protein expression can not be precisely predicted and estimated at gene transcript levels in apoplast. Second, the activities of apoplastic proteins can be regulated by posttranslational modifications during ER-Golgi secretion pathways or inhibited by pathogen-derived inhibitors. Therefore, the readout at the activity level is crucial for deciphering the functions of apoplastic proteins in defense. Third, the apoplastic proteome of a tomato leaf is less complicated than the leaf proteome. This will enhance the separation and identification of proteins by gel electrophoresis and MS analysis. We characterized FP profiling of tomato AFs, applied comparative ABPP to defense-related tomato AFs, and applied competitive ABPP to test if a pathogen-derived inhibitor can outcompete FP labeling.

2.1.2.1 Characterization of FP labeling

To take the advantages of both fluorescent probe for quick detection of profiling signals and biotin-tagged probe for affinity purification of labeling targets, we used both fluorescent FPpRh and biotin-tagged FPpBio in this study (Figure 1-1). First, we compared the labeling profiles of FPpRh and FPpBio probes. Tomato AFs were labeled with FPpRh and FPpBio, and labeled proteins were detected on protein gels by fluorescence scanning and on protein blots with streptavidin-HRP, respectively. Both FPpRh and FPpBio caused similar labeling patterns mainly with two strong signals at 70-kDa and 56-kDa, and four weak signals at 40-kDa, 36-kDa 33-kDa and 26-kDa, though the relative intensity of each signal may vary between two labeling profiles (Figure 1-5A, lane 2). FPpRh labeling can be globally suppressed by preincubation with excess FPpBio, and FPpBio labeling can be globally suppressed by preincubation with excess FPpRh (Figure 1-5A, lanes 3). This "mutual competition" indicates that FPpRh and FPpBio label the same set of enzymes in tomato AFs, and the signals that FPpRh visualizes are identical to the signals that

23

FPpBio identifies. Both FPpRh and FPpBio labeling profiles contain no background signals (Figure 1-5A, lane 1).
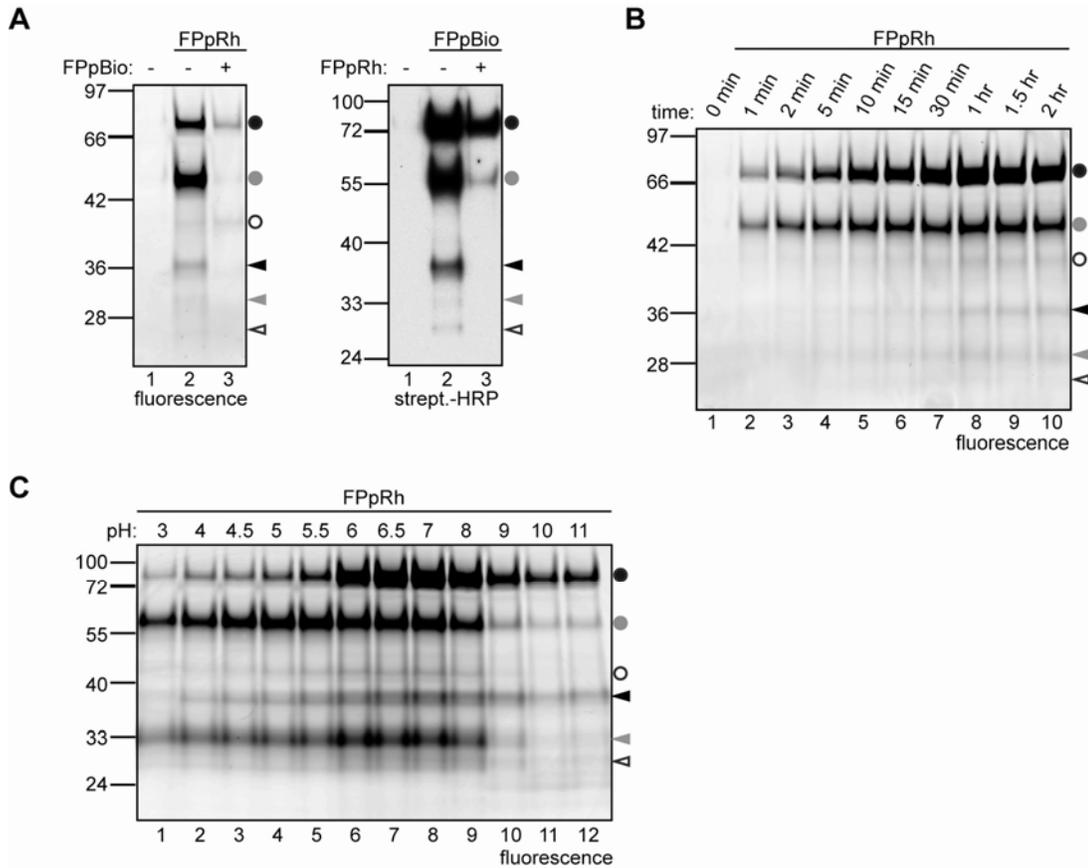
FIGURE 1-5 Characterization of FP profiling in tomato apoplastic fluids.
A, FPpRh and FPpBio label the same targets in AFs. Left panel: AFs were incubated with 0.2 μM FPpRh for 2 hr at pH 6 with or without a preincubation of 30 minutes with 2 μM FPpBio. Right panel: AFs were incubated with 0.2 μM FPpBio for 2 hr at pH 6 with or without a preincubation of 30 minutes with 2 μM FPpRh. Please note that FPpRh and FPpBio share very similar labeling profiles, and one can outcompete the other's labeling. *B*, Time course of FPpRh labeling. AFs were labeled with 0.2 μM FPpRh at pH 6 for different time. *C*, pH dependency of FPpRh labeling. AFs were labeled for 3 hr with 0.2 μM FPpRh at different pH values.

Labeling time is a crucial parameter for competitive ABPP with reversible inhibitors. To characterize the time course of FP profiling, labeling of tomato AFs was followed over different periods (Figure 1-5B). This shows that FP labeling occurs within 1 minute, and the labeling of all targets reaches the maximum within 1 hour. Therefore, a short labeling time is required for kinetically controlled competition assays with putative reversible inhibitors, as FP labeling is relatively fast.

The above experiments were performed at pH 6, the apoplastic pH. Because protein activities can be tightly controlled or flexibly regulated by different pH, we tested FP labeling of tomato AFs at various pH values. This pH dependency experiment showed that optimal pH range for labeling of both 70-kDa and 36-kDa signals is pH 6-11, and for 56-kDa and 33-kDa signals is pH 4-8 (Figure 1-5C). At pH 6, all signals can be labeled maximally, indicating that the target serine hydrolases in tomato AF are indeed active at their physiological pH (Figure 1-5C, lane 6). We used pH 6 for all subsequent FP profiling experiments in this study.

2.1.2.2 FP profiling of apoplastic fluids of defense-related tomato plants

Salicylic acid (SA) is a signal molecule that increases endogenously upon pathogen infection and triggers local defense and systemic acquired resistance (Shah, 2003). Benzothiadiazole (BTH) is a functional analog of SA with higher mobility in plants, and exogenous application of BTH triggers SA-dependent defense responses (Lawton *et al.*, 1996). The advantages of defense induction in plants by BTH over live pathogens are apparent. First, since no pathogenic organism is involved, the research system is significantly simplified. Second, plant defense induction can be readily synchronized. Third, the effects of chemical induction can be tightly controlled in a dosage-dependent manner.

Tomato plants were drenched with H_2O or with BTH solution, and AFs of adult leaves were extracted at 5 days post treatment and labeled with FPpRh. Sufficient induction of defense responses was indicated by the accumulation of PR proteins in the AFs from BTH-treated tomato plants (Figure 1-6A). FPpRh profiling of AFs from H_2O- or BTH-drenched tomato plants revealed extensive differentials of serine hydrolase activities on 1D gel (Figure 1-6B). The 70-kDa and 33-kDa signals were strongly upregulated upon BTH treatment, while the 56-kDa signal was downregulated, suggesting that their functions may relate to the SA-mediated apoplastic defense (Figure 1-6B, black dot, grey arrowhead and grey dot, respectively). 36-kDa and 26-kDa signals remained similar in H_2O- and BTH-treated samples, implying that both may have a housekeeping function not directly involved in plant defense (Figure 1-6B, black and open arrowhead).
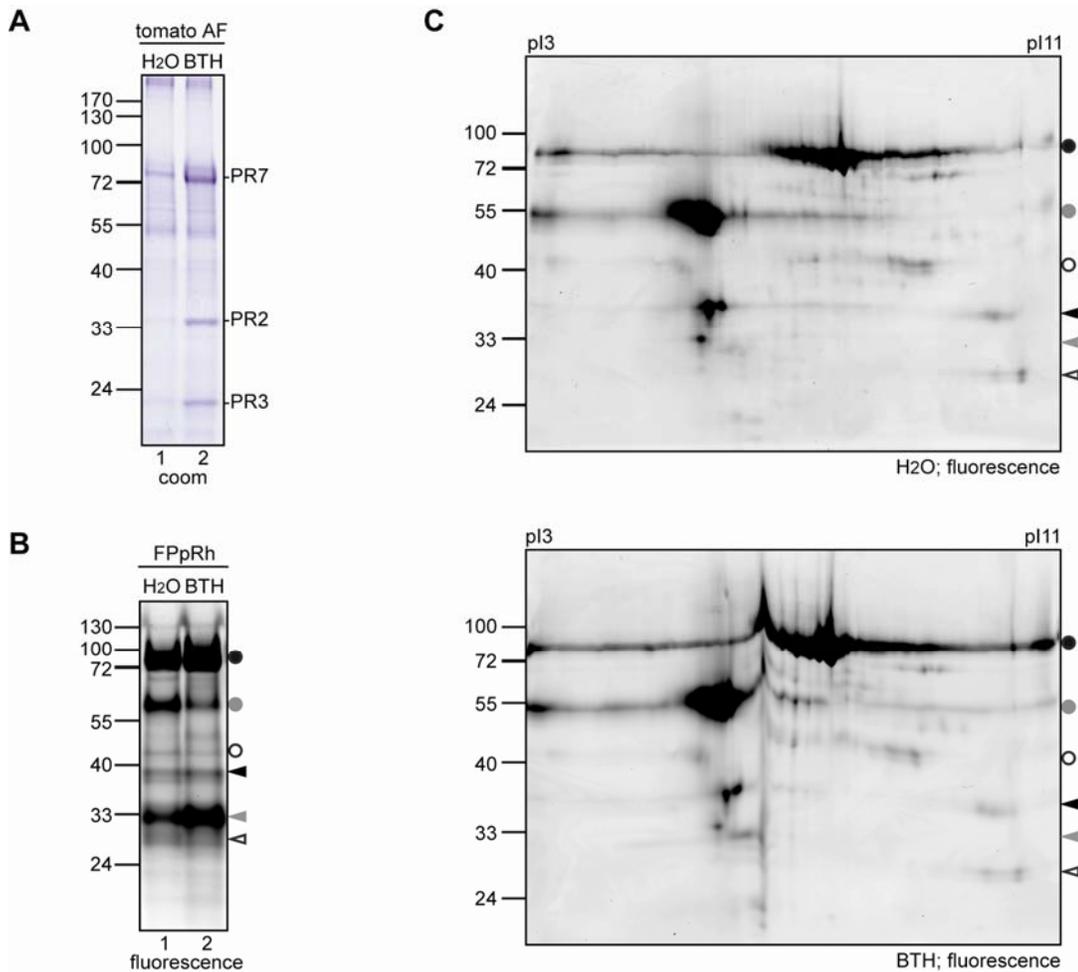
FIGURE 1-6 Differential activities of secreted FPpRh targets in BTH-treated tomato plants.
A, Apoplastic PR protein accumulation in BTH-treated tomato plants. Five-week-old tomato plants were treated with H_2O or BTH. AFs were isolated after 5 days, and equal volumes were separated on a 12% protein gel to visualize PR protein accumulation in the AF. *B and C*, Tomato plants were drenched with H_2O or 300 μM BTH for 5 days, and apoplastic fluids were isolated. Equal volumes were used for protein activity profiling with FPpRh. Proteins were separated by 1DE (*B*) or 2DE (*C*).

We further separated the FPpRh-labeled serine hydrolases on 2D gels, resulting in a better separation of the signals (Figure 1-6C). The strong 70-kDa signal has different isoforms, whose activities may be differentially regulated during plant defense (Figure 1-6C, black dot). Identification of purified FP targets on 2D gels will provide a detailed reference map of active serine hydrolases in tomato AFs, and facilitate studies on the activity regulation of target proteins.

2.1.2.3 FP labels P69B whose activity is upregulated in defense

To identify the FP profiling targets, leaf AFs from H_2O- and BTH-drenched tomato plants were labeled with FPpBio. The biotinylated proteins were purified on streptavidin agarose beads, and separated by 1DE. The profile of captured biotinylated signals on streptavidin blots is identical with the profile on coomassie-stained gel (Figure 1-7A). The coomassie-stained protein bands were excised from the gel, digested with trypsin and subjected to MS analysis. MS analysis was performed by Tom Colby at Proteomics Service Center of MPIZ in Cologne, Germany. The MS data demonstrated that both 70-kDa and 33-kDa signals contain specific peptides of P69B, a subtilisin-like serine protease that resides in tomato apoplast (Tornero *et al.*, 1997). Due to technical limitations, the tryptic peptides from other coomassie-stained protein bands could not be detected by MS. The identity of the two identified signals was confirmed by showing that purified biotinylated proteins cross-react with the antiserum specific to N-terminal peptide of P69 subtilase (Figure 1-7B; Tian *et al.*, 2004). The activity of P69B is upregulated in AFs when the tomato plants are treated with BTH (Figure 1-7). These results are consistent with pathogenesis-related (PR) nature of P69B which is induced and accumulates in the tomato apoplast upon pathogen attack or treatments with SA or BTH (Vera *et al.*, 1989; Jorda and Vera, 2000; Tian *et al.*, 2004).
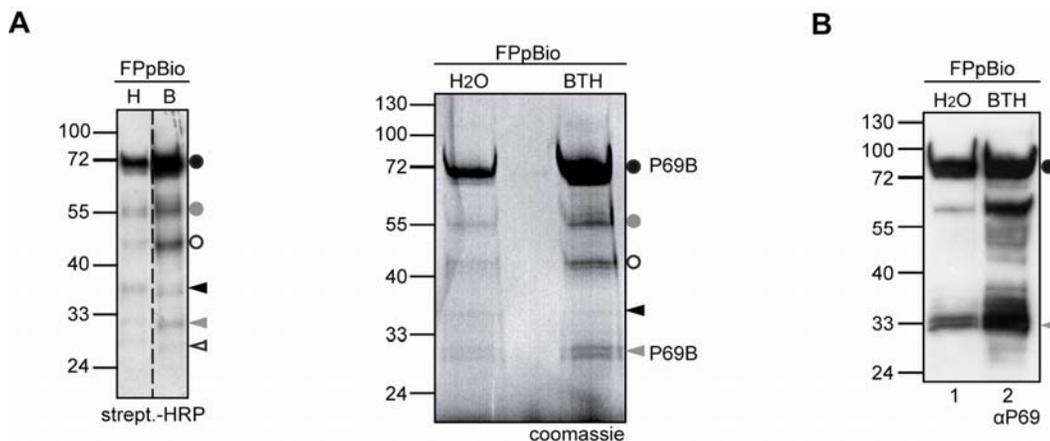
FIGURE 1-7 Identification of major FPpBio target in tomato apoplastic fluids.
A, Purification and identification of FPpBio-labeled proteins from AFs. Tomato plants were drenched with H_2O or 300 μM BTH for 5 days, and AFs were isolated. Equal volumes of AFs from H_2O- or BTH-treated plants were labeled with FPpBio, and biotinylated proteins were captured and purified on streptavidin-agarose beads. Proteins eluted from these beads were

analyzed on protein blots using streptavidin-HRP (left panel), and on protein gels stained with coomassie-blue (right panel). Coomassie-blue-stained protein bands were excised, digested with trypsin and analyzed by tandem MS. P69B was identified as major component of two major signals indicated with arrowheads. *C*, Confirmation of P69B as the major FPpBio target in tomato AFs. Two major signals were confirmed to be P69B using anti-P69 antibody on the purified proteins. Please note that activities of P69B in tomato AFs were upregulated upon BTH treatment.

2.1.2.4 EPI1a can not outcompete FP labeling of P69B in tomato apoplastic fluids

EPI1 is an extracellular protease inhibitor secreted by *Phytophthora infestans* during infection and has been shown to inhibit the tomato apoplastic subtilisin-like serine protease P69B (Tian *et al.*, 2004). EPI1 contains two domains homologous to the Kazal family of serine protease inhibitors: an atypical Kazal domain EPI1a and a typical Kazal domain EPI1b (Figure 1-8A, upper panel). Using enzymatic assays with colorimetric substrates and coimmunoprecipitation assays, Kamoun and coworkers showed that the EPI1 inhibits and interacts with P69B, and the inhibition and interaction are achieved only through EPI1a domain, but not EPI1b domain (Tian *et al.*, 2005). We ectopically expressed recombinant EPI1a in *Escherichia coli*, and performed competitive ABPP to examine if EPI1a can outcompete FP labeling of P69B.

The rEPI1a has an N-terminal FLAG tag from expression vector pFLAG-ATS (Figure 1-8A, bottom panel; Tian *et al.*, 2005). Using anti-FLAG affinity gel, we purified rEPI1a from *E. coli* culture media, and determined the purity of the recombinant protein with silver nitrate staining. The purified rEPI1a has an expected size of 10-kDa, and has high purity mainly in elution fraction-2 (Figure 1-8B, arrowhead). rEPI1a was then used as a reference inhibitor of P69B for competition assays with FP labeling of tomato AFs.

To apply competitive ABPP, we preincubated 50 μL AFs from either H_2O- or BTH-treated tomato plants with 100 nM rEPI1a for 30 minutes, and then added 50 nM FPpRh in to label for another 30 minutes. Surprisingly, FPpRh profiling showed that EPI1a can not outcompete FP labeling of P69B in AFs of either H_2O- or BTH-treated samples (Figure 1-8C). This suggests that rEPI1a may not affect the accessibility of FP probe to the catalytic serine residue at the active site of P69B protease.
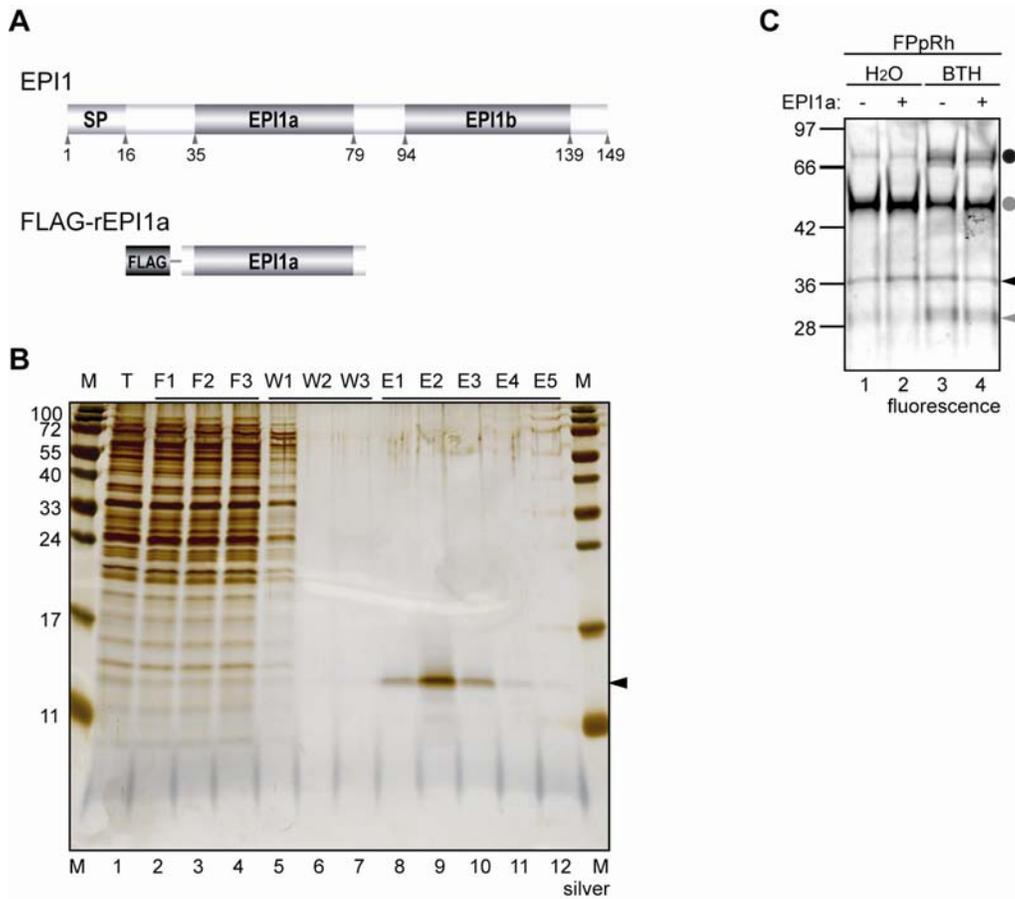
FIGURE 1-8 EPI1a can not outcompete FP labeling of P69B in tomato apoplastic fluids.
A, Schematic diagram of EPI1 and FLAG-rEPI1a structures. The signal peptide (SP), two Kazal domains (EPI1a and EPI1b) and FLAG-tag are represented in dark gray. The numbers indicate the amino acid positions from N-terminus. The diagram was modified from Tian *et al*, 2004. *B*, Ectopic expression and affinity purification of Kazal domain EPI1a of EPI1. Recombinant EPI1a with FLAG epitope tag at N terminus was ectopically expressed in *E. coli*, and purified with anti-FLAG affinity gel from the culture medium. Silver nitrate staining shows the purity of the eluted protein. Elute fraction 2 was used in competition assays of FPpRh profiling. M, protein size marker. T, total input. F, flow-through. W, wash. E, elute. *C*, EPI1a can not outcompete FP labeling of P69B in tomato AFs. 50 μL of AFs from H_2O- or BTH-treated plants were preincubated for 30 minutes with or without 100 nM EPI1a, and then labeled with 50 nM FPpRh for another 30 minutes.

2.2 ABPP with epoxide probe DCG-04

2.2.1 PLCP activities and AVR2 inhibition of PIP1 in tomato apoplastic fluids

Considering that invasion of the plant apoplast is a critical phase of the infection cycle of numerous pathogens, it can be postulated that this compartment serves as a molecular battlefield that contributes to the success of pathogen infection and plant resistance. Infection of tomato with various pathogens triggers the accumulation of a large amount of pathogenesis-related (PR) proteins in the apoplast, some of which directly target those pathogens by degrading their cell wall components (Kombrink *et al.*, 1988; Joosten and De Wit, 1989; Van Loon *et al.*, 2006; Ferreira *et al.*, 2007). Pathogens, on the other hand, secrete different effector proteins during infection to prevent this degradation (Rose *et al.*, 2002; Tian *et al.*, 2004, 2005; Van den Burg *et al.*, 2006; Van Esse *et al.*, 2007).

Although apoplast-localized plant proteases can play a role in defense, they might also act in signaling or perception upon pathogen infection (Van der Hoorn and Jones, 2004). For example, RCR3, a secreted PLCP of tomato, is essential for the function of the tomato resistance gene *Cf-2*, which mediates recognition of the pathogenic fungus *Cladosporium fulvum* carrying the avirulence gene *Avr2* (Krüger *et al.*, 2002). RCR3 is transcriptionally regulated as a PR protein, and the secreted AVR2 protein binds and inhibits RCR3. This mechanism of perception suggests that RCR3 is rather a virulence target of AVR2 that became guarded by the Cf-2 resistance protein to monitor pathogen entry (Van der Hoorn et al., 2002; Rooney et al., 2005; Jones and Dangl, 2006). The hypothesis that PLCPs can be virulence targets is also supported by the discovery that *Phytophthora infestans* secretes PLCP inhibitors during infection of tomato (Tian *et al.*, 2007).

These data indicate that tomato plants secrete PLCPs during defense to create a proteolytic apoplast that is harmful to pathogens. However, it is unknown what the full content of apoplastic PLCP activities is and to what extent these secreted PLCPs are inhibited by AVR2 and other pathogen derived inhibitors. In this study, we used ABPP with PLCP-specific fluorescent ABP TMR-DCG-04 to investigate which

PLCPs are active in the tomato apoplast during the benzothiadiazole (BTH)-triggered defense response and to determine the extent to which these PLCPs are inhibited by AVR2.
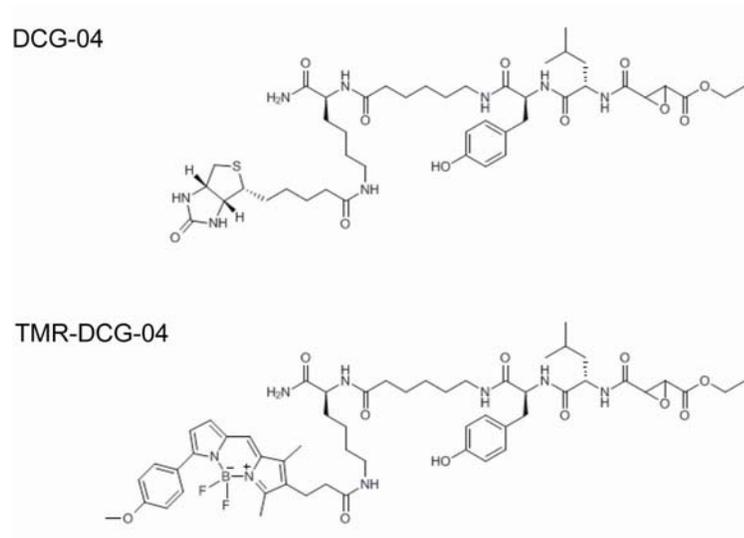
FIGURE 2-1 Structures of activity-based probes DCG-04 and TMR-DCG-04.
Both carry the same epoxide reactive group, binding group and linker, and differ in reporter groups: biotin in DCG-04 and BODIPY-TMR in TMR-DCG-04.

2.2.1.1 BTH treatment results in increased PLCP activity in the tomato apoplastic fluids

We employed protease activity profiling as a tool to display activities of PLCPs in the tomato AFs (Van der Hoorn *et al.*, 2004). Protease activity profiling is based on the use of a BODIPY-TMR-tagged, broad-range PLCP inhibitor E-64 (called TMR-DCG-04; Figure 2-1, lower panel), which reacts with the catalytic Cys residue of the protease in an activity-dependent manner (Greenbaum *et al.*, 2000). E-64 lacks specificity-determining binding groups and is often used for diagnostic purposes since it is reactive to a wide range of PLCPs. Although the readout does not contain information on substrate specificity and conversion rates, signals represent the availability and abundance of active sites of PLCPs.
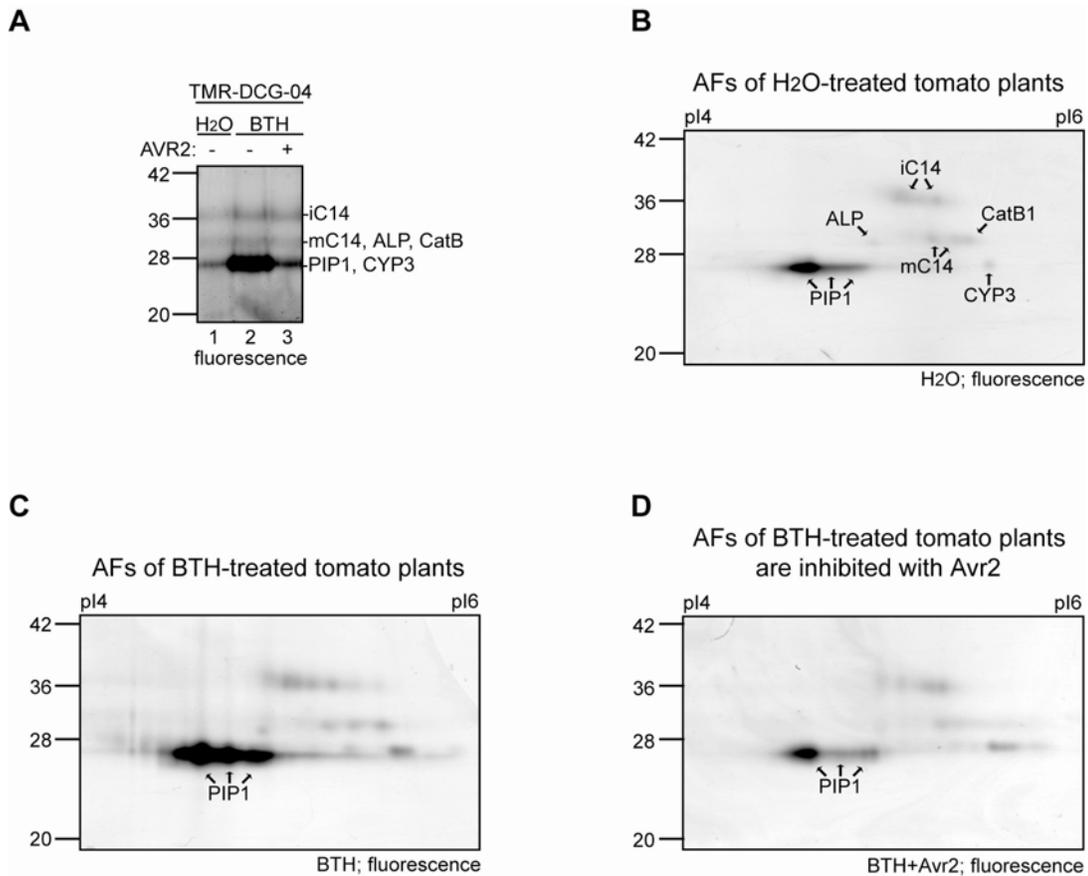
FIGURE 2-2 PIP1 is induced by BTH treatment and inhibited by AVR2 in the tomato apoplastic fluids.

A, 1D fluorescent protease activity profiling of tomato AFs. Plants were treated with H_2O or BTH for 5 days, and AF was isolated. Equal volumes of AF were used for protease activity profiling with TMR-DCG-04. The same volume of AF of BTH-treated tomato plants were also preincubated with 83 nM AVR2 before adding TMR-DCG-04 to label the remaining noninhibited proteases. Proteins were separated by 1D gel electrophoresis. Please note that only 25-kDa signal coinciding with PIP1 is significantly stronger from BTH-treated plants, and suppressed by addition of AVR2. **B and C**, 2D fluorescent protease activity profiling of PLCPs in tomato AFs. Plants were treated with H_2O (**B**) or BTH (**C**) for 5 days, and AF was isolated. Equal volumes of AF were used for protease activity profiling with TMR-DCG-04. Proteins were separated by 2D gel electrophoresis. Signals on the 2D map (**B**) represent PLCPs identified by *in vitro* DCG-04 labeling, affinity purification and tandem MS analysis, and are indicated with arrows. Please note that only signals coinciding with PIP1 are significantly stronger from BTH-treated plants (**C**). **D**, 2D fluorescent protease activity profiling of PLCPs in tomato AFs in the presence of AVR2. Same volume of AF of BTH-treated tomato plants were preincubated with 83 nM AVR2 before adding TMR-DCG-04 to label the remaining noninhibited proteases. Proteins were separated by 2D gel electrophoresis. Please note that only signals coinciding with PIP1 are significantly weaker in the presence of AVR2.

To investigate secreted PLCP activities during the defense response of tomato, we isolated apoplastic fluids (AFs) 5 days after treating tomato plants with H_2O or with the salicylic acid (SA) analog BTH. The AF of BTH-treated tomato contains the expected PR proteins, demonstrating that the BTH treatment was successful (Figure 1-6A).

Protease activity profiling with TMR-DCG-04 revealed three fluorescent signals in AF of H_2O-treated tomato plants: a strong signal at 25-kDa, a weaker signal at 30-kDa, and a weak signal at 35-kDa (Figure 2-2A, lane 1). All three of these signals can be competed by adding an excess of E-64 during labeling (data not shown). These three signals are upregulated in AF of BTH-treated tomato plants (Figure 2-2A, lane 2). The differential activities of 30-kDa and 35-kDa signals are less pronounced than the 25-kDa signal, which dominates the overall PLCP activities in AF of BTH-treated tomato plants. Thus, tomato plants create a proteolytic apoplast by secreting active PLCPs upon BTH treatment, especially the 25-kDa PLCP.

2.2.1.2 Tomato apoplast contains activities of different PLCPs

To identify the PLCPs in the tomato apoplast, AFs were labeled with DCG-04 (Figure 2-1, top) and biotinylated proteins were purified, separated by 2DE, and identified by tandem MS. Target purification, 2DE and MS analysis were performed by Renier van der Hoorn, Anne Harzen and Tom Colby, respectively, at Proteomics Service Center of MPIZ in Cologne, Germany. This established 2D reference map of PLCP activities in tomato apoplastic fluids for comparative ABPP of BTH treatment and AVR2 inhibition mentioned below with 2D fluorescent profiling. The advantages of profiling PLCP activities in tomato AFs by 2DE with fluorescent TMR-DCG-04 probe are apparent. First, 2DE provides indispensably excellent separation of plant PLCPs, as subsets of them share extremely similar molecular weight (MW) and therefore could not be efficiently detected and distinguished by 1DE (Van der Hoorn *et al.*, 2004). Second, fluorescent profiling offers sensitive measurement of fluorescent signals with superb dynamic range, so that ensures reliable quantification of signal intensities. Third, it escapes, compared to biotin-streptavidin blots, background noises from the endogenously biotinylated proteins and unspecific binding of the second reporter or

luminescence reagents. Forth, it avoids introducing signal variations among different gels, so that makes multiple gels quantitatively comparable.

Comparison of the fluorescent 2D map (Figure 2-2B) with the Coomassie blue-stained 2D gel containing purified PLCPs (Shabab *et al.*, 2008) indicates that we can detect the activities of PIP1, C14, CatB1, CYP3, and perhaps even ALP simultaneously in the AF of H_2O-treated tomato plants using fluorescent protease activity profiling. The horizontal rows of spots for most of the proteases probably come from different isoforms that exist in planta or are generated during extraction.

2.2.1.3 PIP1 is induced by BTH treatment and inhibited by AVR2 in the tomato apoplastic fluids

The three signals detected by fluorescent protease activity profiling on 1D gel are consistent with those observed on 2D gels (Figure 2-2A-D). 1D gels show that BTH treatment results in a strong upregulation of the 25-kDa PIP1 and CYP3 signals and weak upregualtions of the 30-kDa and 35-kDa signals of mature isoform of C14 (mC14), ALP, CatB and intermediate isoform of C14 (iC14), respectively (Figure 2-2A, lane 1 and 2).

Comparison of the fluorescent 2D activity profiling maps of AFs of H_2O- and BTH-treated tomato plants indicates that only the signal corresponding to PIP1 is significantly upregulated upon BTH treatment (Figure 2-2B and C). The signals corresponding to the other PLCPs remain similar when compared with the control. These data indicate that PIP1 dominates the increased PLCP activity during BTH treatment. The induction of PIP1 by BTH treatment is similar to those of *PR* genes (Sanz-Alferez *et al.*, 2008), indicating that PIP1 gene expression is regulated through the SA pathway and that it can be considered as being a PR protein.

Having identified the PLCPs that pathogens encounter when they invade the tomato apoplast, we next investigated which PLCPs are inhibited by AVR2 of the fungus *C. fulvum* (Rooney *et al.*, 2005). AVR2 was produced as an N-terminally FLAG-tagged protein in *E. coli* by Mohammed Shabab.

To investigate the inhibition of PLCPs by AVR2 in crude AFs of BTH-treated tomato plants, we preincubated these AFs for 30 min with AVR2 and then added TMR-DCG-04 to label the remaining, noninhibited proteases. These assays were analyzed by 1DE and revealed that AVR2 prevents the labeling of most of the 25-kDa proteases, whereas the other signals remain unaltered (Figure 2-2A, lanes 2 and 3).

To determine the selectivity of AVR2 inhibition in more detail, we performed fluorescent protease activity profiling using TMR-DCG-04 on AF of BTH-treated tomato plants with and without preincubation with AVR2 and analyzed the samples on 2D gels. The 2D images were normalized using the fluorescent protein size markers and compared. Comparing the 2D fluorescent maps in the absence or presence of AVR2 shows that fluorescent labeling of C14, ALP, CYP3, and CatB1 is unchanged, whereas labeling of PIP1 is significantly reduced in the presence of AVR2 (Figure 2-2C and D). These data indicate that AVR2 selectively targets PIP1 and does not inhibit other C14, ALP, CYP3, or CatB1 in the tomato apoplast.

2.2.2   C14 activities and EPIC1/2B inhibition of C14 in tomato apoplastic fluids

Tomato is a host for numerous other leaf pathogens with miscellaneous lifestyles. The oomycete pathogen *Phytophthora infestans*, for example, is a hemibiothrophic pathogen that requires living cells during the initial stage of infection, but then causes extensive necrosis at a later stage (Kamoun and Smart, 2005). The defense response of tomato against such pathogens is universal and includes the accumulation of proteins like cysteine proteases in the apoplast that are potentially harmful for these pathogens (Tian *et al.*, 2005, 2007; Van Loon *et al.*, 2006; Ferreira *et al.*, 2007). These defense-related enzymes are thought to directly target the pathogens e.g. by degrading their cell wall components. Successful tomato pathogens evolved means to suppress these defense responses. For example, *P. infestans* secretes cystatin-like EPIC1 and EPIC2B proteins to inhibit tomato secreted papain-like cysteine proteases RCR3 and PIP1 (Tian *et al*., 2007; Song *et al*., 2009). These observations are consistent with the hypothesis that pathogen effectors evolve to inhibit harmful secreted proteases.

However, emerging concept is that most effectors have multiple targets (Hogenhout *et al*., 2009), and PIP1 and RCR3 are not the only PLCPs that are encountered by these pathogens during infection. Tomato secretes seven different papain-like cysteine proteases (PLCPs) into the apoplast that belong to four distinct classes. Besides RCR3 and PIP1 (subfamily 5), tomato secretes five other PLCPs that belong to different subfamilies. These PLCPs are C14 (subfamily 1), aleurain-like ALP and CYP3 (subfamily 7) and cathepsin B-like CatB1 and CatB2 (subfamily 8) (Beers *et al*., 2004). C14 is unique amongst these proteases since it carries a C-terminal granulin domain with unknown function (Yamada *et al*., 2001). Like its Arabidopsis ortholog RD21, tomato C14 exists in two active isoforms, depending on the presence or absence of a C-terminal granulin domain. The intermediate isoform (iC14) carries the granulin domain and is 40-kDa, whereas the mature isoform (mC14) is 30-kDa and lacks the granulin domain. Here, we investigated which of the tomato secreted PLCPs are targeted by the EPIC1 and EPIC2B effectors of *P. infestans*.

2.2.2.1 Characterization of DCG-04 labeling of recombinant C14

In order to investigate the activities of the secreted PLCPs of tomato individually and the potential inhibition by EPICs, we produced tomato C14 by agroinfiltration in *Nicotiana benthamiana* by expressing C14 with the silencing inhibitor p19, and use extracts of agroinfiltrated leaves for activity-based protein profiling (ABPP) (Shabab *et al.*, 2008). Ectopic overexpression of the recombinant tomato C14 (rC14) with the silencing inhibitor p19 ensures high levels of proteins produced *in planta* with all required post-translational modifications (Voinnet *et al.*, 2003; Van der Hoorn *et al.*, 2000). rC14 was produced by Raju Chintha at MPIZ in Cologne, Germany.

Labeling of *N. benthamiana* leaf extracts containing overexpressed rC14 with 2 μM DCG-04 at pH 5 reveals one strong signal at 30-kDa and one weak signal at 40-kDa, which represent two active isoforms of rC14: the 30-kDa mature rC14 and the 40-kDa intermediate rC14 (Figure 2-3A, B, C; indicated by black and gray arrowheads, respectively; Shabab *et al.*, 2008). This indicates that the mature isoform of rC14 dominates the overall activities of rC14 produced from agroinfiltration in *N. benthamiana*.
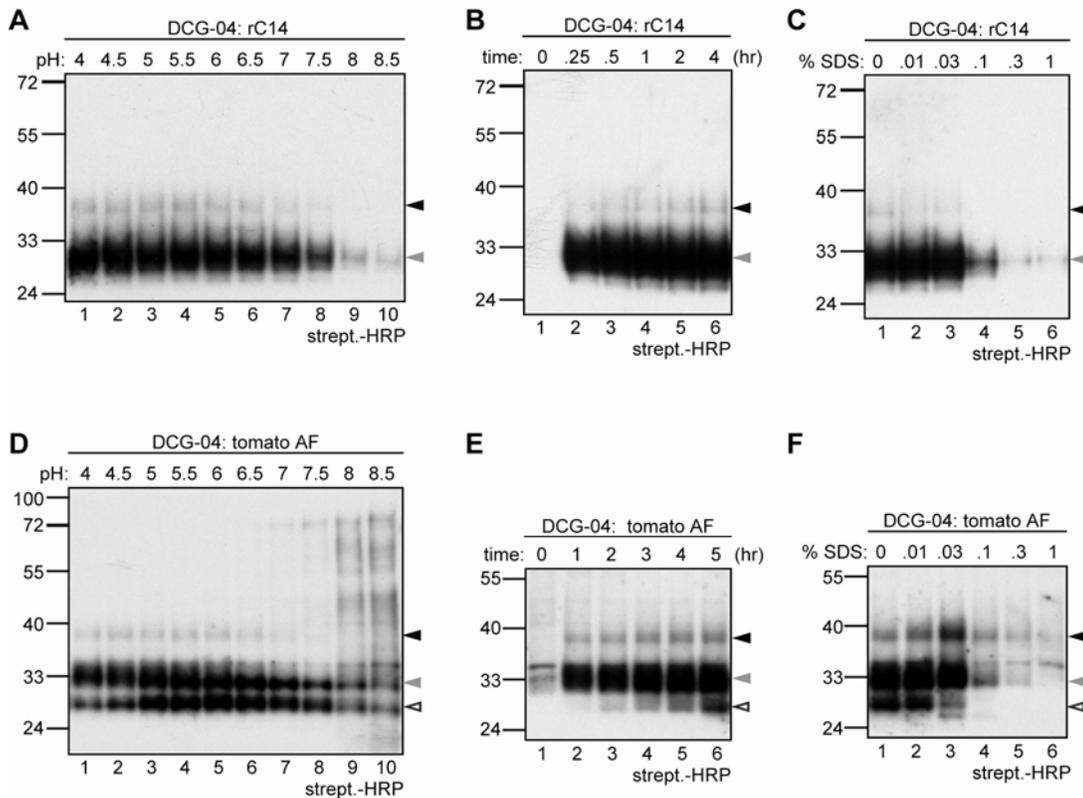
FIGURE 2-3 Characterization of DCG-04 profiling of recombinant C14 and of tomato apoplastic fluids.
A, pH dependency of DCG-04 labeling of rC14. Extracts from agroinfiltrated *N. benthamiana* leaves overexpressing rC14 were used as a source of rC14, and were labeled at different pH values. *B*, Time course of DCG-04 labeling of rC14. rC14-containing extracts were labeled at pH 5, and the labeling reactions were terminated at various time points by adding cold acetone to a final concentration of 67%. *C*, SDS effects on DCG-04 labeling of rC14. rC14-containing extracts were labeled at pH 5 in presence of different SDS concentrations. *D*, pH dependency of DCG-04 labeling of tomato AFs. AFs were extracted from tomato plants, and labeled at different pH values. *E*, Time course of DCG-04 labeling of tomato AFs. AFs were labeled at pH 5, and the labeling reactions were terminated at various time points by adding cold acetone to a final concentration of 67%. *F*, SDS effects on DCG-04 labeling of tomato AFs. AFs were labeled at pH 5 in the presence of different SDS concentrations. Black arrowhead, iC14; grey arrowhead, mC14; open arrowhead, PIP1.

The pH value is an important parameter for enzyme activities *in vitro*. Labeling at different pH causes different profiles (Figure 2-3A). Optimal pH range for labeling both intermediate and mature rC14 is at pH 4-6, consistent with the physiological pH of tomato apoplast (~pH 5.5). Activities of rC14 dramatically decrease at pH higher

than pH 7, which is characteristic for apoplastic PLCPs. Therefore, labeling of rC14 was conducted at pH 5 in the rest of this work.

Labeling kinetics is crucial for competitive ABPP to detect reversible inhibitors. To characterize the time course, labeling was followed over different periods (Figure 2-3B). This shows that labeling occurs within 15 minutes and the labeling of both intermediate and mature rC14 reaches saturation within 2 hours.

As an anionic surfactant, SDS can modify conformation, interaction and activity of proteins at certain concentrations. To study the effects of SDS as an additive to the activity of rC14, rC14-containing extracts were labeled with DCG-04 in the presence of different concentrations of SDS. 0.01-0.03% of SDS decreases the labeling of intermediate rC14, while has no effect on the labeling of mature rC14 (Figure 2-3C, lane 2 and 3). 0.1-1% of SDS completely prevents the labeling of intermediate rC14 and dramatically reduces the labeling of mature rC14 (Figure 2-3C, lane 4 to 6). These experiments show that low concentrations (0.1%-1%) of SDS decrease the labeling of rC14 with DCG-04.

2.2.2.2 Characterization of DCG-04 labeling of tomato apoplastic fluids

Labeling of crude apoplastic fluids (AFs) of tomato plants under normal growth conditions with 2 μM DCG-04 at pH 5 reveals three signals, one signal at 40-kDa representing intermediate C14 (iC14), one signal complex at 30-kDa including mature C14 (mC14), ALP and CatB, and one signal at 25-kDa mainly consisting of PIP1 (Figure 2-3D, E, F; indicated by black, gray and open arrowheads, respectively; Chapter 2.2.1.2 of this thesis). On 1D gel, we can not accurately distinguish mC14, ALP or CatB within the 30-kDa signal.

Different pH values affect labeling profiles of three hallmark signals differently (Figure 2-3D). Optimal pH range for labeling of 40-kDa iC14 and 30-kDa signals is from pH 4 to pH 6, and the labeling of those two signals dramatically decreases at pH higher than pH 6.5. 25-kDa PIP1 is active through the experimented pH range of pH 4-8.5, while its optimal pH range for labeling is at pH 5.5-6.5. At basic pH of pH 8-8.5, labeling of iC14 is completely abolished and the background increases globally

(Figure 2-3D, lane 9 and 10). These results indicate that all the DCG-04-labeled PLCPs in tomato AFs have acidic pH ranges optimal for their activities, which is in concert with their apoplastic location. Compared to the studies on rC14, iC14 in tomato AFs has identical pH profile as intermediate rC14, and the 30-kDa signal has a pH profile similar to mature rC14 (Figure 2-3, A and D). Thus, rC14 produced from *N. benthamiana* can represent C14 from the native proteome of tomato AF in the biochemical aspect of pH dependency of DCG-04 labeling.

Time course study on DCG-04 profiling of tomato AFs shows that the labeling of 40-kDa iC14 and 30-kDa signal complex occurs within 1 hour and reaches the maximal within 3 hours (Figure 2-3E). These observations on 40-kDa iC14 signal and 30-kDa signals in tomato AFs are consistent with the time course of labeling of iC14 and mC14 ectopically overexpressed in recombinant forms, respectively (Figure 2-3, B and E). In contrast, the labeling of 25-kDa PIP1 is slower: it starts to appear after 2 hours and does not yet saturate in 5 hours.

When we studied the effects of SDS at different concentrations on DCG-04 labeling of tomato AFs, we found that SDS at 0.1% or higher prevents the labeling of 30-kDa signals, and SDS at 0.03% or higher strongly prevents the labeling of PIP1 (Figure 2-3F). Interestingly, the labeling of iC14 tolerates SDS at the concentrations from 0.01% to 1%, and 0.03% SDS can significantly increase this labeling, which is drastically different from its effect on the labeling of ectopically-overexpressed recombinant iC14 (Figure 2-3, C and F, lane 3). Thus, 0.03% SDS shows contrasting effects on the activity of iC14 in native tomato AFs and in a recombinant form overexpressed in *N. benthamiana*.

2.2.2.3 Characteristics of EPIC1/2B inhibition of recombinant C14

In order to study the inhibitory effects of *P. infestans*-secreted cystatin-like effector proteins EPIC1 and EPIC2B on tomato C14, EPIC1 and EPIC2B were ectopically expressed in *E. coli*, and affinity-purified by Mohammed Shabab. The *N. benthamiana* leaf extracts containing overexpressed rC14 were preincubated with EPIC1 and EPIC2B at different concentrations for 30 minutes, and then incubated with DCG-04 at pH 5 to label the non-inhibited proteases. We studied the strong

interaction between tomato PLCP C14 and EPICs by using long labeling times (3 hours), at relatively high DCG-04 concentrations (300 nM), and low EPIC concentrations (4-65 nM). Under these conditions, weak, reversible interactions will not be detected since DCG-04 reacts irreversibly and would eventually label all proteases.
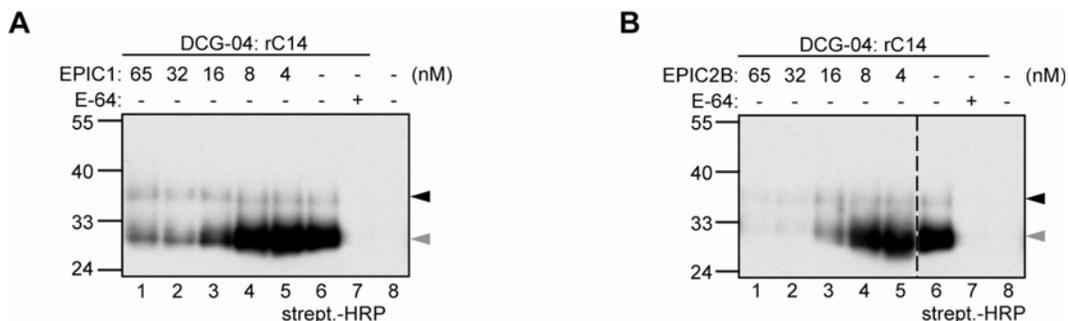
FIGURE 2-4 EPIC1/2B outcompete DCG-04 labeling of recombinant C14.
EPIC1 (*A*) and EPIC2B (*B*) outcompete DCG-04 labeling of rC14 at low nM concentrations. rC14-containing extracts were incubated with different concentrations of EPIC1 (*A*) or EPIC2B (*B*) for 30 minutes at pH 5. DCG-04 was added after preincubation to label the non-inhibited rC14s. Please note that the rC14 labeling is slightly stronger in the presence of 4 nM EPIC1 or EPIC2B, than the no-inhibitor control. Black arrowhead, intermediate rC14. Grey arrowhead, mature rC14.

Competitive ABPP reveals that EPIC1 inhibits mature rC14 at concentrations above 16 nM, but not intermediate rC14 even at 65 nM (Figure 2-4A). Similarly, EPIC2B inhibits mature rC14 potently at concentrations above 16 nM, but it also inhibits intermediate rC14 at concentrations above 32 nM (Figure 2-4B). This indicates that EPIC1 and EPIC2B have similar yet not identical affinity for rC14, and EPIC2B outcompetes DCG-04 labeling of both intermediate and mature rC14 more thoroughly than EPIC1 at concentrations above 32 nM (Figure 2-4 A and B, lane 1 and 2). Interestingly, we observed that at low concentrations (4-8 nM) both EPIC1 and EPIC2B enhance DCG-04 labeling of mature rC14 (Figure 2-4 A and B, lane 4 and 5). This indicates that EPIC1 and EPIC2B activate target PLCPs at low concentrations.

2.2.2.4 Characteristics of EPIC1/2B inhibition of PLCPs in tomato apoplastic fluids

To investigate if the inhibitory effects of EPIC1 and EPIC2B on C14 also occur in secreted proteomes, we preincubated apoplastic fluids isolated from tomato with 65 nM EPIC1 or EPIC2B for 30 minutes, and then labeled with 500 nM DCG-04 at pH 5 for 3 hours. This competitive ABPP demonstrates that EPIC1 prevents biotinylation of iC14, while EPIC2B prevents biotinylation of iC14 and of 30-kDa signals and PIP1 weakly (Figure 2-5A). The selective inhibition of iC14 indicates that, under stringent conditions, these two inhibitors target iC14 and form tight complex that persist over long incubation time.

The competition assays described above were done at 65 nM inhibitor concentrations. To investigate inhibition at lower inhibitor concentrations, tomato AFs were incubated with or without various concentrations of EPIC1 or EPIC2B respectively for 30 minutes, and then incubated with 500 nM DCG-04 at pH 5 for 3 hours. This revealed that EPIC1 inhibits iC14 at the concentration of 65 nM (Figure 2-5B, left panel, lane 2), and EPIC2B inhibits C14 at concentrations above 32 nM (Figure 2-5B, right panel, lane 2 and 3). 65 nM EPIC2B also weakly inhibits 30-kDa mC14-containing signals and the lowest signal which predominantly represents PIP1 (Figure 2-5B, right panel, lane 2). This competitive ABPP demonstrates that EPIC2B is a more potent competitor than EPIC1 to DCG-04 labeling of PLCPs in tomato AFs, which is consistent with their inhibitory characteristics to rC14 (Figure 2-4A and B, and 2-5B).

At last, we tested the EPIC1 and EPIC2B inhibition of iC14 in tomato AFs by competitive ABPP with DCG-04 labeling in the presence of 0.03% SDS, as 0.03% SDS can maximally uncover the activities of iC14 in tomato AFs *in vitro* (Figure 2-3F). Surprisingly, we found that in the presence of 0.03% SDS, EPIC2B can not only inhibit iC14 but also other 30-kDa signals and PIP1 (Figure 2-5C, lane 5), and EPIC1can inhibit all three signals that DCG-04 can profile even stronger (Figure 2-5C). In the presence of 0.03% SDS, both EPIC1 and EPIC2B exhibit broad inhibition of all PLCPs in tomato AFs, and EPIC1 exhibits more potent inhibition of iC14 than EPIC2B in contrast to its inhibition of iC14 in tomato AFs or of rC14 without SDS.

41
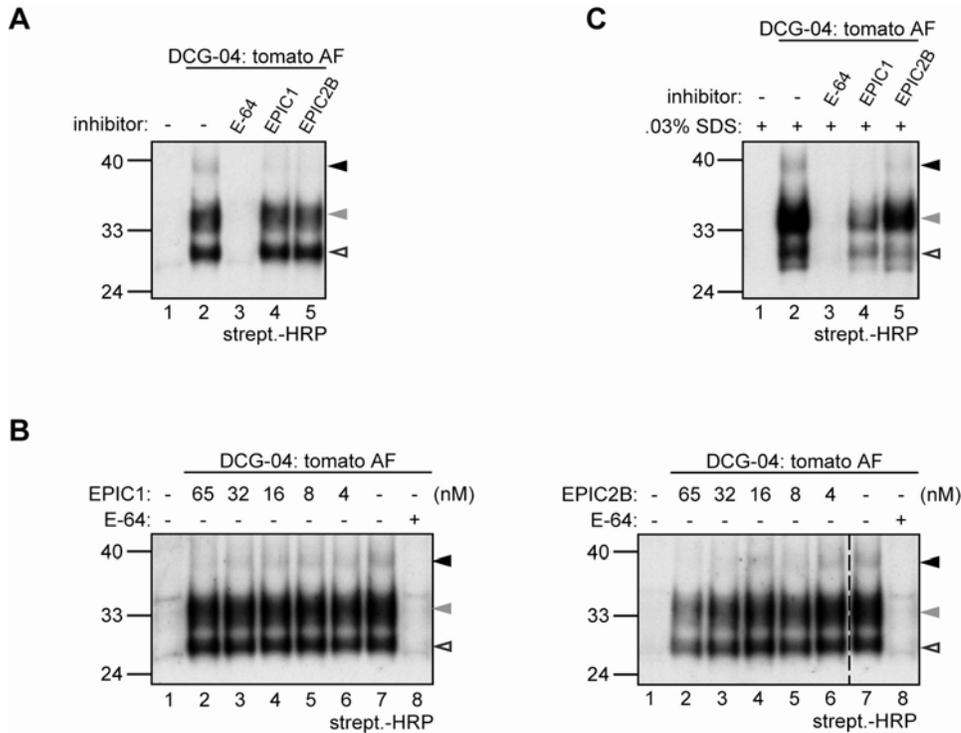
FIGURE 2-5 EPIC1/2B selectively inhibit PLCPs in tomato apoplastic fluids.
A, EPIC1 and EPIC2B outcompete DCG-04 labeling of iC14 in tomato AFs. AFs were preincubated with 65 nM EPIC1, 65 nM EPIC2B or 40 μM E-64 at pH 5 for 30 minutes before adding DCG-04 to label the remaining non-inhibited PLCPs. *B*, EPIC1 (left panel) and EPIC2B (right panel) outcompete DCG-04 labeling of iC14 at low nM concentrations in tomato AFs. AFs were incubated with different concentrations of EPIC1 or EPIC2B at pH 5 for 30 minutes. DCG-04 was added after preincubation to label the non-inhibited PLCPs. *C*, EPIC1 and EPIC2B selectively inhibit PLCPs in tomato AFs in the presence of 0.03% SDS. In the presence of 0.03% SDS, AFs were incubated with EPIC1 or EPIC2B at pH 5 for 30 minutes. DCG-04 was added after preincubation to label the non-inhibited PLCPs. Please note that in the presence of 0.03% SDS, EPIC1 and EPIC2B also outcompete DCG-04 labeling of mC14-containing signals and PIP1. Black arrowhead, iC14. Grey arrowhead, mC14-containing signals. Open arrowhead, PIP1.

2.3   ABPP with vinyl sulfone probe MV151

Plants are able to adapt to changing environments and undergo drastic developmental changes. These processes require effective and selective protein turnover machinery. Turnover of most cytosolic and nuclear proteins is mediated by the ubiquitin/proteasome system (Sullivan *et al.*, 2003). This system is highly conserved in eukaryotes and well studied in yeast. The 26S proteasome is a large multisubunit protease residing in the cytosol and nucleus and consists of a 20S core protease (CP) and a 19S regulatory particle (RP). The RP accepts ubiquitinated substrates, unfolds them and feeds them into the CP (Kurepa and Smalle, 2008).

The CP is structured as a 670-kDa hollow cylinder formed by four stacked rings of seven subunits (Groll *et al.*, 1997). The outer rings consist of seven different α subunits, while the inner rings consist of seven different β subunits, stacked together in the 'αββα' configuration. The proteolytic activity resides in three of the seven β subunits which are located in the inner cavity of the cylinder. Subunit β1 has caspase-like activity (cleaving after acidic residues); β2 has trypsin-like activity (cleaving after basic residues); and β5 has chymotrypsin-like activity (cleaving after hydrophobic residues) (Dick *et al.*, 1998). Together, these subunits degrade the substrate proteins into peptides of 3-20 amino acids that are released into the cytosol or nucleus.

ABPP is a powerful tool to track protease activities in proteomes and living cells, and ABPs based on vinyl sulfone (VS) reactive groups were shown to label the catalytic subunits of the mammalian proteasome (Kessler *et al.*, 2001; Verdoes *et al.*, 2006). To generate new approaches to study plant proteasome functions, we proposed to optimize *in vitro* activity-based profiling to display activities of all three catalytic subunits of the Arabidopsis proteasome using VS-based probes, and develop MV151 as readout of proteasome activities in plants. This would facilitate the identification and selection of subunit-specific inhibitors, and enables the display of activities of the different catalytic subunits during biological processes, by, for example, investigating proteasome activities during defense responses.
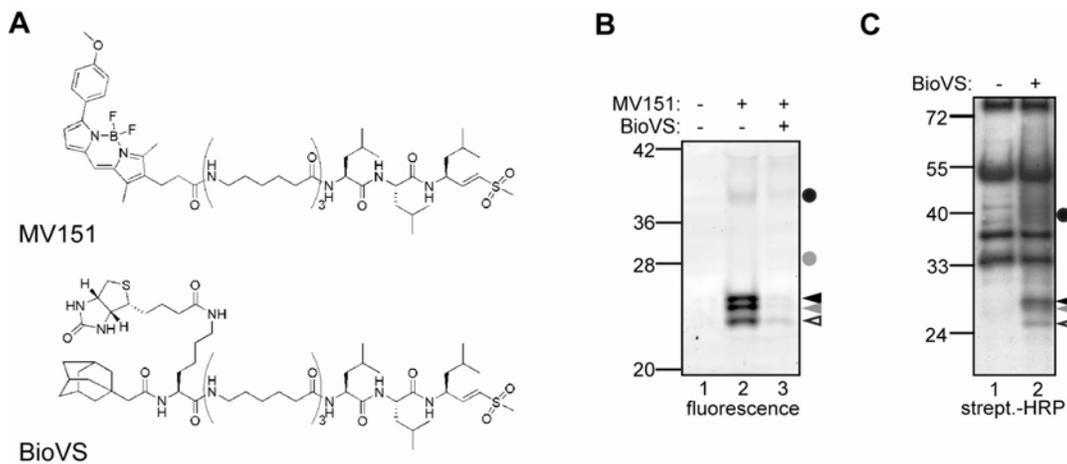
FIGURE 3-1 Labeling by VS probes of Arabidopsis leaf extracts.
A, Molecular structures of the VS probes used in this study. Both probes carry a vinyl sulfone (VS) reactive group; a Leucine tripeptide binding group; and a long linker region. MV151 carries a BODIPY fluorescent reporter tag. BioVS (also called AdaK(Bio)Ahx3L3VS, Kessler *et al.*, 2001) carries a biotin reporter tag and an adamantane to enhance membrane permeability. *B and C*, Labeling profiles of MV151 and BioVS. Arabidopsis leaf extracts were labeled for 3.5 hours with 0.4 µM MV151 or for 2.5 hours with 2 µM BioVS. Labeled proteins were detected on protein gel by fluorescence scanning (*B*) or on protein blot using strept.-conjugated HRP (*C*). Specific signals are indicated with circles and triangles.

2.3.1 Characterization of MV151 labeling

Two activity-based probes were used in this study (Figure 3-1A). Both probes carry a vinyl sulfone (VS) reactive group, a leucine tripeptide binding group, and a long nonnatural peptide linker. The probes differ, however, in the reporter tags. MV151 contains a Bodipy fluorescent group for fluorescent imaging (Verdoes *et al.*, 2006), whereas BioVS (previously called AdaK(Bio)Ahx3L3VS, Kessler *et al.*, 2001) contains a biotin tag for detection and affinity purification.

Labeling of Arabidopsis leaf extracts with 0.4 µM MV151 reveals three strong fluorescent signals at 25-kDa, and two weak signals at 30- and 40-kDa (Figure 3-1B, lane 2, indicated by triangles and dots, respectively). As will be demonstrated later (Figure 3-3A), the strong 25-kDa signals represent the three proteasome catalytic subunits whereas the weak 30- and 40-kDa signals represent PLCPs. All these signals are suppressed by preincubation with 20 µM BioVS, indicating that BioVS competes for the same target proteins as MV151 (Figure 3-1B, lane 3). Labeling of Arabidopsis leaf extracts with 2 µM BioVS also causes three signals at 25-kDa, and a few

additional signals (Figure 3-1C, lane 2). Many of these additional signals are also present in the no-probe-control, indicating that these are caused by endogenous biotinylated proteins (Figure 3-1C, lane 1). We choose to use MV151 labeling for activity profiling for the low background, ease of work and signal quantification.

To characterize labeling at different MV151 concentrations, Arabidopsis leaf extracts were labeled with 0.01-4 μM MV151 and fluorescent signals were quantified and plotted against the concentration. These data show that at low MV151 concentrations there is a preference of labeling of the upper two 25-kDa proteins (β2 and β5 subunits) and that labeling of the lowest signal (β1 subunit) and 40-kDa (RD21A) is saturated at concentrations above 1 μM (Figure 3-2A).

To characterize this labeling further, labeling was followed over different periods, and the fluorescence quantified and plotted in a time-course. This shows that labeling occurs within minutes and that the strong 25-kDa signals label consecutively at increasing MV151 concentrations: first the middle signal (β5), then the upper signal (β2) and finally the lower signal (β1) (Figure 3-2B). Labeling of the 40-kDa signal (RD21A) is slower and saturates after 1 hour (Figure 3-2B). Thus, although the labeling occurs quickly, incubation times of four hours are required to saturate labeling of the β1 subunit.

The above labeling experiments were performed at pH 7.4. Labeling at different pH causes different profiles (Figure 3-2C). At pH 4, there is no labeling of the 25-kDa signals, whereas the signals at 40- and 30-kDa become stronger, and an additional 50-kDa signal appears. At pH 5 there are multiple weak signals in the 25-kDa region. At increasing pH (pH 6-7) some of these signals become stronger and others weaker. Profiles at pH 7-8 are similar with three strong 25-kDa signals. At basic pH (pH 9-11) the 25-kDa signals become weaker, the background increases and a new signal appears at 70-kDa. The 70-kDa signal and the background signals can not be competed with MG132 and E-64 and are therefore considered to be nonspecific (data not shown). The 40-kDa signals (RD21A) have a constant intensity at neutral and basic pH and are increasingly intense at low pH. These experiments show that MV151 labeling profiles strongly depend on pH and that the 25-kDa proteasome-derived signals are strongest at pH 7.5.
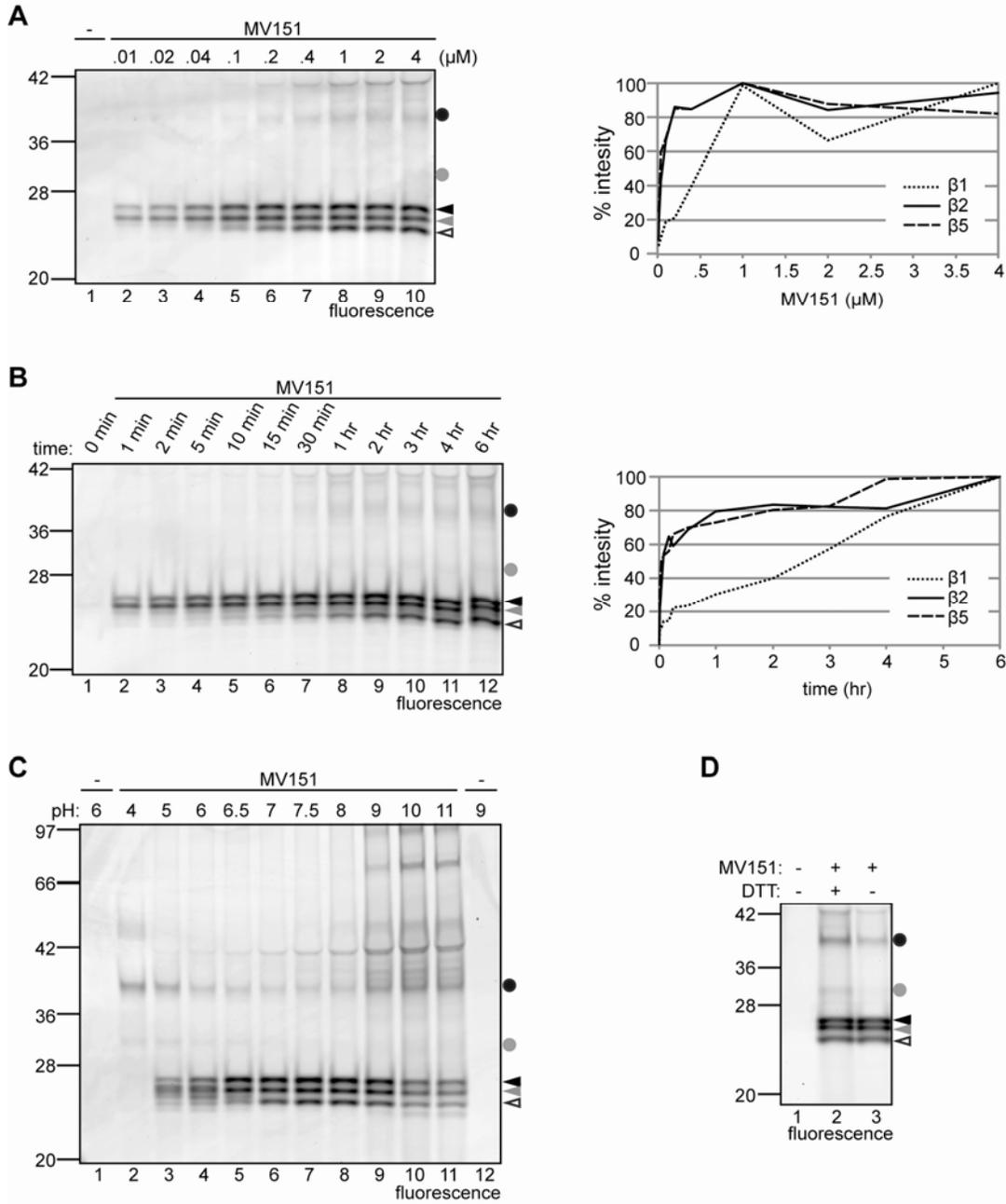
FIGURE 3-2 Characteristics of MV151 labeling.
A, Concentration dependency of MV151 labeling. Arabidopsis leaf extracts were labeled for three hours with different concentrations of MV151 (left panel). Signals were quantified and plotted in a graph (right panel). *B*, Time course of MV151 labeling. Arabidopsis leaf extracts were labeled with 0.4 μM MV151 for different time points (left panel). Signals were quantified and plotted in a time course graph (right panel). *C*, pH dependency of MV151 labeling. Arabidopsis leaf extracts were labeled for 2 hr with 0.4 μM MV151 at different pH. *D*, Reducing agent DTT increases labeling of some proteins. Arabidopsis leaf extracts were labeled for 4 hr with 0.4 μM MV151 in the absence or presence of 1 mM dithiothreitol (DTT). The upper two signals (dots) are increased by adding DTT, whereas the others (triangles) are not.

To optimize labeling further we added a series of putative cofactors like ATP, NAD, magnesium and calcium ions and reducing agents during labeling. These cofactors had no effect on the labeling profile (data not shown), except for the reducing agent DTT. Adding 1 mM DTT enhances labeling of the 30- and 40-kDa signals but does not alter the intensities of the 25-kDa signals (Figure 3-2D). This is consistent with the notion that activities of PLCPs can be induced with reducing agents.

2.3.2 Identification and confirmation of the probe targets

To identify the labeled proteins, Arabidopsis leaf extracts were treated with BioVS. The resulting biotinylated proteins were purified on streptavidin beads and detected on a coomassie-stained gel. Three signals at 25-kDa coincided with the three biotinylated signals detected by protein blotting (Figure 3-3A). These protein bands were excised, digested with trypsin, and subjected to tandem mass spectrometry. The MS data revealed that the upper signal represents the β2 catalytic subunit of the proteasome (PBB1, At3g27430), the middle signal represents subunit β5 (PBE1, At1g13060), and the lower signal subunit β1 (PBA1, At4g31300) (Figure 3-3B). There were no specific peptides identified from PBB2 and PBE2 in this analysis, but PBB2 has been detected from the upper 25-kDa signal in a repetition experiment (data not shown). The identified peptides are all from the mature subunits and not from the prodomain, which is autocatalytically removed before the proteasome assembly (Heinemeyer *et al.*, 1997). None of the peptides carries the catalytic Threonine which resides at the N-terminus of the mature protein. Labeling of this residue by BioVS probably makes the N-terminal peptide too large to be detected by MS. MS analyses were performed by Tom Colby at Proteomics Service Center of MPIZ in Cologne, Germany.

To independently demonstrate that PBA1 is amongst the purified biotinylated proteins, we took advantage of an antibody that has been raised against PBA1 (Yang *et al.*, 2004). Probing the purified BioVS-labeled proteins with this PBA1 antibody revealed a single strong signal at 23-kDa, demonstrating that the lowest of the three signals is indeed PBA1 (Figure 3-3A). Furthermore, western blot analysis of MV151-labeled proteomes with PBA1 antibody revealed a second signal at a slightly higher molecular weight, consistent with being MV151-labeled PBA1 (Figure 3-3C).

47
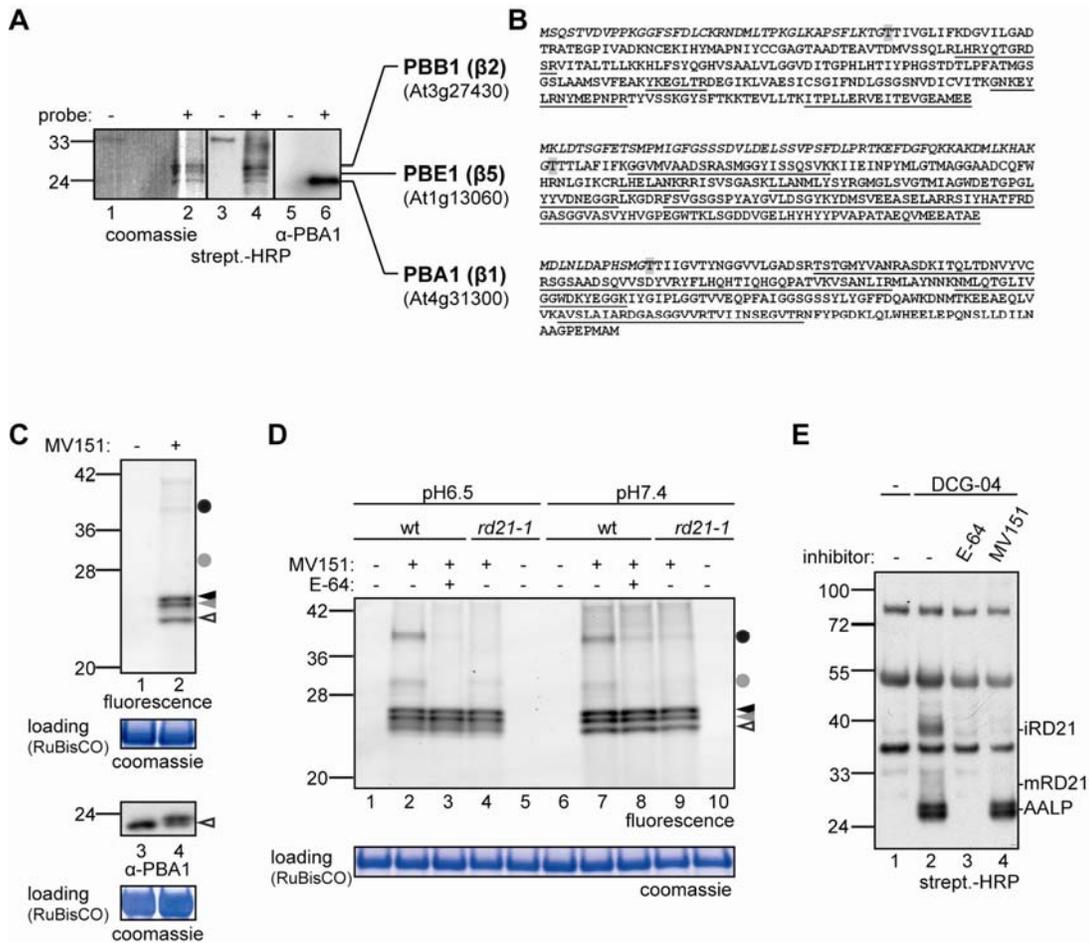
FIGURE 3-3 Identification and confirmation of the MV151 labeled proteins.
A, The three 25-kDa signals represent the three catalytic β-subunits of the proteasome. Arabidopsis leaf extract was labeled with BioVS and biotinylated proteins were purified, separated on protein gel, and stained with coomassie (left panel). Proteins from the three bands were digested by trypsin and analyzed by MS/MS. Proteins were identified as PBB1, PBE1 and PBA1, respectively. The identity of PBA1 is confirmed with a PBA1 antibody (right panel). *B*, Sequences of the three catalytic subunits with the identified peptides. Italics, prodomain; grey, boxed T, catalytic Threonine; underlined, identified peptides. *C*, Labeling by MV151 causes a shift in gel migration of PBA1. Leaf extracts were labeled with 0.4 μM MV151 and proteins were detected by fluorescent scanning and PBA1 antibody. *D*, The 40-kDa signal is absent in the *rd21A-1* knockout line. Arabidopsis leaf extracts from wild-type (wt) and *rd21A-1* mutant plants were preincubated with or without 40 μM E-64 and labeled for 4.5 hours with 0.4 μM MV151 at pH 6.5 and pH 7.4. *E*, MV151 prevents labeling of RD21A by DCG-04. Arabidopsis leaf extracts were preincubated with 40 μM MV151 and labeled with 2 μM 24 DCG-04. Labeling of intermediate (i) RD21A is prevented by preincubation with MV151, whereas labeling of Arabidopsis aleurain-like protein (AALP) is not.

Analysis of proteins at the 30- and 40-kDa regions revealed peptides of PLCP RD21A (data not shown). The identification of PLCPs is consistent with our previous study when identifying *in vivo* targets of MVA178, which is an azide-labeled version of MV151 (Kaschani *et al.*, 2009a). *In vivo* labeling with MVA178 causes strong labeling at 30- and 40-kDa. Purification of these labeled proteins using click-chemistry revealed that the 40-kDa signal contains RD21A (At1g47128), whereas the 30-kDa signals contain RD21A, RD19A (At4g39090) and RD21C (At4g16190). Consistent with the observation that PLCP labeling *in vivo* is stronger than *in vitro* (Kaschani *et al.*, 2009a), the signals detected with MV151 are weak, but probably caused by labeling the same PLCPs.

To confirm that PLCPs are causing the 30- and 40-kDa signals in the MV151 labeling profile, we preincubated leaf extracts with and without E-64, which were then labeled with MV151 at pH 6.5 and 7.4. Preincubation with PLCP inhibitor E-64 prevented labeling at 30- and 40-kDa, and had no effect on labeling of the signals at 25-kDa (Figure 3-3D). To demonstrate that RD21A causes the signal at 40-kDa, we labeled extracts of leaves of the rd21A-1 knockout line (Wang *et al.*, 2008). The 40-kDa signal in extracts of rd21A-1 knockout line is missing, confirming that this signal is caused by RD21A (Figure 3-3D). The signal at 30-kDa is reduced in the rd21A-1 knockout line. This is consistent with the fact that RD21A exists as 30- and 40-kDa isoforms which are both active (Yamada *et al.*, 2001; Van der Hoorn *et al.*, 2004). The remaining 30-kDa signals in the MV151 labeling profile of rd21A-1 lines are probably caused by RD19A or RD19C, or other PLCPs, since these PLCPs were found in this region during *in vivo* labeling with VS-based probes (Kaschani *et al.*, 2009a).

To confirm that MV151 targets PLCPs, we preincubated leaf extracts with 40 μM MV151 and then labeled with 2 μM DCG-04, a biotinylated derivative of E-64 which labels PLCPs (Greenbaum *et al.*, 2000). Labeling with DCG-04 on Arabidopsis leaf extracts results in a typical activity-based profile containing intermediate (i) RD21A at 40-kDa, a mixture of various PLCPs at 30-kDa, and Arabidopsis aleurain-like protease (AALP) at 25-kDa (Van der Hoorn *et al.*, 2004). Preincubation with E-64 prevents labeling of all these signals (Figure 3-3E, lane 3). Interestingly, preincubation with MV151 prevents labeling of the 40- and 30-kDa signals but not of

the 25-kDa AALP signal (Figure 3-3E, lane 4), indicating that MV151 labels many PLCPs but not all.

2.3.3 Proteasome inhibitors

We next tested if MV151 labeling can be used to identify subunit-specific inhibitors. MG132 (zLLLcho) is a tri-leucine aldehyde and a frequently used proteasome inhibitor in plant science. Preincubation of leaf extracts with MG132, followed by labeling with MV151 demonstrates that MG132 blocks MV151 labeling of β1 and β5 subunits and suppresses labeling of the β2 subunit (Figure 3-4A, lane 4). Importantly, MG132 also prevents labeling of the 40-kDa RD21A. Preincubation with PLCP inhibitor E-64 prevents MV151 labeling of the 40-kDa RD21A signal, but not the proteasome-derived signals (Figure 3-4A, lane 3), consistent with the presumed high selectivity of E-64 (Powers *et al.*, 2002).

The availability of many commercial peptide aldehyde-based inhibitors and the observation that MG132 only partially inhibits β2 subunit, prompted us to test other peptide aldehydes for selective inhibition of the proteasome. These inhibitors all carry a C-terminal aldehyde but differ in the residues of the peptide. Many of these peptide aldehyde-based inhibitors are designed to inhibit caspases, which are selective for aspartate (D) at the P1 position of the inhibitor. Preincubation with these inhibitors was followed by MV151 labeling to reveal the remaining activities (Figure 3-4A, top). The signals were quantified and plotted in a heat map (Figure 3-4A, bottom).

Interestingly, many of these caspase inhibitors prevent MV151 labeling of the β1 subunit, which is consistent with the caspase-like activity of this subunit (Figure 3-4A). Labeling of the β1 subunit can also be blocked by AcLLMcho (Figure 3-4A, lane 12), which carries a methionine (M) at the P1 position. Furthermore, IEPDcho is not effective in inhibition of β1, but IETDcho is, indicating that the proline (P) at the P2 position prevents inhibition of the β1 subunit. Labeling of the β2 subunit can be prevented by leupeptin (AcLLRcho), which is a frequently used PLCP inhibitor (Figure 3-4A, lane 6), and originally described as a proteasome inhibitor (Wilk and Orlowski, 1980). The fact that leupeptin can suppress labeling of the β2 subunit is consistent with the presumed trypsin-like activity (cleaving after basic residues) of the

β2 subunit, since leupeptin carries an arginine (R) at the P1 position. Labeling of the β5 subunit can only be inhibited with MG132 and MG115 (zLLNvacho) (Figure 3-4A, lanes 4 and 5). This is consistent with the presumed chymotrypsin-like activity (cleaving after hydrophobic residues) of the β5, since both inhibitors carry a leucine at the P1 position. Finally, labeling of the 40-kDa RD21A signal can be prevented by E-64, MG132, MG115, leupeptin and LLMcho, but not by caspase inhibitors (Figure 3-4A, lanes 3-13). This is consistent with the fact that PLCPs like RD21A are selective for substrates having hydrophobic residues at the P2 position.
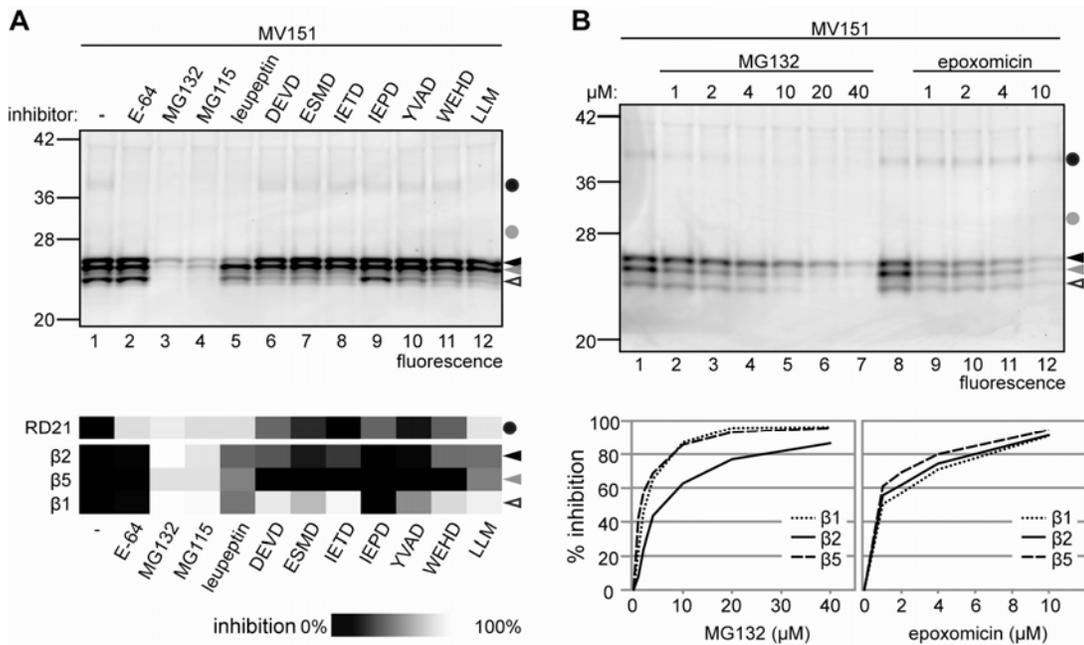
FIGURE 3-4 Selective inhibition of proteasome catalytic subunits.
A, Inhibition of MV151 labeling. Arabidopsis leaf extract was preincubated with various inhibitors (50 μM) and then labeled with MV151 (0.5 μM). Fluorescent signals indicate the absence of inhibition. Signals were quantified, normalized to the DMSO control (lane 1), and plotted in a heat map (bottom) indicating the remaining activities (black). *B*, Concentration dependency of inhibition. Arabidopsis leaf extracts were preincubated at different concentrations of MG132 and epoxomicin and then labeled for 2 hours with 0.4 μM MV151. Proteasome-derived signals were quantified and plotted against the inhibitor concentration in dose-response graphs (bottom).

A dilution series of MG132 confirms that MG132 preferentially inhibits β5 and β1 (Figure 3-4B, lanes 2-7). Epoxomicin carries an epoxy ketone reactive group and is a selective inhibitor of the proteasome (Meng *et al.*, 1999). Preincubation with epoxomicin indeed prevents MV151 labeling of all three subunits, but not of 40-kDa RD21A (Figure 3-4B, lane 10). Quantification of the signals from an epoxomicin dilution series indicates that epoxomicin inhibits β1, β2, and β5 with similar affinities (Figure 3-4B, lanes 8-12).

2.3.4 MV151 profiling of other Arabidopsis organs and leaves of other plant species

To expand the use of MV151 profiling, we tested labeling of other Arabidopsis organs. Labeling of seed, stem and root extracts revealed similar profiles as those from leaf extracts, but the relative intensities differ (Figure 3-5A, lanes 2, 6 and 10). Signals at 30- and 40-kDa were only observed in stem and root. These signals are caused by PLCPs, since they are absent after preincubation with PLCP inhibitor E-64 (Figure 3-5A, lanes 4, 8 and 12). The three signals at 25-kDa differ in overall intensity between the organs and the lowest signal is usually the weakest. These signals probably represent proteasome catalytic subunits since labeling can be suppressed by MG132 but not by E-64 (Figure 3-5A, lanes 3, 4, 7, 8, 11 and 12). The differences in intensities of the proteasome signals in different tissues can be caused by differences in proteasome concentrations and differences between the content of the extracts and are subject to optimization of labeling conditions.

To test if MV151 profiling can also be used in other plant species we labeled leaf extracts of tomato (*Solanum lycopersicum*), bean (*Vicia faba*) and barley (*Hordeum vulgare*) with MV151. The resulting labeling profiles are different, but share similarities (Figure 3-5B). PLCPs can be distinguished, since these signals can be competed by preincubation with E-64 and MG132. PLCPs are labeled in tomato at 35-kDa, in bean at 30-, 27- and 40-kDa, and in barley at 40- and 32-kDa. These data are consistent with the different DCG-04-labeling profiles of different plant species (Van der Hoorn *et al.*, 2004). The stronger signals are probably caused by proteasome labeling since this can only be competed by MG132. In tomato extracts there is a strong signal at 25-kDa and a weak signal just below, in bean a strong signal at 25-

kDa, a medium intense signal at 23-kDa and a very weak signal in between, and in barley, three equally intense signals at 23-, 24- and 25-kDa. Some of these signals might be a combined signal from two proteasome subunits. These data indicate that there are slight size differences in the catalytic subunits of the proteasome between different plant species. Thus, although the profiles are different between different plant species, all display strong proteasome derived signals in the 25-kDa region and several weaker PLCP-derived signals at 30-40-kDa.
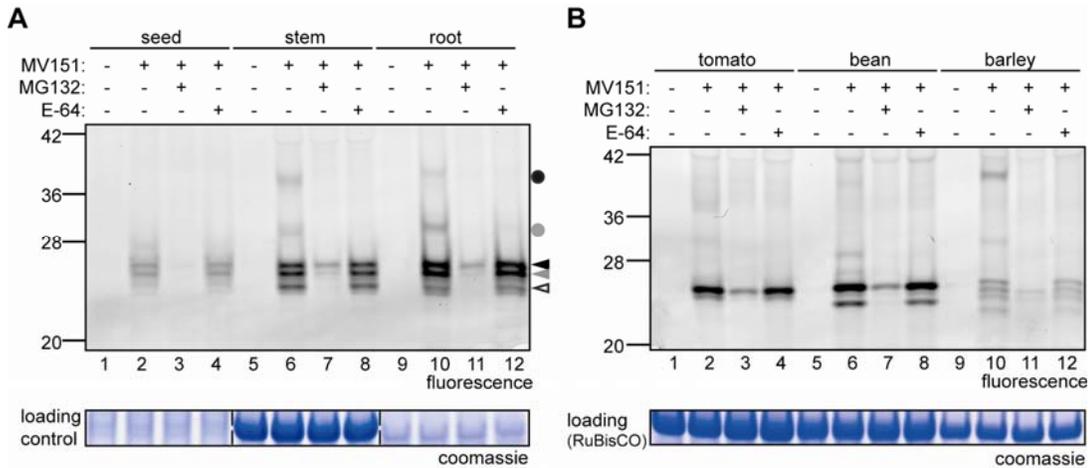
FIGURE 3-5 MV151 labeling of other tissues and other plant species.
Extracts from Arabidopsis seed, stem and root (**A**) and from leaves of tomato, bean and barley (**B**) were preincubated with and without 40 μM MG132 or E-64, and then labeled for 3 hours with 0.4 μM MV151.

2.3.5 Proteasome activity is induced during defense

To investigate if proteasome activities change during defense, we sprayed Arabidopsis plants with and without benzothiadiazole (BTH), which induces the salicylic acid (SA) signaling pathway, resulting in a defense response (Kohler *et al.*, 2002). Extracts from H_2O- and BTH-treated plants were subjected to MV151 profiling. Interestingly, BTH-treatment results in increased activity of proteasome. This upregulation occurs at one day after BTH treatment and remains for at least five days (Figure 3-6A).

Although the upregulation is moderate, it occurs consistently in independent leaves and in different biological replicates (Figure 3-6B). Quantification showed a 1.46 ± 0.17 (n=7) -fold upregulation of the 25 kDa signals, and is statistically significant (Students *t*-test: P = 0.000013). Western blot analysis show equal levels of PBA1, indicating that the proteasome levels are equal between water and BTH treated plants and that the activity is post-translationally upregulated (Figure 3-6C).

To show that the elevated proteasome activity in BTH-treated plants depends on the SA signaling pathway, we investigated BTH-induced proteasome activities in Arabidopsis SA signaling mutant *npr1*. When *npr1* mutant plants were treated with BTH, proteasome activities were elevated in wild-type, but not in *npr1* lines (Figure 3-6D). These data show that the proteasome activity is not directly induced by BTH, but requires NPR1 function, indicating that elevated proteasome activities are a response to the SA signaling pathway.

To investigate in which cellular compartment the increased proteasome activity resides upon BTH-treatment, we fractionated extracts from H_2O and BTH-treated plants in a nuclear-depleted (ND) and nuclear-enriched (NE) fraction and subjected those to MV151 profiling. Subcellular markers, phosphoenolpyruvate carboxylase (PEPC) for the cytoplasm and histone H3 for the nucleus (Noel *et al.*, 2007; Cheng *et al.*, 2009), confirmed that the fractions were not cross-contaminated (Figure 3-6E). The increased PEPC level upon BTH-treatment is consistent with the BTH-inducibility of this gene (www.genevestigator.com; Zimmerman *et al.*, 2004; Von Rad *et al.*, 2005). Labeling of the proteasome in the nuclear-enriched fractions did not occur, presumably because the high DNA concentration causes a low pH and improper labeling conditions. However, the nuclear-depleted fraction, containing over 90% of the proteasomes, shows an elevated labeling upon BTH-treatment (Figure 3-6E), demonstrating that BTH-induced activity occurs in the cytoplasm.
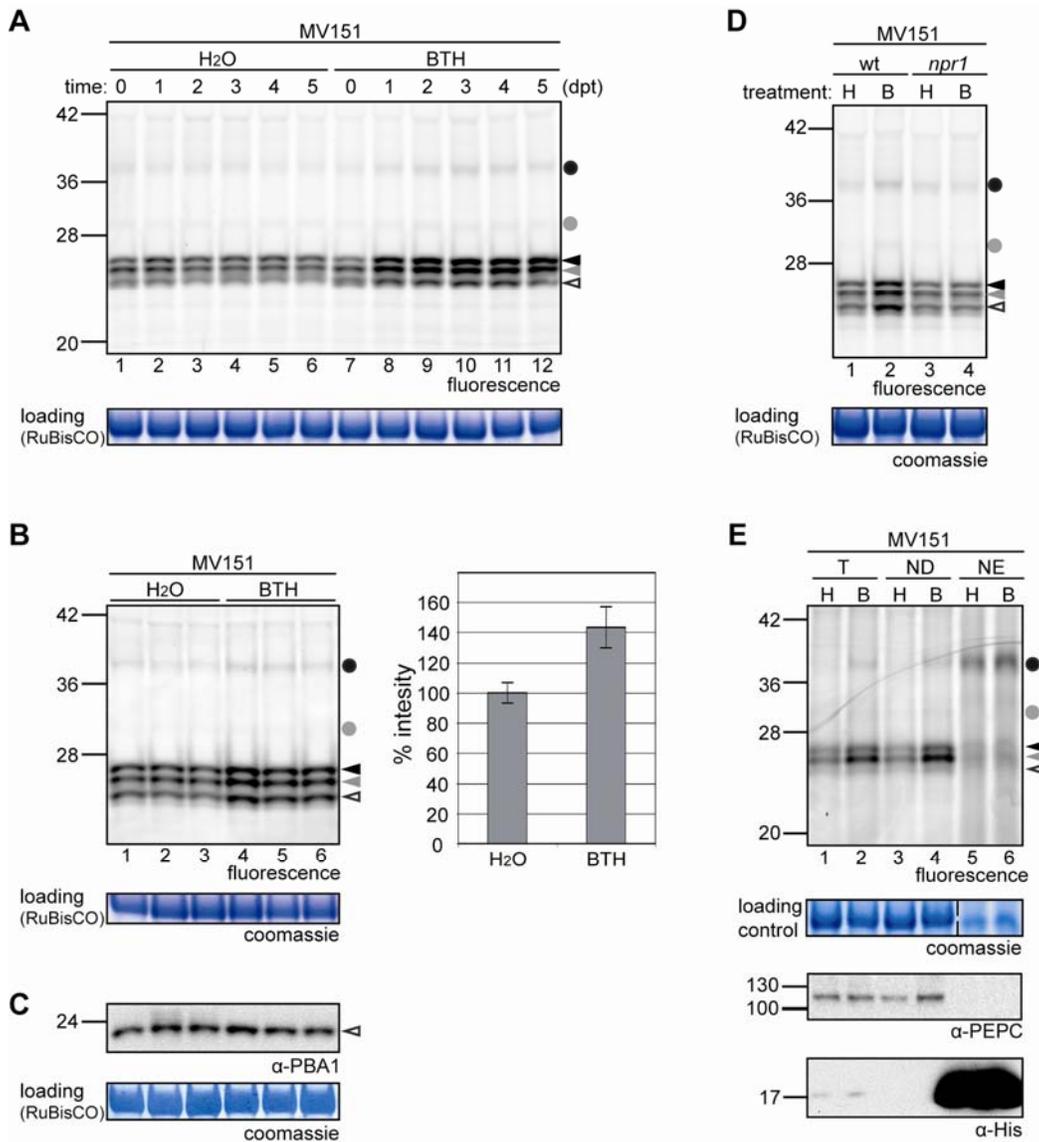
FIGURE 3-6 Upregulated proteasome activities in BTH-treated plants.
A, Increased proteasome activity upon BTH treatment. Arabidopsis plants were sprayed with H_2O or benzothiadiazole (BTH). Leaf proteins were extracted and equal quantities were labeled with MV151 at different days post treatment (dpt). *B*, Reproducibility of BTH-induced proteasome activities. Three different pots with each four plants were sprayed with H_2O or BTH. Extracts of four leaves of each pot were labeled with MV151. Shown is a representative of three biological replicates (left panel). Signals were quantified and plotted in a graph (right panel). *C*, Proteasome activation occurs post-translationally. Extracts from *B* were detected with anti-PBA1 antibody. *D*, BTH-induced proteasome activity is NPR1 dependent. Wild-type and *npr1* mutant plants were treated with H_2O (H) or BTH (B) and leaf extracts were labeled with MV151. *E*, Proteasome activation occurs in the cytoplasm. Total cell extracts (T) from H_2O (H) and BTH (B) treated plants were separated into nuclear depleted (ND) and nuclear enriched (NE) fractions, and labeled with MV151. Anti-phosphoenolpyruvate carboxylase (α-PEPC) and anti-histone H3 (α-His) are markers for cytoplasmic and nuclear proteins, respectively.

2.4   Labeling of β-lactone probe IS4

The genome of the model plant *Arabidopsis thaliana* encodes ~320 putative serine and ~140 putative cysteine proteases, including large families of ~60 subtilase-like proteases, ~60 serine carboxypeptidase-like proteins and ~30 papain-like cysteine proteases (PLCPs) (Beers *et al.*, 2004). Some of these proteases have key regulatory roles in defense and development, but the roles, substrates and activation mechanisms of most of these enzymes are unknown (Van der Hoorn, 2008).

ABPP is a powerful tool to track protease activities in proteomes and living cells, and ABPs for serine and cysteine have been generated for PLCPs, caspases, legumains, gingipains, deubiquitinating and desumoylating enzymes, granzymes and other serine proteases in animal research (reviewed in the Introduction chapter). However, to date the applications of ABPP are still limited in plant fields (reviewed in the Introduction chapter).

To expand the range of serine and cysteine proteases that can be monitored by activity-based protein profiling (ABPP) in plants, we designed a new series of ABPs containing a β-lactone reactive group. This reactive group is found in covalent inhibitors of lipases, cysteine proteases and the proteasome (Dick *et al.*, 1997; Lall *et al.*, 1999; Drahl *et al.*, 2005). The recent use of β-lactone reactive groups in ABPs resulted in probes that label various enzyme classes in bacterial proteomes, including proteases (Böttcher and Sieber, 2008). This labeling, however, requires side chains on the β-lactone that probably confer binding affinity for various enzymes. To target β-lactone probes to serine and cysteine proteases, we added a peptide backbone with a variant amino acid. We then tested the labeling of Arabidopsis leaf extracts with these non-directed β-lactone probes.

2.4.1   Labeling leaf proteomes with β-lactone probes

To design a new class of ABPs for serine and cysteine proteases, we used a threonine-based β-lactone linked to a variant amino acid, an amide linker and biotin ("IS" probes, Figure 4-1A). The IS probe collection consists of six probes (IS#; 2, 3, 4, 5, 8

56

and 9) with various amino acid residues representing hydrophilic, aromatic or aliphatic side chains (Figure 4-1A). For all of the probes except IS9, nonbiotinylated derivatives (IS#-n; 2, 3, 4, 5 and 8) were synthesized to serve as competitors of IS labeling (Figure 4-1A). Probe syntheses were conducted by in-group organic chemists Zheming Wang and Rengarajan Balamurugan at Chemical Genomics Center in Dortmund, Germany.
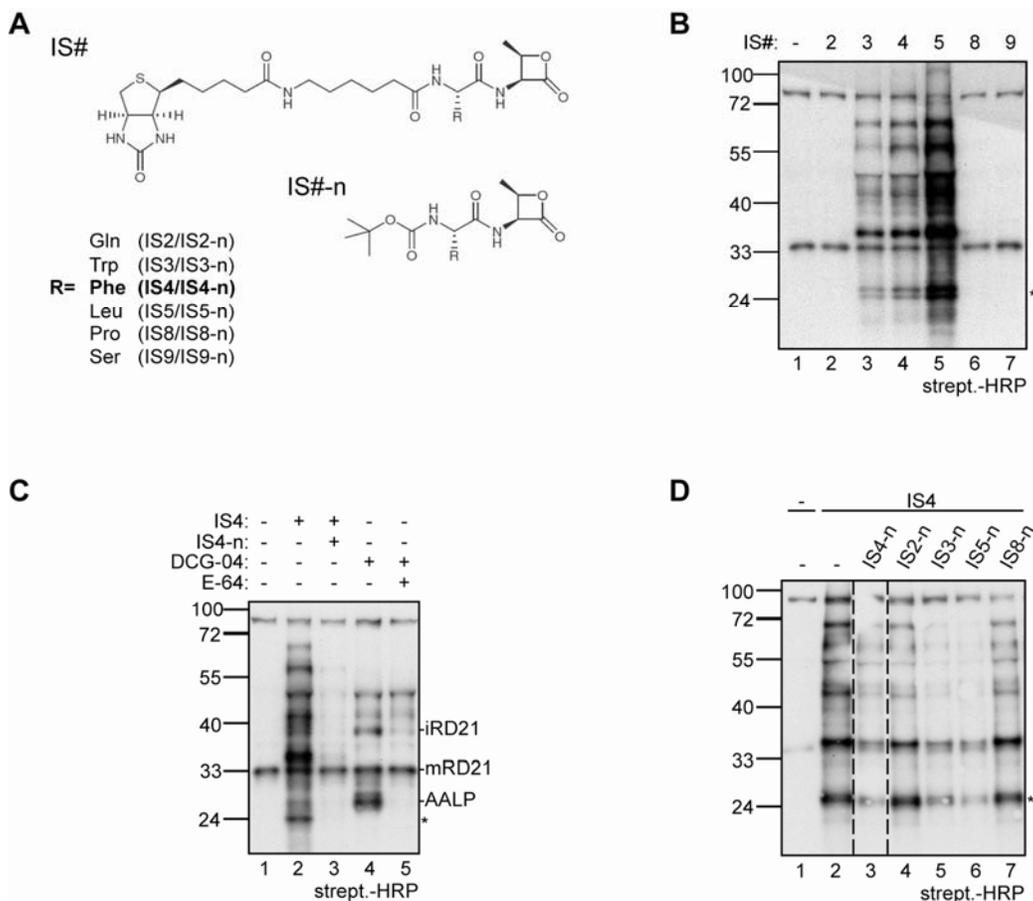
FIGURE 4-1 β-lactone probes and their labeling of leaf extracts.
A, Structures of β-lactone probes. Biotinylated (IS#) and nonbiotinylated (IS#-n) β-lactone derivatives were synthesized with various amino acid residues (R) next to the threonine-based β-lactone moiety. *B*, Labeling with IS probes yielded similar profiles with various intensities. IS probes (2 μM) were incubated with Arabidopsis leaf extracts, and biotinylated proteins were detected on protein blots using streptavidin-HRP. *C*, Labeling with IS4 and DCG-04 is specific and distinct. Arabidopsis leaf extracts were incubated for 2 h with 2 μM DCG-04 or IS4 in the absence or presence of nonbiotinylated 200 μM E-64 or 60 μM IS4-n, respectively. DCG-04 labeled AALP and the intermediate (i) and mature (m) isoforms of RD21. *D*, Inhibition of IS4 labeling by IS#-n. Arabidopsis leaf extracts were preincubated with 30 μM IS#-n for 30 min, and 2 μM IS4 was added and incubated for 1 hour. Dashed lines indicate lanes that were left out from the blot. *, Hallmark band.

We first incubated Arabidopsis leaf extracts with the IS probes and detected biotinylated proteins on protein blots probed with streptavidin–horseradish peroxidase (HRP). IS3, IS4 and IS5 had similar labeling profiles, with strong signals at 23- and 36-kDa (Figure 4-1B). In contrast, IS2, IS8 and IS9 did not cause any labeling compared to the no-probe control (Figure 4-1B). Thus, IS probes with glutamine, proline and serine do not label, whereas IS probes with hydrophobic residues tryptophan, phenylalanine and especially leucine have similar labeling profiles with multiple signals.

IS4 labeling was further investigated, as it was synthesized in the largest quantity. Because IS probes potentially target serine and cysteine proteases, we compared IS4 labeling to that of DCG-04, which labels PLCPs (Greenbaum *et al.*, 2000). DCG-04 labels six PLCPs in Arabidopsis leaf extracts, including AALP and intermediate and mature isoforms of RD21 (Van der Hoorn *et al.*, 2004). The RD21 intermediate isoform carries an additional C-terminal granulin domain of unknown function that is proteolytically removed during maturation (Yamada *et al.*, 2001). As shown previously, the DCG-04 activity profile contains signals from the 40-kDa RD21 intermediate isoform, 30-kDa RD21 mature isoform and 25-kDa AALP, all of which were competed by adding an excess of E-64 during labeling (Figure 4-1C). The remaining 30-kDa and 80-kDa signals are background signals, as these were also present in the no-probe control. IS4 labeling was of strong intensity compared to the DCG-04 activity profile, and its profile was different, indicating that IS4 does not label the same set of PLCPs (Figure 4-1C). The presence of an excess of nonbiotinylated IS4-n during IS4 labeling outcompeted the biotinylation, indicating that the labeling is specific (Figure 4-1C). IS4 labeling was also competed by IS3-n and IS5-n, but not by IS2-n or IS8-n (Figure 4-1D). These observations are consistent with the labeling of the biotinylated IS series, indicating that the same set of proteins is labeled with IS3, IS4 and IS5.

Further characterization of IS4 labeling revealed that it occurs mainly at pH 7-9, with an optimum pH of 8 (Figure 4-2A) and requires the presence of a reducing agent (Figure 4-2B).
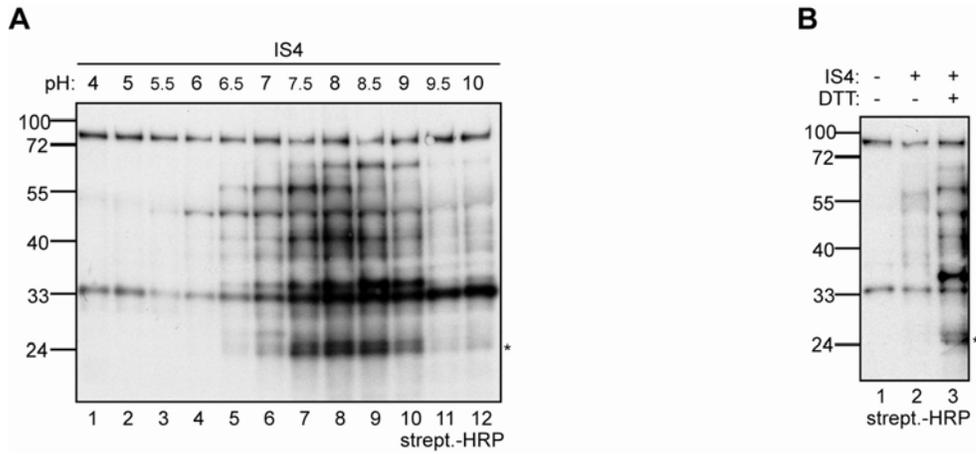
FIGURE 4-2 Labeling with IS4 depends on pH and reducing agent.
Arabidopsis leaf extracts were labeled with IS4 at different pH (*A*) or with or without 1 mM DTT (*B*). *, Hallmark band.

2.4.2 IS4 labels PsbP at the N-terminus

In all labeling experiments, there were consistent strong signals at 36- and 23-kDa. The 23-kDa protein was identified through large-scale affinity capture on streptavidin magnetic beads (Figure 4-3A) and tandem MS. The other biotinylated proteins could not be captured efficiently on streptavidin beads. MS data (explained in detail below) indisputably showed that the 23-kDa protein represents protein P of the oxygen-evolving complex of photosystem II (PsbP) (Yi *et al.*, 2007). The identity was confirmed by showing that purified, biotinylated proteins cross-react with PsbP-specific antiserum (Figure 4-3A).

PsbP has a mature size of 23-kDa and is abundant in leaf extracts (Yi *et al.*, 2007). The labeling of PsbP by IS4 is notable, as PsbP is not a serine or cysteine protease, and no nucleophilic serine or cysteine residues have been reported for this protein. To identify the labeling site, we examined the MS spectra in detail. Comparison of the spectra of the IS4-labeled sample and the no-probe control revealed a series of peptides specific for the IS4-labeled sample (Figure 4-3B, top). Most of these peptides matched the predicted tryptic PsbP peptides, covering 65% of the mature protein (Figure 4-3B, bottom). The fact that these peptides were found with the predicted,

59

unmodified masses indicates that IS4 was not attached to these regions of PsbP. Among the 'missing' peptides of PsbP was the N-terminal peptide, which should have a mass of 1,351.70 Da. Notably, the spectrum of the IS4-specific sample contained an additional mass of 1,938.99 Da (Figure 4-3B, top inset), which fits the sum of the masses of the N-terminal peptide and the predicted mass of IS4 (Figure 4-3B, bottom). The second additional mass at 1,954.99 Da from the IS4-specific sample is the oxidized version of this labeled N-terminal peptide.

To determine the site of IS4 labeling within the N-terminal peptide, we investigated the peptide fragmentation data of the labeled N-terminal peptide. The N-terminal peptide has the sequence AYGEAANVFGKPK. The MS/MS data contained a long series of y ions with the predicted masses, indicating that IS4 is not attached to any of the C-terminal peptide series, up to GEAANVFGKPK (Figure 4-3C, y3-11). In contrast, masses for N-terminal peptide fragments up through AYGE were found as b ions in the MS/MS spectrum, but only if the mass of IS4 was added (Figure 4-3C, b4-7). The presence of the b4 ion indicates that IS4 is attached to the N-terminal alanine. The MS/MS spectrum also contained the mass of IS4 itself (b3), indicating that the linkage between IS4 and alanine is likely to be an amide bond, as these bonds break during post source fragmentation (Figure 4-3C, b3). The b2 and b1 ions indicate that IS4 loses masses corresponding to a threonine and phenylalanine, respectively, indicating that the peptide bonds in IS4 are preserved and no other modifications occurred (Figure 4-3C, b2 and b1). Taken together, these data indicate that IS4 is attached to the N-terminus of PsbP through a peptide bond between a C-terminal threonine of the probe to the N-terminal alanine of PsbP (Figure 4-3D). MS analyses were performed by Tom Colby at Proteomics Service Center of MPIZ in Cologne, Germany.

To investigate whether other proteins are labeled by IS4 at primary amino groups, we treated the leaf proteome with sulfo-N-hydroxysuccinimide acetate (sulfo-NHS-Ac). Sulfo-NHS-Ac reacts with deprotonated primary amino groups of N-termini above pH 7 and lysines above pH 9. Pretreatment of the leaf proteome with sulfo-NHS-Ac in PBS buffer (pH 7.5) suppressed labeling by IS4 globally (Figure 4-3E), indicating that IS4 is linked to N-termini of labeled proteins.
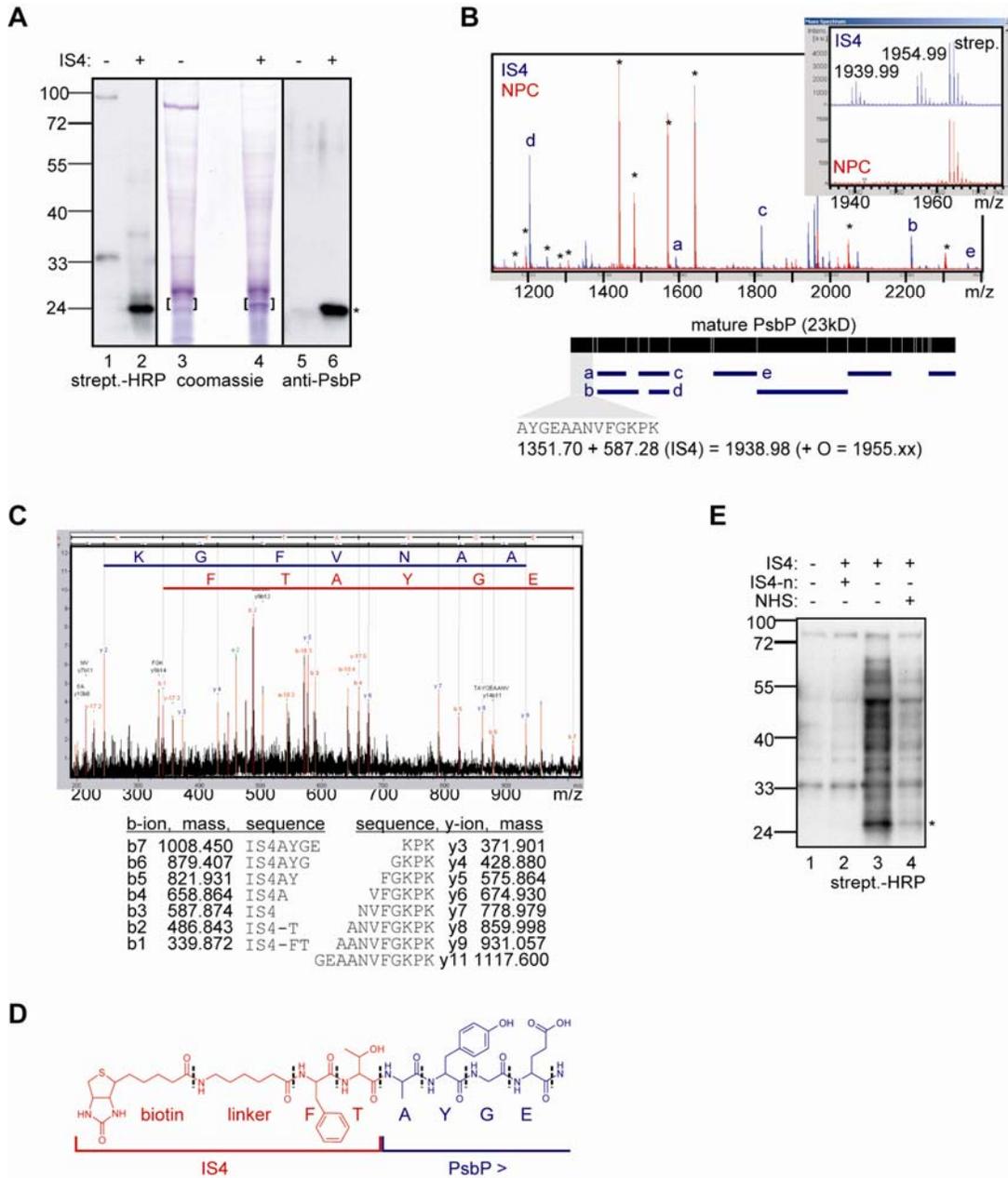
60

A, Purification of IS4-labeled proteins from Arabidopsis leaf extracts. Arabidopsis leave extracts were labeled with and without IS4 and biotinylated proteins were captured and purified on magnetic streptavidin beads. Proteins eluted from these beads were analyzed on protein blot, probed with streptavidin-HRP (left), and on coomassie-stained protein gel (middle). The differential protein band at 23-kDa was isolated (brackets), analyzed by tandem mass spectrometry and confirmed as being PsbP using specific PsbP antisera on the purified proteins (right). The additional protein on the coomassie gel is streptavidin that leaked from the beads. **B**, Peptide-mass fingerprint (PMF) of the 23-kDa protein band. Proteins isolated from the 23-kDa region of the IS4-labeled proteins (blue) and no-probe control (NPC; red) were analyzed by MS. Only part of

the PMF is shown. Peptides from bovine serum albumin (*), streptavidin and trypsin were present in both the IS4 and NPC samples. The remaining IS4-specific peptides covered most of the 23-kDa mature PsbP protein (bottom). Peptides a-e are indicated on the PMF; the other matching peptides were outside the shown region. The section of the PMF with the IS4-modified, N-terminal peptide is shown in the inset and explained by the calculation on the bottom. Both the IS4-labeled peptide and its oxidized form have predicted masses that match the masses in the PMF inset. *C*, Fragmentation data of the IS4-labeled N-terminal peptide. The predicted y ions (bottom right) are found in the spectrum at the expected masses (top). The b ions are also found in the spectrum, with the additional mass of IS4. IS4 itself and fragments of IS4 are also found in the spectrum (b1, b2 and b3 ions). *D*, Proposed structure of the N-terminus of IS4-labeled PsbP, based on the peptide fragmentation data. IS4 is linked by a normal threonine through a peptide bond to the N-terminal alanine of PsbP. *E*, IS4-labeling is prevented by primary amine modification. Arabidopsis leaf extracts were preincubated with or without 200 μM Sulfo-NHS-Ac (NHS) or 200 μM IS4-n for 1 hour at pH 7.5. Treated proteomes were then labeled with 2 μM IS4. *, PsbP.

2.4.3   IS4 labeling requires cysteine protease RD21

The mechanism by which IS4 labels the N-terminus of PsbP was puzzling, given that PsbP is not a serine or cysteine protease and that labeling does not occur at serine or cysteine residues. However, a clue to the mechanism of IS4 labeling came when protease inhibitors were studied. IS4 labeling was inhibited with cysteine protease inhibitors E-64 and leupeptin, but not with serine protease inhibitor PMSF (Figure 4-4A). Because E-64 specifically targets PLCPs, these data suggest that a PLCP is required for IS4 labeling.

The Arabidopsis genome encodes ~30 PLCPs, of which at least 10 are expressed in leaves (http://www.genevestigator.ethz.ch/) and 6 were previously identified by DCG-04 labeling in leaf extracts (Van der Hoorn *et al.*, 2004). We reasoned that one of these leaf PLCPs could be responsible for IS4 labeling. We therefore generated PLCP-knockout lines by selecting lines carrying a T-DNA insertion in the genes encoding leaf-expressed PLCPs. IS4 labeling of extracts from these mutant plants revealed that labeling occurs in leaf extracts of all mutants except those of the *rd21-1* line (Figure 4-4B). The absence of IS4 labeling was confirmed with an independent knockout line, *rd21-2* (data not shown). These data indicate that only RD21 is required for IS4 labeling in leaf extracts.
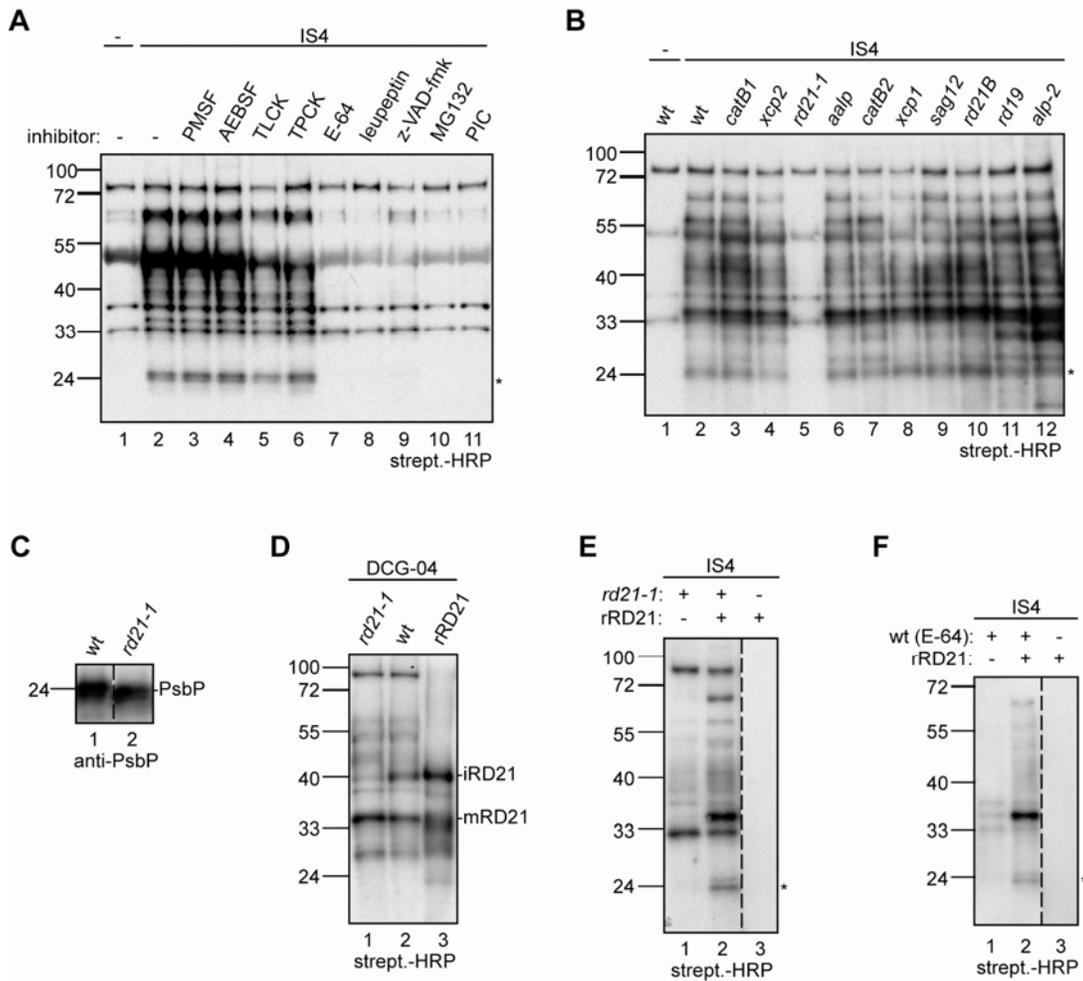
FIGURE 4-4 IS4 labeling requires active cysteine protease RD21.
A, IS4 labeling requires cysteine, but not serine, protease activities. Arabidopsis leaf extracts were preincubated with 40-400 μM protease inhibitors and then incubated with 2 μM IS4. PIC, protease inhibitor cocktail (diluted to 1 x according to the Instruction Manual, Roche, Switzerland). **B**, IS4 labeling requires the PLCP RD21. Leaf extracts of Arabidopsis PLCP knockout lines were incubated with IS4. wt, wild type. **C**, Absence of IS4 labeling in extracts of *rd21* plants is not due to the absence of PsbP. PsbP was detected in leaf extracts using protein blots probed with PsbP antibodies. Dashed line indicates lanes that were left out from the blot. **D**, Recombinant RD21 (rRD21) activity compared to that in Arabidopsis leaf extracts. RD21 was overexpressed by agroinfiltration in *Nicotiana benthamiana* and used as a source of rRD21. Leaf extracts from agroinfiltrated leaves and from Arabidopsis leaves of wild-type and *rd21* mutant plants were labeled with DCG-04 at pH 8 to reveal relative RD21 activities. To get similar levels of RD21 activities, 40x less protein was loaded from agroinfiltrated leaves compared to Arabidopsis leaves. **E**, rRD21 complements IS4 labeling in extracts of *rd21* mutant plants. Leaf extracts from wild-type and rd21 mutant plants were labeled with IS4 in the absence or presence of rRD21-containing extracts. **F**, Recombinant RD21 complements IS4 labeling in E-64-treated proteomes from wild-type Arabidopsis leaves. Leaf extracts were treated with 20 μM E-64. Excess E-64 was removed by gel filtration, and extracts were labeled with IS4 in the absence or presence of rRD21-containing extracts. Dashed lines indicate lanes that were left out from the blot. *, PsbP.

63

The absence of labeling in the *rd21* lines could be caused by the absence of PsbP and other acceptor proteins. To exclude this possibility, the *rd21-1* proteome was probed with antibody to PsbP and compared to signals from the wild-type proteome. This western blot showed that PsbP is present in both wild-type and *rd21-1* mutant plants, unaltered in size or quantity (Figure 4-4C). Thus, the absence of IS4 labeling is not caused by the absence of acceptor proteins in *rd21* mutants.

2.4.4 RD21 complements IS4 labeling *in vitro*

Having determined that RD21 is required for IS4 labeling, we tested whether RD21 could also complement IS4 labeling in *rd21* or E-64-treated proteomes. We produced Arabidopsis RD21 by agroinfiltration in *N. benthamiana* by expressing RD21 with the silencing inhibitor p19 (Van der Hoorn *et al.*, 2000; Voinnet *et al.*, 2003). This procedure ensures high levels of recombinant proteins produced *in planta* with all required post-translational modifications. RD21 production was confirmed using RD21-specific antibodies (data not shown). Extracts containing recombinant RD21 were diluted to a concentration at which RD21 activity was similar to that of Arabidopsis leaf extract (Figure 4-4D).

We next tested whether recombinant RD21 could complement IS4 labeling in proteomes of *rd21-1* mutant plants. Adding recombinant RD21 to proteomes of *rd21-1* mutant plants complemented IS4 labeling (Figure 4-4E). This restoration of IS4 labeling did not occur when recombinant RD21-deficient extracts of agroinfiltrated *N. benthamiana* were added, again indicating that recombinant RD21 is required to restore IS4 labeling (data not shown). No IS4 labeling was observed in recombinant RD21-containing extracts themselves, because these were diluted to adjust the recombinant RD21 concentration (Figure 4-4E).

To investigate the mechanism by which E-64 inhibits IS4 labeling, we incubated leaf extracts of wild-type plants with E-64 to inactivate RD21 and other PLCPs. The excess of E-64 was removed by gel filtration, and the E-64-treated proteome was used for IS4 labeling. No IS4 labeling occurred on these E-64-treated proteomes (Figure 4-4F). However, IS4 labeling was restored to normal levels by adding recombinant RD21 (Figure 4-4F). These results indicate that E-64 does not act by occupying IS4-

binding sites on the target proteins, but rather by inactivating PLCPs, presumably RD21.
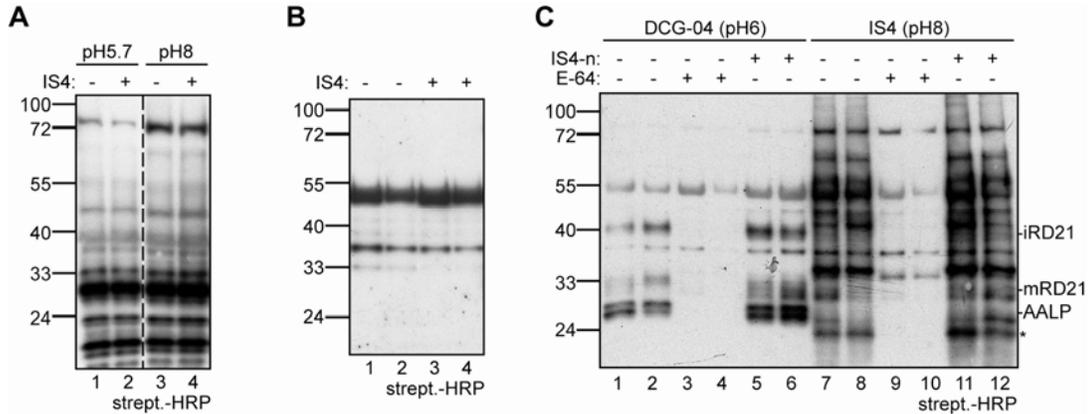
FIGURE 4-5 *In vivo* labeling with IS4.
A, Labeling with IS4 can not be detected in Arabidopsis cell cultures. 2-week old Arabidopsis cell cultures were washed and incubated for 4 hours with 20 μM IS4. Dashed lines indicate lanes that were left out from the blot. *B*, Labeling with IS4 can not be detected in detached Arabidopsis leaves.6-week old Arabidopsis leaves were detached and incubated with their petiole in solutions containing 10 μM IS4 for 6 hours. Proteins were extracted and analyzed on protein blots probed with streptavidin-HRP. The experiment was done in duplo and repeated twice with similar results. *C*, IS4-n can not prevent IS4 or DCG-04 labeling of detached Arabidopsis leaves. 6-week old Arabidopsis leaves were detached and incubated with their petiole in 100 μM E-64 or 150 μM IS4-n for 4 hours. Proteins were extracted and labeled with 2 μM DCG-04 at pH 6 or IS4 at pH 8 for 1 hour, and proteins were analyzed on protein blots probed with streptavidin-HRP. The experiment was done in duplo and repeated twice with similar results. *, PsbP.

We also investigated whether IS4 could label in living cells. We used both Arabidopsis cell cultures and detached leaves. Incubation of cell cultures with IS4 did not label specific proteins, even when the pH was increased from 5.7 to 8 (Figure 4-5A). Similarly, no IS4-specific labeling was detected when detached leaves were incubated with IS4 (Figure 4-5B). To test whether the nonbiotinylated IS4-n could enter the tissue and reach RD21, leaves were preincubated with IS4-n and E-64 *in vivo*, and then proteins were extracted and used for labeling with DCG-04 and IS4. Preincubation with E-64 blocked labeling of RD21 by DCG-04 and prevented IS4 labeling, indicating that E-64 inhibits RD21 activity *in vivo* (Figure 4-5C). In contrast, preincubation with IS4-n did not block labeling of RD21 by DCG-04, indicating that

there is no inhibition of RD21 by IS4-n *in vivo*. Extracts from leaves pretreated with IS4-n could be labeled with IS4, consistent with the absence of inhibition of RD21 by IS4-n (Figure 4-5C). Thus, IS4-n may not be reaching RD21 in living tissues because it is unstable *in vivo* or not membrane permeable. Limited *in vivo* labeling of β-lactone probes was also noted in studies on bacterial cell cultures (Böttcher and Sieber, 2008).

2.4.5   Binding of β-lactones to RD21

The above data show that labeling of IS4 to other proteins is mediated by RD21. To investigate whether RD21 itself is labeled by IS4, we analyzed purified IS4-labeled proteins with RD21-specific antisera. Neither intermediate nor mature RD21 signals were detected among the labeled proteins, indicating that RD21 is not labeled by IS4 (Figure 4-6A, bottom panel). These data are consistent with our previous observation that the IS4-labeling pattern does not contain signals of the size of intermediate RD21 (Figure 4-1C).

These findings suggest that IS4 binds to RD21 as an unstable intermediate that is not retained during purification of the labeled proteins. To show that IS4 binds to RD21, we labeled Arabidopsis leaf extracts with DCG-04 in the presence of excess nonbiotinylated IS4-n and IS2-n. IS4-n prevented labeling of intermediate RD21 by DCG-04, suggesting that IS4 occupies the substrate binding groove of RD21 (Figure 4-6B). In contrast, IS2-n could not prevent labeling of iRD21 by DCG-04 (Figure 4-6B), indicating that IS2 does not label (Figure 4-1B) because it does not interact with iRD21. Notably, AALP was labeled by DCG-04, indicating that this protease does not bind IS4-n (Figure 4-6B).

We next tested the pH dependency of IS4-n binding. RD21 reacts with DCG-04 at pH 5-10 (Figure 4-6C), indicating that RD21 is active at a wide pH range. However, preincubation with IS4-n prevented DCG-04 labeling of RD21 at pH 6-9 (Figure 4-6C), indicating that IS4-n binds to RD21 only in this pH range. The range of IS4-n binding coincides with that of IS4 labeling (pH 7-9; Figure 4-2A), except for pH 6. These data suggest that at pH 6, IS4 binds to RD21, but there is no transfer onto other proteins.
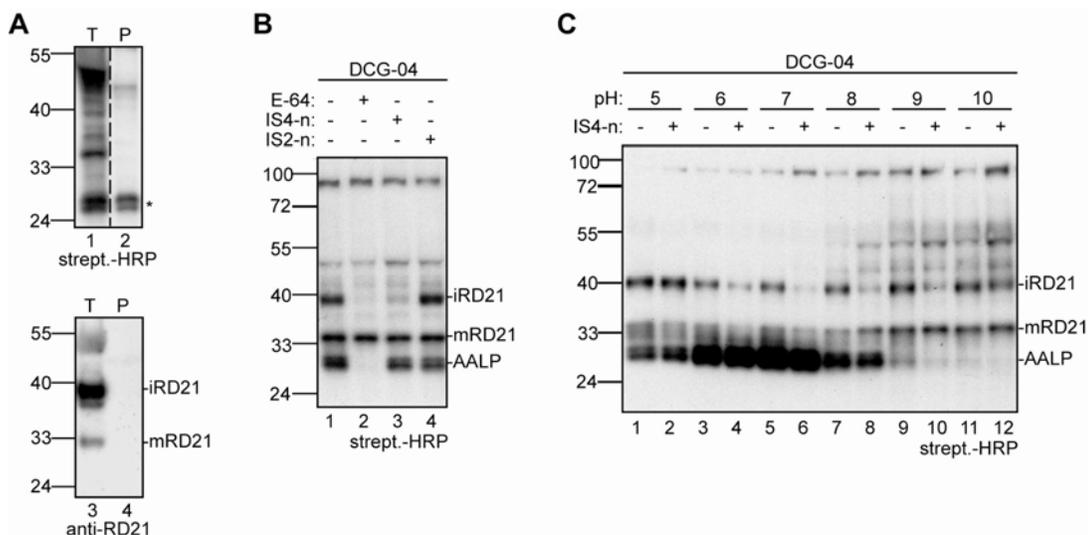
FIGURE 4-6 Binding of β-lactones to RD21.
A, IS4 does not label RD21. Arabidopsis leaf extracts were labeled with IS4 and the total labeled extract (T) and purified biotinylated proteins (P) were detected with streptavidin-HRP (left) and RD21 antiserum (right). Both intermediate (i) and mature (m) isoforms of RD21 were detected. Dashed lines indicate lanes that were left out from the blot. *B*, Nonbiotinylated IS4-n prevents intermediate RD21 isoform (iRD21) labeling in leaf extracts. Arabidopsis leaf extracts were labeled with 2 μM DCG-04 in the presence or absence of 200 μM nonbiotinylated E-64, IS2-n or IS4-n. *C*, IS4-n prevents iRD21 labeling at pH 6-9. Arabidopsis leaf extracts were incubated with 1 μM DCG-04 with or without 200 μM IS4-n at various pH values. *, PsbP.

2.4.6 RD21 ligates peptides

Given the above results, we hypothesized that IS4 binds to RD21 and forms a thioester intermediate that can be transferred to the N-terminus of PsbP. Because a thioester bond is common to all intermediates of PLCPs with their substrates, we tested whether thioesters formed from peptides could also be ligated to other proteins by RD21. To ensure that the peptides would bind RD21, we designed them based on sequences of IS4 (Bio-FTβ) and the N-terminus of PsbP (AYGEAAN). Three peptides were synthesized: the biotinylated peptides Bio-FTAYGE (PepA) and Bio-FTA (PepB) and the nonbiotinylated peptide AYGEAAN (PepC; Figure 4-6A). These peptides are nonelectrophilic agents that combine key recognition elements of IS4 and the N-terminus of PsbP.
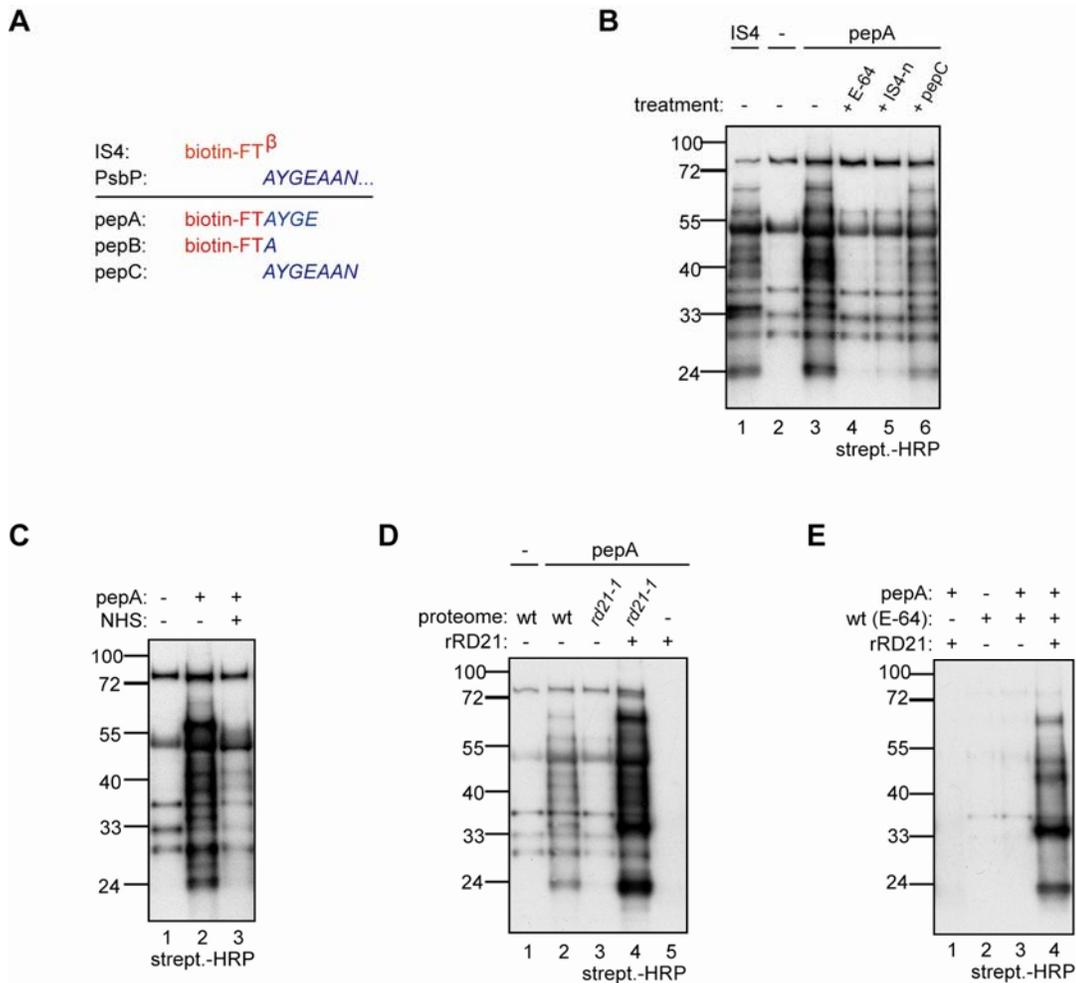
FIGURE 4-7 RD21 can ligate peptides.
A, Biotinylated peptides PepA, PepB and PepC were compared to sequences of IS4 (red) and PsbP (blue). *B*, PepA labeling can be prevented by E-64, IS4-n and PepC. Leaf extracts were preincubated with or without 120 μM E-64, 120 μM IS4-n or 300 μM PepC and labeled with or without 20 μM PepA or 3 μM IS4. Only half of the IS4-labeled sample was loaded. *C*, PepA labeling occurs at primary amino groups. Leaf extracts were preincubated with or without 600 μM sulfo-NHS-Ac (NHS) at pH 7.4 to block the N-terminal amino groups and then labeled with 30 μM PepA. *D*, PepA labeling is RD21 dependent. Leaf extracts of wild-type and *rd21* mutant plants were labeled with PepA in the presence or absence of recombinant RD21 (rRD21). *E*, rRD21 complements PepA labeling in E-64-treated proteomes. Leaf extracts were treated with 20 μM E-64. Excess E-64 was removed by gel filtration, and extracts were labeled with 30 μM PepA in the absence or presence of rRD21. wt, wild type.

Labeling of leaf extract with PepA resulted in a profile very similar to that of IS4 (Figure 4-7B). PepB, in contrast, did not cause any biotinylation (data not shown). Analogous to labeling by IS4, PepA labeling was prevented by adding E-64 or IS4-n and required the reducing agent DTT (Figure 4-7B). PepA labeling was reduced by

adding the nonbiotinylated PepC (Figure 4-7B), indicating that PepC competes with PepA labeling of acceptor proteins such as PsbP. Labeling by PepA was suppressed by preincubation with sulfo-NHS-Ac (Figure 4-7C), indicating that PepA labels at primary amines, presumably N-termini. Labeling with PepA was absent in *rd21-1* mutant proteomes and was complemented by recombinant RD21 (Figure 4-7D). Finally, PepA labeling was absent from E-64-treated proteomes but was complemented by recombinant RD21 (Figure 4-7E). Taken together, these observations indicate that RD21 ligates the N-terminal moiety of PepA to the N-termini of acceptor proteins.

CHAPTER 3: DISCUSSION

3.1   ABPP with fluorophosphonate probe FP

3.1.1   FP profiling of Arabidopsis leaf extracts

We optimized ABPP of Arabidopsis leaf extracts with FP, resulting in a highly reproducible and robust FP labeling. We next characterized FP labeling in more detail, and found that the labeling of most targets occurs maximally at cytosolic pH 8, and is saturated within 15 minutes. Among tested enzyme cofactors and chemical additives, only 0.1% SDS was found to affect FP labeling. FP labeling is absolutely absent in the heat-denatured leaf proteome, indicating that the labeling is activity-dependent. The knowledge obtained from this characterization greatly facilitated the large-scale purification of the labeling targets, and led to the identification of over 50 Arabidopsis serine hydrolase activities from more than 10 different serine hydrolase families including many proteases, lipases and esterases (Kaschani *et al.*, 2009b).

Two FP probes that only differ in linker region confer different profiling properties. In general, FP probes having a PEG linker label with stronger intensities and more signals than those with a hydrocarbon linker (Figure 1-2). This was also found in animal proteomes and is probably due to the increased water solubility and accessibility of this probe (Kidd *et al.*, 2001).

The Arabidopsis genome encodes for 198 serine proteases and even more nonproteolytic serine hydrolases (Van der Hoorn and Jones, 2004), but not all those serine hydrolases were detected with FP profiling. The absence of the other serine hydrolases can have different reasons. First, many Arabidopsis serine hydrolase genes are not expressed in leaves under the conditions tested. This holds, for example, for many genes encoding subtilases (Rautengarten *et al.*, 2005). Second, some serine hydrolases may not be active under the conditions tested. We showed, for example, that labeling depends on pH (Figure 1-2A), indicating that many enzymes cannot be labeled at non-optimal conditions. Third, some FP-labeled serine hydrolases might not be abundant enough to be detected with gel-based target identification or even with

MudPIT. Fourth, FP may not react with every serine hydrolase. For example, there are other FP probes available that label different serine hydrolases (Dijkstra *et al.*, 2008). Differences in labeling profiles between FP-Bio and FPpBio indeed indicate that labeling depends on the probe used.

Profiling with FP is a powerful tool to assist in the functional analysis of serine hydrolases, *e.g.* to monitor serine hydrolase activities in defense-induced or pathogen-infected Arabidopsis plants. We treated Arabidopsis plants with BTH to trigger SA-dependent defense responses, and labeled leaf extracts with FP to detect serine hydrolase activities during plant defense. This type of plant defense induction is independent of living pathogens and provides opportunities to study the changes in protein activities solely from the plant side. FP profiling revealed that BTH extensively upregulates activities of several serine hydrolases (Figure 1-3A). The identities of these specific FP targets still need to be clarified. Nevertheless, they may play roles in plant defense, and therefore may become host targets for invading pathogens to inhibit or suppress. Extensive changes in serine hydrolase activities were also observed in leaf extracts of wild-type Arabidopsis or in *sid2* mutant plants infected with virulent or avirulent strains of bacterial pathogen *P. syringae* (Figure 1-3B). The protein activity changes are dynamic during the first three days of infection, and may reflect serine hydrolase activities from both Arabidopsis and Pseudomonas. Identification and functional characterization of those differential serine hydrolases will greatly enrich our knowledge on the dynamic interactions between Arabidopsis and Pseudomonas during early infection stages.

We used 1D protein gel analysis to monitor the infection of Arabidopsis by *B. cinerea* and provide a first glimpse into the differential hydrolase activities during Botrytis infection. Both Arabidopsis and Botrytis hydrolases were detected in infected *pad3* mutant plants (Figure 1-4). Botrytis cutinases and lipases are thought to play a key role in Botrytis infection process because Botrytis infects by dissolving the cuticle (Van Kan, 2006). However, knock-out strains lacking cutinase CutA and lipase lip1 did not cause reduced virulence (Van Kan *et al.*, 1997; Reis *et al.*, 2005). Our data indicate that CutA is not the dominant cutinase during infection and that at least two Botrytis cutinase-like lipases are produced and active during infection. This activity information, combined with the Botrytis genome sequence, is essential information

for focused strategies to further investigate Botrytis pathogenesis. Several Arabidopsis enzymes show differential activities during Botrytis infection. The activities of methylesterases MES2 and MES3, for example, were down-regulated (Figure 1-4). It is unknown whether these effects are mediated by the pathogen to promote infection or mediated by the plant to suppress pathogen invasion. MES2/3 activities, for example, might be down-regulated by Botrytis to suppress salicylic acid signaling pathways. These FP labeling experiments illustrate the kinds of questions that are raised by investigating plant-pathogen interactions using ABPP. However, more experiments are required to confirm the differential activities and to reveal their molecular mechanisms and biological functions.

3.1.2　FP profiling of tomato apoplastic fluids

We used tomato apoplastic fluids as a research model for investigating secreted proteases and their functions in plant apoplastic defense, and applied ABPP with FP profiling to study the serine hydrolase activities in SA-dependent plant defense responses. Biochemical characterization of FP labeling of tomato AFs revealed that most of the FP targets are maximally active at pH 6, which is consistent with the physiological pH of the acidic apoplast. Treatment of tomato plants with BTH, a functional analogue of SA, results in substantial changes in serine hydrolase activities. Two major FP targets, whose activities are significantly upregulated upon BTH treatment, were identified as P69B, a secreted subtilisin-like serine protease. This is consistent with previous findings that P69B is a PR protein which is induced by pathogen attack or SA treatment and accumulates in tomato leaf apoplast (Tornero *et al.*, 1997; Jorda and Vera, 2000).

Various interactions occur in apoplast during plant development and responses to the environment full of stresses. Therefore, it is pivotal to study the proteins in plant apoplastic space. Apoplastic proteins are usually secreted from the plant cell through ER-Golgi secretion pathway, and are involved in non-self recognition, development, nutrition and responses to abiotic and biotic stresses (Berger and Altmann, 2000; Boller, 2005; Tasgin *et al.*, 2006; Kusumawati *et al.*, 2008; Paungfoo-Lonhienne *et al.*, 2008). There are at least three major material resources for plant apoplastic secretome research: extracellular medium of suspension cell culture, xylem sap and leaf

apoplastic fluid (Lee *et al.*, 2004; Djordjevic *et al.*, 2006; Tran and Plaxton, 2008). Tomato leaf apoplastic fluid is native, dynamic and experimentally easy to obtain, and is particular useful for studies on apoplastic plant-microbe interactions, as the tomato apoplast is the entry site of numerous pathogens. Previously, tomato AF was successfully used to study the interactions between apoplastic proteases and effector proteins secreted from different pathogens (Tian *et al.*, 2004; Rooney *et al.*, 2005).

We focused on serine hydrolases including serine proteases in tomato leaf AF, and monitored the activities of tomato apoplastic serine hydrolases using ABPP with FP labeling. Particularly, we sought for serine hydrolases whose activities are altered upon BTH treatment, as they may function in SA-dependent defense responses and may become host targets for pathogens to inhibit. SA biogenesis, signaling network and downstream defense responses within plant cells were comprehensively surveyed in last decade (Loake and Grant, 2007), but SA effects on plant apoplastic defense remains less characterized. Chitinase and β-1,3-glucanase, for example, are among few well-studied apoplastic PR proteins that can be induced by exogenously-applied SA (Bowles, 1990). Besides of those, Park and coworkers recently treated Arabidopsis cell culture with SA and identified a dozen of SA-responsive secreted proteins including GDSL-like lipase-1 (GLIP1), which is implicated in plant resistance to the fungus *Alternaria brassicicola* (Oh *et al.*, 2005). Popova and coworkers found that SA differentially regulates the activities of antioxidant enzymes in the apoplast of winter wheat by enzymatic activity assays (Tasgin *et al.*, 2006). Williamson and coworkers observed that SA stimulates the secretion of mannitol dehydrogenase (MTD) into tobacco leaf apoplast (Cheng *et al.*, 2009). The authors hypothesized that these SA-induced MTDs may serve to eliminate the antioxidant mannitol secreted by fungal pathogens, and consequently coordinate reactive oxygen species (ROS)-mediated plant defenses. We recently investigated PLCPs in tomato AFs using ABPP with DCG-04 labeling, and detected at least seven PLCP activities when plant defense was triggered with BTH treatment (Shabab *et al.*, 2008). We identified PIP1 as an apoplastic PR protein whose activity is upregulated by BTH, and found that fungal effector protein AVR2 from *C. fulvum* inhibits PIP1. The tomato leaf apoplast contains a large variety of uncharacterized hydrolytic proteins. To expand the spectrum of the hydrolases, we profiled tomato AF with the serine hydrolase-specific probe FP.

While profiling tomato AFs with FP, we used two probes, FPpRh and FPpBio, with identical reactive group and linker but different reporter groups for quick detection and affinity purification of labeling targets, respectively (Figure 1-1). FPpRh and FPpBio cause similar but not identical labeling profiles, although mutual competition assay suggested that both probes target almost the same set of serine hydrolases (Figure 1-5A). The subtle differences between two labeling profiles may be an outcome of different reactivity of each probe towards distinct targets. For example, in comparison to the 70-kDa hallmark signal, FPpRh labels the 56-kDa signal much stronger than FPpBio does (Figure 1-5A, grey dot). Furthermore, a 40-kDa signal can only be labeled with FPpRh but not with FPpBio. This observation is consistent with the fact that FPpBio can not efficiently outcompete FPpRh labeling of this 40-kDa signal (Figure 1-5A). Finally, the FPpRh profiling revealed that the activity of 56-kDa target was downregulated in AFs of BTH-drenched tomato plants (Figure 1-6B). Unfortunately, this 56-kDa signal is absent when tomato AFs were labeled with FPpBio, and therefore we could not identify this FPpRh target (Figure 1-7A). We postulate that the 56-kDa signal on 1D gel contains several FP labeling targets, and that one serine hydrolase in this mixture is downregulated upon BTH treatment and can be labeled only with FPpRh but not with FPpBio. The distinct effects of reporter tags on the reactivity of FP probes has been noted by Cravatt and coworkers, as the trifunctional FP probe labels much less serine hydrolase targets than FP probes with either a biotin tag or a rhodamine tag (Benjamin Cravatt, personal communication). The development and synthesis of an FP probe with an affinity tag that can both detect and purify this 56-kDa of SA-regulated enzyme should be a priority for future investigations.

The 70-kDa FP signal in tomato AFs was identified as P69B by affinity purification and MS analysis, and confirmed by western blotting with anti-P69B antibody (Figure 1-7). We found that P69B is upregulated upon BTH treatment both at activity level (Figure 1-7) and expression level (data not shown). These results are in line with P69B being a pathogenesis-related (PR) protein. P69B is induced and accumulates in the tomato apoplast upon citrus exocortis viroid infection or SA or BTH treatment (Vera *et al.*, 1989; Jorda and Vera, 2000; Tian *et al.*, 2004). P69B is a subtilisin-like serine protease (subtilase) with a molecular weight of ~69-kDa, and a member of P69 subtilase subfamily consisting of six highly-homologous subtilases, P69A-F (Tornero

et al., 1997; Jorda *et al.*, 1999, 2000). Vera and coworkers investigated the expression profiles of all six P69s by promoter analysis with GUS reporter in transgenic Arabidopsis plants, and showed that P69A is constitutively expressed in all tissues expect roots and flowers; P69D is transiently expressed in cotyledons and emerging leaves; P69E is only expressed in roots; and the expression of P69F is restricted in the leaf hydathodes (Jorda *et al.*, 1999, 2000). P69A, D, E and F are not induced by virulent/avirulent Pseudomonas infections or SA treatment. In contrast, P69B and P69C are not constitutively expressed in all developmental stages, but are strongly induced locally and systemically by both Pseudomonas and SA. Induced expression of P69B is restricted in leaf veins, while induced expression of P69C is scattered all over the leaf lamina (Jorda *et al.*, 1999; Jorda and Vera, 2000). However, we found that FP labels all P69A, P69B, P69C, P69E and P69F in the leaf AFs of H_2O-treated tomato plants; and the activities of all five P69s are significantly upregulated upon BTH treatment (Kaschani *et al.*, unpublished data). Improved separation of purified FP target proteins on 2D gel is expected to lead to the identification of different P69 isoforms and their post-translational modifications, and differential activities during SA-mediated defense responses.

The 33-kDa BTH-inducible FP target in tomato leaf AFs was also identified and confirmed to represent P69B (Figure 1-7). FP is believed to covalently react with Ser-531, the conserved putative catalytic residue of P69B (Tornero *et al.*, 1997), and the anti-P69B antibody was raised against the N-terminal peptide of P69B (aa114-126; Tian *et al.*, 2004). Any P69B isoform that can both be labeled with FP and be recognized by anti-P69B antibody should have a size larger than ~45-kDa, but the 33-kDa signal is much smaller than this theoretical minimal size. We speculate two possibilities for it. The first possibility is that certain alternative splicing event may occur to the P69B transcript, leading to a loss of peptide sequence prior to Ser-531 and a shortened translation product of P69B. Indeed, sequence alignment analysis indicated that tomato P69 subtilases has a long peptide sequence insertion prior to the catalytic serine and a long C-terminal peptide sequence after the catalytic serine when compared to non-plant subtilases (Tornero *et al.*, 1996, 1997). The second possibility is that this 33-kDa signal is a degradation fragment of mature P69B, in which amino acid other than Ser-531 was labeled by FP or a peptide other than aa114-126 could be

bound by anti-P69B antibody. Affinity purification and MS analysis of the 33-kDa signal and identification of the FP-labeling site will give a final answer to this puzzle.

Though as a PR protein P69B is induced by pathogen attack or SA treatment and may play a role in SA-mediated plant defenses, the biological function of P69B is still unknown. Unlike the majority of PR proteins whose expression is delimited to the necrotic zones caused by HR when the plants are challenged with pathogens, the virulent and avirulent Pseudomonas-triggered accumulation of P69B is not preferentially around the necrotic lesions (Jorda and Vera, 2000). The authors postulated that P69B may process apoplastic substrate proteins to remodel the extracellular matrix and/or to activate signal transduction, rather than directly interact with invading pathogens. Nevertheless, the involvement of P69B in plant defense implies that this protease may become a host target for pathogen-derived effector proteins. Kamoun and coworkers discovered a Kazal-like extracellular effector protein EPI1 from *P. infestans* which is expressed during infection and inhibits tomato P69B (Tian *et al.*, 2004). This inhibition of P69B is accomplished by the atypical Kazal domain EPI1a but not by the typical Kazal domain EPI1b, which was demonstrated with in-gel protease activity assay at pH 8 using colorimetric substrates (Tian *et al.*, 2005). Kazal-like EPI1a is an active-site inhibitor and inhibits the target subtilases by sterically blocking the active-site to the substrates (Read *et al.*, 1983). We found, however, that EPI1a can not outcompete FP labeling of P69B in leaf AFs of either H_2O- or BTH-treated tomato plants (Figure 1-8C), and therefore were unable to show EPI1a inhibition of P69B by competitive ABPP with FP labeling. This raises the question on the fidelity of ABPP, which in principle readouts active-site accessibility of the target enzymes, in reflecting the enzymatic activity of the probe targets, which is defined as "moles of substrate converted per unit time". When EPI1a interacts with P69B and resides on the active site of the serine protease to repel the substrates from approaching the active site, it may not cut off the access of the FP warhead to the catalytic serine residue of P69B. For this reason, FP profiling of P69B in the presence of EPI1a may bring false interpretation of P69B activity.

Another conflicting result we obtained is on the pH dependency of P69B enzymatic activity and FP labeling of P69B. During biochemical characterization of P69s, Conejero and coworker showed that viroid-induced P69s (mainly P69B and P69C) are

maximally active at pH 8.5-9 but not active at all at pH 6 using fluorogenic casein and RuBisCO as substrates (Vera and Conejero, 1988). While profiling tomato AFs with FP, we found that the pH optimum of FP labeling of P69s is pH 6-8 (Figure 1-5C), meaning that P69s are more active at pH 6 than at pH 9, which is not in agreement with the results from Conejero group. In order to maximally mimic the biologically relevant environment, we used pH 6, which is close to the physiological pH of tomato leaf apoplast, for *in vitro* FP profiling. The different pH values chosen in enzymatic assays (pH 8) and competitive ABPP (pH 6) for EPI1a inhibition of P69B may be the cause of the contradictory outcomes. In general, conclusions from ABPP results on protein activities should be drawn with care, and if possible, enzymatic assays with specific substrates should be performed in parallel with ABPP to ensure the consistency of the activity readouts.

3.2   ABPP with epoxide probe DCG-04

3.2.1   PIP1 is induced by BTH treatment and inhibited by AVR2 in the tomato apoplastic fluids

The apoplast, a battlefield between plant defending cells and invading pathogens, is likely to be ancient, predating the evolution of translocation mechanisms for effector proteins by which pathogens manipulate the host cytoplasm and suppress host defense responses. Therefore, understanding the nature of plant defenses in the apoplast and the counter defense mechanisms that pathogens evolved to overcome these defenses is essential for a comprehensive understanding of host-pathogen interactions and should complement the body of knowledge that has emerged on cytoplasmic effectors and defense mechanisms.

We used the apoplast of tomato (*Solanum lycopersicum*) as a research model, which is easily accessible for biochemical experiments and ideal for studying apoplastic molecular plant-pathogen interactions. We focused on papain-like proteases in the tomato apoplast by applying protease activity profiling to study the activities of the PLCPs and the interactions between the PLCPs and pathogen-secreted inhibitors. This

sub-project revealed seven active PLCPs in the apoplast of tomato, using the broad-range active site-directed probe TMR-DCG-04, which reacts with a wide range of PLCPs (Van der Hoorn *et al.*, 2004). The seven PLCPs that we detected are probably not the full set of secreted PLCPs but certainly comprise the majority of active PLCPs in the tomato apoplast. It is likely that extracellular pathogens will encounter these secreted PLCPs during infection.

PIP1 is strongly upregulated at activity level upon BTH treatment, and the upregulated activity of PIP1 is correlated with the transcript accumulation (data not shown). This indicates that the *PIP1* gene is under control of the SA signaling pathway and that PIP1 belongs to the class of PR proteins that accumulate during the basal immune response. Consistent with BTH induction, PIP1 is upregulated during infection with *P. syringae* and *P. infestans* (Zhao *et al.*, 2003; Tian *et al.*, 2007). However, since SA signaling is not the only pathway that is active during infection, the final levels of PLCPs will strongly depend on the time point, cell type, and pathogen. Infection of tomato with *P. syringae*, for example, induces the expression of C14 but not CatB2 (Zhao *et al.*, 2003). Furthermore, infection of potato plants with avirulent *P. infestans* results in upregulation of both C14 and CatB2 (Avrova *et al.*, 1999, 2004). Thus, although the other PLCP genes are not induced by the SA analog BTH, their expression can be induced during infection, probably through other pathways.

We showed that the *C. fulvum* AVR2 effector protein specifically targets the defense-related protease PIP1 in tomato apoplastic fluids, using ABPP with TMR-DCG-04. The fact that only BTH-induced PIP1 is inhibited by AVR2 is an interesting observation; although it cannot be excluded that *C. fulvum* secretes other proteins that target other PLCPs. Although these data suggest that PIP1 plays a role in defense in the absence of Cf-2, this remains to be demonstrated. Recently, De Wit and coworkers showed that AVR2 is a genuine virulence factor of *C. fulvum* in both Arabidopsis and tomato plants (Van Esse *et al.*, 2008).

The approach taken in this study to identify secreted proteases and analyze their inhibition by pathogen-derived proteins has revealed interesting aspects of an apoplastic molecular battlefield between plants and pathogens. Given these

observations, it seems likely that many pathogens secrete PLCP inhibitors during infection and that these inhibitors, the proteases, and their substrates are involved in a continuous coevolutionary battle. How coevolution shaped the apoplastic defense, and how these defense-related proteases discriminate between self and non-self remain exciting questions to resolve.

3.2.2 C14 activities and inhibition by EPIC1/2B in tomato apoplastic fluids

Suppression of host defense responses is an important strategy of adapted plant pathogens. This study revealed that the EPIC1 and EPIC2B effector proteins of the oomycete pathogen *P. infestans* both target and inhibit intermediate isoform of tomato C14, an abundant, ubiquitous, stress-related protease that is typified by an additional C-terminal granulin domain and resides mostly inside the host cell. C14, a partially secreted tomato PLCP, is supposed to play a role in plant basal defense in apoplast as its activity is slightly upregulated upon BTH treatment (Figure 2-2A, lane 1 and 2). The oomycete EPIC proteins are strong inhibitors of C14, since the EPIC-C14 interaction is specific and occurs at low inhibitor concentrations. The EPICs are supposed to suppress C14-related defense machinery and facilitate the pathogen to colonize the host plant.

C14 is a highly conserved protease that occurs throughout the plant kingdom. C14-like proteases are characterized by a unique, C-terminal granulin-like domain that shares homology to animal growth hormones that are released upon wounding (Bateman and Bennett, 1998). The tomato C14 is relatively abundant and has been studied many times under the names TDI-65, CYP1 and SENU1, and is known to be transcriptionally induced by heat, cold, drought and senescence (Schaffer and Fisher, 1988, 1990; Drake *et al.*, 1996; Harrak *et al.*, 2001). The potato ortholog of C14 is called CYP1 and is transcriptionally induced in resistant potato cultivars early during infection of *P. infestans* (Avrova *et al.*, 1999). The Arabidopsis ortholog is named RD21, and accumulates in vesicles (Hayashi *et al.*, 2001; Yamada *et al.*, 2001). Although the function of C14-like proteases is currently unknown, these data suggest that C14-like proteases have an intrinsic function related to general stress responses.

C14 is not the only target of EPICs. This is consistent with the emerging concept in effector biology that most effectors have multiple targets in the host (Hogenhout *et al.*, 2009). It was previously shown that EPIC2B but not EPIC1 inhibits PIP1 (Tian *et al.*, 2007). In addition, EPIC1 and EPIC2B both inhibit RCR3, which is closely related to PIP1 (Song *et al.*, 2009). Short labeling times and different probe and inhibitor concentrations were used in these assays to show that EPICs prevent biotinylation of PIP1 and RCR3. The specificity and biological function of EPIC1 and EPIC2B inhibition of each tomato PLCP secreted into apoplast remains to be further elucidated. Particularly for C14, profiling of apoplastic fluids from *P. infestans*-infected tomato plants with DCG-04 could reveal if C14-EPIC interaction occurs *in vivo*.

To characterize the EPIC inhibition of tomato C14, we monitored the activities of both recombinant C14 ectopically overexpressed in *N. benthamiana* and C14 in the crude tomato apoplastic fluids. rC14 produced with agroinfiltration retains necessary modifications taking place only *in planta* (Van der Hoorn *et al.*, 2000), and offers opportunities to study the activities of both iC14 and mC14 simultaneously, because in tomato AFs mC14 could not be efficiently separated from CatB and ALP by 1DE. 2DE with fluorescent DCG-04 profiling is a robust analytical platform to monitor the activity of mC14 in tomato AFs (Figure 2-2B), and will facilitate the study on EPIC-mC14 interaction in the apoplast.

DCG-04 labeling of recombinant iC14 is identical in pH dependency and time course compared to the labeling of iC14 in tomato AFs, indicating that C14s have a similar physicochemical properties in different biological context. However, addition of 0.03% SDS differentially affects iC14 activities *in vitro*: it suppresses DCG-04 labeling of recombinant iC14 while enhances DCG-04 labeling of iC14 in tomato AFs. SDS is an anionic detergent widely used in protein research. At high concentrations it denatures, unfolds and negatively charges proteins, while at low concentrations it may activate proteins as shown for the proteasome, matrix metalloproteases, cysteine proteases and other enzymes (Tanaka *et al.*, 1989; Springman *et al.*, 1990; Yamada *et al.*, 1998; Cong *et al.*, 2009). The fact that SDS activation of iC14 in tomato AFs can be detected by DCG-04 profiling demonstrates that 0.03% SDS can cause structural changes around the active site of the enzyme, leading to the enhanced accessibility of the probe to the active site.

In this case, there might be several possible mechanisms for this activation of iC14 by SDS. First, the active site of iC14 may be buried inside by a secondary structure of the intermediate form of the protease (e.g. the granulin domain), and 0.03% SDS may alter the protein conformation and expose the active site to the probe and substrates. A similar regulation model was recently reported by Decker and coworkers that SDS activates phenoloxidase by twisting its intrinsically flexible Hc domain I from domain II and III, and exposing the entrance to the active site (Cong *et al.*, 2009). Second, iC14 may form face-to-face dimer and mask the active site of one monomer by the other, and 0.03% SDS may dissociate the dimerization and activate the protease by unmasking the active sites. SDS dissociates, as reported by Prakash and coworkers, multimeric protein carmin into its monomers at low concentrations (Sudhindra and Prakash, 1993). Third, under normal conditions *in vitro*, the active site of iC14 may be predominantly occupied by endogenous inhibitory proteins or small molecules to keep it in an inactive form, and 0.03% SDS may break such relatively weak interactions between iC14 and its inhibitory ligands to activate iC14. SDS interferes with many protein-protein or protein-small molecule interactions. For example, Tóth and coworkers found that low concentration of SDS detaches the ligand tetrahydropterin from its stabilizing enzyme type-III nitric oxide synthase, while does not disturb the quaternary structure of the enzyme itself (Tóth *et al.*, 1998).

Nevertheless, SDS activation of iC14 in tomato AFs suggests that the activity of iC14 can be regulated in its physiological environment, and 0.03% SDS is a way to release its full activity. We hypothesized that the endogenous iC14 is mainly in an inactivated form as a reservoir of proteolytic potential, to be activated promptly upon specific signals.

The fact that EPIC1 and EPIC2B are strong inhibitors against C14 and other tomato PLCPs was also highlighted by their strong inhibition of tomato AFs in the presence of 0.03% SDS. EPIC1 and EPIC2B show high similarity in amino acid sequences, and close relationship from phylogenetic analyses (Tian *et al.*, 2007). However, they also exhibit differentials in inhibitory potency to recombinant iC14 and iC14 in tomato AFs. Recently, Michaud and coworkers tried to tailor the specificity of tomato cystatin *Sl*CYS8 toward cysteine proteases, and successfully fine-tuned its specificity by single mutations at positively selected amino acid sites (Goulet *et al.*, 2008). This

research demonstrates that subtle amino acid differences at defined positions in cystatin can cause diverse selectivity to their target cysteine proteases. Thus, single amino acid replacement in EPIC1 and EPIC2B may identify their target selectivity and dissect their functions against different PLCPs in tomato AFs.

The most interesting observation in this research is that at low EPIC1 or EPIC2B concentrations of 4-8 nM both *P. infestans*-derived inhibitors can moderately activate the mature isoform of rC14. Recently, Von Pawel-Rammingen and coworkers also found that human protease inhibitor cystatin C activates Streptococcal IgG-cleaving cysteine protease IdeS, which contains a typical papain-like structural fold (Vincents *et al.*, 2008). In this research, fluorogenic substrates were used to measure cysteine protease activities, and kinetic analysis revealed that cystatin C significantly accelerated the proteolytic velocity of the pathogen-derived cysteine protease. In our case, low concentrations of EPIC1 and EPIC2B may modify the active site of mC14, making it more accessible to probe or substrates. As enhanced accessibility of the enzyme active site to substrates may lead to accelerated substrate cleavage of the protease, our DCG-04 profiling may shed lights on the mechanism of this atypical cysteine protease activation by cystatins.

Another lesson from this observation is that it is of instrumental importance to measure *in vivo* the ratio of pathogen-derived inhibitors and the plant proteases during pathogen infection. Only by doing that we could then more precisely determine the effects of inhibitors on their interacting host proteases at biologically-relevant concentrations *in vitro*, and clarify whether these plant proteases are inhibited or hijacked for functional analysis of these pathogen-derived inhibitors.

3.3   ABPP with vinyl sulfone probe MV151

It has been widely accepted that substrate specificity of the proteasome is mostly determined by selective ubiquitination of target proteins (Sullivan *et al.*, 2003). However, proteasome activities also play regulatory roles itself. Interferon treatment of mammalian cells results in the production of "immunoproteasomes" which contain

different catalytic β-subunits to release hydrophobic peptides for antigen presentation (Rock *et al.*, 1994; Goldberg *et al.*, 2002). In some mammalian tissues proteasomes occur as subpopulations with different subunit compositions and different proteolytic activities (Drews *et al.*, 2007). Nearly all proteasome subunits in Arabidopsis are encoded by two genes, suggesting that proteasome subpopulations may occur (Kurepa and Smalle, 2008). The catalytic subunits, for example, are encoded by PBA1 (β1), PBB1 and PBB2 (β2) and PBE1 and PBE2 (β5). In tobacco, transcript levels encoding a β1 catalytic subunit are specifically upregulated during defense, suggesting the existence of "plant defense proteasomes" (Suty *et al.*, 2003).

Developing tools to monitor the activity of the proteasome is instrumental to study proteasome functions. Monitoring proteasome activities during development and defense could lead to the identification of novel proteasome inhibitors and activators of endogenous or exogenous origin, as well as changes in the composition of the proteasome complex. Furthermore, selection of specific inhibitors for each catalytic subunit can be used to determine the role of each proteasome subunit. Genetic approaches to address subunit-specific roles are limited, since inactivation of one subunit usually affects the assembly and activity of the other subunits (Heinemeyer *et al.*, 1997).

We showed that VS-based probes can be used to monitor the activity of all three catalytic subunits of the proteasome. The procedure can be used to study the activity of proteasome subunits during different biological processes in different tissues, and in different plant species. The method also facilitates the selection of subunit-selective inhibitors that can be used to address the subunit-specific functions of the proteasome.

The β5 subunit is preferentially labeled at low probe concentrations and short labeling times. This is consistent with the fact that MV151 carries a leucine at the P1 position, which is an ideal inhibitor for β5, since it has chymotrypsin-like activity (cleaving after hydrophobic residues). Equal labeling of all three catalytic subunits can be achieved by prolonged labeling at high probe concentrations. Labeling is optimal at pH 7.5, which coincides with the pH of the cytoplasm and nucleus.

The β2 and β5 subunits are encoded by two highly homologous paralogs, PBB1, PBB2 and PBE1 & PBE2, respectively. The paralogs are difficult to discriminate since the corresponding protein sequences are nearly identical. However, in different assays we have identified specific peptides of PBA1 (β1), PBB1 (β2), PBB2 (β2) and PBE1 (β5) (this manuscript) and PBE1 (β5) and PBE2 (β5) in an *in vivo* labeling experiment (Kaschani *et al.*, 2009a). These data suggest that both paralogous subunits occur simultaneously and indicate that different proteasome complexes may exist in plants.

The VS probes also label some PLCPs like RD21A. This was confirmed by MS analysis, mutant analysis, pretreatment with the PLCP-specific inhibitor E-64, and competition experiments with DCG-04. PLCP labeling was also observed in different Arabidopsis organs and in leaves of other plant species. Labeling of PLCPs is consistent with the fact that VS inhibitors can covalently inhibit PLCPs (Powers *et al.*, 2002). However, not all PLCPs are targeted by VS-based inhibitors, as was demonstrated for AALP (Figure 3-3D). Labeling of PLCPs is weak when compared to labeling of the proteasome, but it can be stronger if a reducing agent is added (Figure 3-2D), or if the labeling is done *in vivo* (Kaschani *et al*, 2009a).

Simultaneous activity-based profiling of the three catalytic subunits and PLCPs is a powerful tool to test the selectivity of protease and proteasome inhibitors. When testing different commercially available inhibitors, we found a striking inconsistency with the advertised selectivity. For example, proteasome inhibitors MG132 and MG115 also target PLCPs, and PLCP inhibitor leupeptin and various caspase inhibitors also target the proteasome. However, since all these inhibitors are aldehyde-based and differ only in the amino acid residues, the inhibitory profiles could be correlated to the residues at the P1 and P2 positions. These data show a consistent picture, since PLCPs are selective for hydrophobic residues at the P2 position, whereas the proteasome catalytic subunits are selective for residues at P1: β1 for acidic residues, β2 for basic residues, and β5 for hydrophobic residues. The ability to design and test subunit selective inhibitors has tremendous potential since these inhibitors would enable to determine subunit-specific functions of the proteasome.

The proteasome is a highly conserved proteolytic complex in eukaryotes. This is underlined by the consistency of our data with previous findings (Kurepa and Smalle, 2008). To expand ABPP of the proteasome in plants we tested different Arabidopsis organs and leaf extracts from different plant species. We could display proteasome activities in each of these organs, as demonstrated with different inhibitors. However, labeling of each subunit remains to be optimized for other Arabidopsis tissues, and the signals from the different plant species probably overlap and require further separation. Nevertheless, these experiments show the broad applicability of the technique.

ABPP with MV151 revealed that proteasome activities are 1.5-fold upregulated in BTH-treated plants in an NPR1-dependent manner. This was unexpected, since transcript levels of genes encoding proteasome subunits are unaltered upon BTH treatment (www.genevestigator.com, Zimmermann *et al.*, 2004; Von Rad *et al.*, 2005). Our data suggest that the upregulated proteasome activity is post-translational. Although the mechanism of this post-translational activation of the proteasome is unknown at this point, it is well-described that the plant proteasome can be post-translationally regulated by e.g. oxidation of proteasome subunits (Basset *et al.*, 2002).

The upregulated proteasome activity is in line with a role of the proteasome in various defense responses. The avrRpm1-induced hypersensitive response requires proteasome activity (Hatsugai *et al.*, 2009) and induction of NPR1-regulated genes require degradation of phosphorylated NPR1 by the proteasome (Spoel *et al.*, 2009). Furthermore, *Pseudomonas syringae* pv. *syringae* produces proteasome inhibitor Syringolin A which contributes to their virulence (Groll *et al.*, 2008). Besides regulatory roles, the proteasome may also play a role in releasing amino acids for the synthesis of defense-related proteins and compounds, and protect cells against the reactive oxygen species and pathogen-inflicted damage. BTH causes a severe change in metabolism to generate defense-related proteins and compounds (Dietrich *et al.*, 2004). We speculate that an increased proteasome activity in the cytoplasm is required for efficient, large scale proteolytic processes during defense. Defense-related proteasomes may even have different enzymatic activities, similar to mammalian 'immunoproteasomes' which releases hydrophobic peptides for antigen presentation (Rock *et al.*, 1994; Goldberg *et al.*, 2002). Interestingly, plant defense proteasomes

are thought to occur in tobacco where transcript levels encoding a β1 catalytic subunit is specifically upregulated during elicitation (Suty *et al.*, 2003). The properties and role of defense-related proteasomes will be subject to future studies.

In conclusion, proteasome activity profiling is a simple and robust method to discover changes in proteasome activities. This method will significantly support our future analysis of proteasome activities during pathogen infection, and is now available to the plant research community to study proteasome activities in a wide range of biological processes.

3.4   Labeling with β-lactone probe IS4

The data are consistent with a model in which β-lactones and peptides bind to RD21 and form a thioester bond that is transligated to abundant, unmodified N termini of acceptor proteins (Figure 4-8). The binding of donors to RD21 is probably mediated by a phenylalanine residue at the P2 position, which is consistent with a preference for such hydrophobic P2 residues by PLCPs (Powers *et al.*, 2002). Transfer of the donor molecule occurs at neutral or basic pH levels, when the N terminus of acceptor molecule is deprotonated and can act as a nucleophile.

The fact that more plant PLCPs are active in leaf extracts (Van der Hoorn *et al.*, 2004), yet no labeling is observed in extracts of rd21 knockout lines, indicates that phylogenetic analysis of the protease domain of RD21 shows that RD21 falls in a separate clade that lacks animal counterparts (http://merops.sanger.ac.uk/). RD21 exists in two active isoforms: a 40-kDa intermediate isoform with granulin domain and a 30-kDa mature isoform without granulin domain (Yamada *et al.*, 2001). Both isoforms are present in leaf extracts, but whether the granulin domain is required for transligation remains to be tested.

At this stage, it is not known whether PsbP is a natural acceptor for RD21 transligation, as all labeling experiments were performed on leaf extracts, and PsbP and RD21 might be compartmentalized in living cells. Post-translational modification

of N termini can be an important regulatory mechanism (Walling, 2006), and RD21 might regulate proteins by ligating donor molecules to their N termini. One way to investigate this further is to examine which proteins are N-terminally modified by RD21 in vivo using labeled donor molecules. The identification of the native N-terminal modification on these natural acceptors might lead to the identification of native donor molecules and the discovery of a novel, plant-specific posttranslational modification.

Although we were unable to detect labeling by IS4 in living cells, it seems likely that transligation can occur at physiological conditions, as it requires RD21, a reducing agent, neutral or basic pH, donor peptides and acceptor proteins with unmodified N termini. RD21 has been detected in vesicles and vacuoles of Arabidopsis (Hayashi *et al.*, 2001; Carter *et al.*, 2004), and the tomato RD21-like protease C14/TDI-65 has been detected in apoplasts, chloroplasts and nuclei (Tabaeizadeh *et al.*, 1995). The pH of some of these compartments would allow transligation reactions. At this stage, however, we can not exclude that RD21 would only act as a transligase in extracts and as a protease on natural substrates *in vivo*.

Studies of some of the presumed plant proteases revealed that they can also catalyze nonproteolytic reactions. Phytochelatin synthase, for example, acts as a glutathione transpeptidase, yielding phytochelatin, which is required for heavy-metal tolerance (Clemens, 2006). A number of serine carboxypeptidase-like proteins act as acyltransferases in the production of sinapoyl secondary metabolites, which protect plants against UV radiation (Lehfeldt *et al.*, 2000). So far, there are two other plant cysteine proteases described that catalyze transpeptidation reactions. Phytochelatin synthase (family C72) cleaves the tripeptide glutathione and ligates the γGlu-Cys moiety to glutathione to produce phytochelatin, which is essential for heavy-metal tolerance (Cobbett and Goldsbrough, 2002). Vacuolar processing enzyme (family C13) is required for the production of a circular peptide (cyclotide) called kalata B1, which might have a role in insect defense (Saska *et al.*, 2007). RD21 is the first representative of a third cysteine protease family (C1A, the PLCPs) that can catalyze transpeptidation reactions.
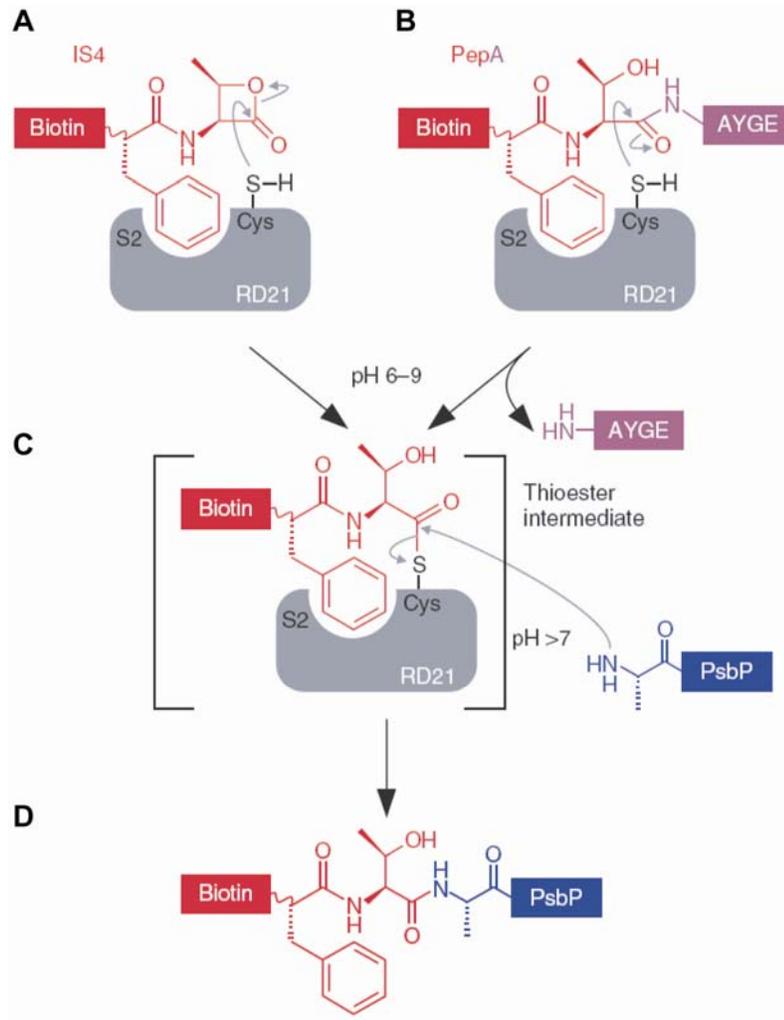
Figure 4-8 Model for β-lactone and peptide labeling of PsbP by RD21.
A to D, β-lactone probes (*A*) and peptides (*B*) bind to RD21. The phenylalanine residue of these acceptor molecules (IS4 and PepA, respectively) is at the P2 position, making contact with the S2 substrate binding pocket of RD21. The active-site cysteine of RD21 acts as a nucleophile, resulting in an unstable thioester intermediate (*C*). At neutral to basic pH, the N-terminal amino group of PsbP acts as a nucleophile on the thioester intermediate, resulting in labeling of the N terminus of PsbP through a peptide bond (*D*).

Little is known of the mechanisms of transpeptidases. The data suggest that water is somehow excluded from the active site to promote transpeptidation reactions. It will be interesting to investigate whether the acceptor molecule is already bound before formation of the thioester intermediate to exclude water from the active site.

The post-translational fusion of peptides or proteins through peptide bonds using enzymes has great potential for applications in research and medicine (Lombard *et al.*, 2005). Sortin, for example, is a bacterial transpeptidase that has been used to ligate peptides to 'sortagged' cell wall proteins on living cells (Popp *et al.*, 2007; Tanaka *et al.*, 2008). Subtiligase, derived from a subtilase, has been used for protein semisynthesis (Chang *et al.*, 1994; Tan *et al.*, 2008). Each of these enzymes has its own opportunities and limitations. The use of RD21-like PLCPs might open new avenues for controlling post-translational modifications, but further optimization and characterization are required. For example, the specificity requirements for the donor and acceptor molecules and the efficiency of transpeptidation compared to proteolysis remain to be addressed.

Although we have designed β-lactone derivatives as non-directed ABPs, the fate of these small molecules in plant extracts seems more complex than we predicted. IS4 labeling does not depend on the activity of the targeted proteins, but rather results from indirect labeling through a presumed protease. This indicates that further investigation of unexpected labeling sites can lead to intriguing molecular mechanisms. The mechanism of transligation, the selectivity for donor and acceptor substrates, and whether these reactions also occur in living cells are topics worthy of further study.

CHAPTER 4: MATERIALS AND METHODS

4.1 Materials

4.1.1 Biological materials

Arabidopsis plant materials

Arabidopsis plants were grown in a growth cabinet on a 12-hr light regime at 24 °C (day) and 20 °C (night). T-DNA insertion mutants of RD21 (At1g47128: SALK_090550 (*rd21-1*) and SALK_065256 (*rd21-2*); At5g43060: SAIL_781H05 (*rd21B*)), SAG12 (At5g45890: SALK_124030), XCP1 (At4g35350; SALK_84789), XCP2 (At4g35350: SALK_057921), RD19 (At4g39090: SALK_031088), AALP (At4g60360: SALK_075550), ALP2 (At3g45310: SALK_088620), CATB1 (At4g01610: SALK_019630) and CATB2 (At1g02300: SALK_110946) were obtained from the Salk Institute Genomic Analysis Laboratory. All are in the ecotype Columbia-0 background (Col-0). Homozygous lines were selected using T-DNA and gene-specific primers designed by SIGnAL (http://signal.salk.edu/cgi-bin/tdnaexpress/). Mutant lines *sid2* (Nawrath and Métraux, 1999) and *pad3* (Glazebrook and Ausubel, 1994) were provided by Dr. Bart Thomma (Wageningen University). Mutant line *npr1* (Cao *et al.*, 1994) was provided by Dr. Jane Parker (Max Planck Institute for Plant Breeding Research).

Usually, leaf proteins were extracted from rosette leaves of 4-8-week-old plants. Stem proteins were extracted from the stems of a 9-week-old plant. Root proteins were extracted from whole roots of 9-week-old potted plants after intensive washing with H_2O. Seed proteins were extracted from 1-day-old germinating seeds soaked in H_2O at 4 °C in the dark. Proteins were usually extracted by grinding plant organs in H_2O in a 1.5 mL Eppendorf tube with a plastic "blue stick" homogenizer and centrifugation.

Arabidopsis cell cultures (ecotype Landsberg; May and Leaver, 1993) were weekly subcultured in medium containing 3% w/v sucrose (pH 5.7), 0.5 mg/l naphthalene acetic acid, 0.05 mg/l 6-benzylaminopurine and 4.4 g MS Gamborg B5 vitamins (Duchefa). Before assays, the medium of a 7-day-old cell culture was replaced with

fresh medium. Cell culture proteins were usually extracted by grinding cells in H_2O in a 1.5 mL Eppendorf tube with a plastic "blue stick" homogenizer (Roth) and centrifugation.

Other plant materials

Nicotiana benthamiana and tomato (*Solanum lycopersicum* cv Money Maker) were grown in a climate chamber at a 14-hr light regime at 22 °C (day) and 18 °C (night). Usually, 4- to 6-week old plants were used for experiments. *N. benthamiana* leaf proteins were usually extracted from the agro-infiltrated leaves at 3 day-post-infiltration, or from the third fully unfolded leaves of a 5-week-old plant for FPpRh profiling. Tomato leaf proteins were extracted from the third fully unfolded compound leaf of a 4-week-old plant. Proteins were usually extracted by homogenizing leaves in H_2O with ice-cold mortar and pestle, and centrifugation.

Bean (*Vicia faba*) plants were grown outside in the show garden of Max Planck Institute for Plant Breeding Research. Leaf proteins were extracted from a young leaf of a 1-meter-high plant. Barley (*Hordeum vulgare* cv. Golden Promise) seedlings were grown in a growth chamber at 20 °C under 16-hour light regime. Leaf proteins were extracted from leaves of 2-week-old plants. Proteins were usually extracted by grinding leaf punches in H_2O in a 1.5 ml Eppendorf tube with a plastic "blue stick" homogenizer and centrifugation.

Other biological materials

E. coli strain XL1-blue containing pFLAG-EPI1a (Tian *et al.*, 2005) was provided by Dr. Sophien Kamoun (The Sainsbury Laboratory). AVR2 protein (Rooney *et al.*, 2005) was provided by Dr. Pierre de Wit (Wageningen University). EPIC1 and EPIC2B (Tian *et al.*, 2007) proteins were provided by Dr. Sophien Kamoun (The Sainsbury Laboratory). *Pseudomonas syringae* pv tomato DC3000 virulent strain and avirulent strain AvrPphB (Puri *et al.*, 1997) were provided by Dr. Scott Peck (University of Missouri). *Botrytis cinerea* strain was provided Dr. Bart Thomma (Wageningen University). *Agrobacterium tumefaciens* strain GV3101 pMP90 was provided by Dr. Csaba Konz (Max Planck Institute for Plant Breeding Research).

4.1.2   Chemical and biochemical materials

Activity-based probes

Fluorophosphonate probes (FP-Bio, FPpBio and FPpRh; Liu *et al.*, 1999; Kidd *et al.*, 2001) were provided by Dr. Benjamin Cravatt (The Scripps Research Institute). Epoxide probes (DCG-04 and TMR-DCG-04; Greenbaum *et al.*, 2000, 2002b) were provided by Dr. Matthew Bogyo (Stanford University). Vinyl sulfone probes (BioVS and MV151; Kessler *et al.*, 2001; Verdoes *et al.*, 2006) were provided by Dr. Herman Overkleeft (Leiden University). β-lactone probes (IS# probes) were synthesized by Dr. Rengarajan Balamurugan and in-group chemist Zheming Wang in Chemical Genomics Centre, Dortmund, Germany. All probes were solved in DMSO to a stock concentration of 1 mM and stored at -20 °C. Fluorescent probes were always kept in the dark.

Chemical inhibitors and other chemicals

Chemical inhibitors E-64, MG132, MG115, leupeptin, WEHDcho, LLMcho, epoxomicin, PMSF, AEBSF, TLCK and TPCK were purchased from Sigma. DEVDcho and VADfmk were purchased from Calbiochem. ESMDcho, IETDcho, IEPDcho, YVADcho were purchased from Bachem. Protease Inhibitor Cocktail (Complete tablet) was purchased from Roche. β-lactone inhibitors (IS#-n inhibitors) were synthesized by Dr. Rengarajan Balamurugan and in-group chemist Zheming Wang in Chemical Genomics Centre, Dortmund, Germany. All inhibitors were solved in DMSO and stored at -20 °C.

BTH 50WG (Actigard/Bion, 50% wettable granule) was ordered from Ciba-Gygi or provided from Tong Lin (Bayer CropScience). Sulfo-NHS-Ac was purchased from Pierce. Biotinylated peptides were ordered from JPT Peptide Technologies. PepA (FTAYGE) and PepB (FTA) contain a Ttds linker (4,7,10-trioxa-1,13-tridecanediamine succinimic acid) with biotin at the N-terminus and a carboxyl at the C-terminus. The AYGAEEN peptide has an amine at the N-terminus and a carboxyl at the C-terminus.

General laboratory chemicals and reagents were mainly purchased from Sigma (St.Lois, USA) and Merck (Darmstadt, Germany).

Antibodies

Anti-P69B antibody (Tian *et al.*, 2004) was provided by Dr. Sophien Kamoun (The Sainsbury Laboratory). Anti-PBA1 antibody (Yang *et al.*, 2004) was purchased from BIOMOL. Anti-PEPC and anti-histone H3 antibodies (Noel *et al.*, 2007; Cheng *et al.*, 2009) were provided by Dr. Jane Parker (Max Planck Institute for Plant Breeding Research). Anti-RD21 antibody was provided by Dr. Carol MacKintosh (University of Dundee). Anti-PsbP antibody was purchased from Agrisera. Bovine HRP-conjugated anti-sheep antibody was purchased from Santa Cruz Biotechnology. Donkey HRP-conjugated anti-rabbit antibody was purchased from Amersham.

4.2 Methods

4.2.1 BTH treatments

To Arabidopsis plants, H_2O solution of 300 μM BTH (Bion, Syngenta) and 0.01% Silwet (Lenne Seeds) was sprayed with a perfume sprayer (Roth) to the leaf surface until the droplets ran off. To tomato plants, the soil in 9 cm x 9 cm pot of each plant was drenched with 80 ml of 300 μM BTH H_2O solution at days 0, 2 and 4, and the plant samples were harvested at day 5.

4.2.2 Pathogen infections

For Pseudomonas infection, *Pseudomonas syringae* pv tomato DC3000 from -80 °C frozen stock was grown overnight at 28 °C in 10 ml LB medium in a 50 ml Falcon tube. The culture was centrifuged at 3000 g for 10 min with a Falcon tube centrifuge (Heraeus), and the bacterial pellet was washed with 10 mM $MgCl_2$ and diluted to OD_{600} of 0.3 (measured by spectrometer Ultrospec II, LKB Biochrom) with 10 mM $MgCl_2$ and 0.01% Silwet. The bacterial suspension was then sprayed with a perfume sprayer to the leaf surface of Arabidopsis plants until the droplets ran off.

For Botrytis infection, *Botrytis cinerea* -80 °C frozen stock of 10^7 spores/ml was thawed to room temperature (22-25 °C) and diluted 10 times to 10^6 spores/ml with LB

medium. Expanded rosette leaves of 4-week-old Arabidopsis plants were inoculated with one 6 μl-droplet of 10^6 *B. cinerea* spores/ml on each leaf, using a 1-ml disposable pipette tip (PD-Tips, Plastibrand) and an automatic pipetter (Handy-step electronic). Inoculated plants were kept in trays with transparent covers to maintain high humidity, and grown under standard conditions in a growth chamber. Inoculated leaves were harvested at 5 day- post-infection and subject to ABPP.

4.2.3   Agro-infiltration in *N. benthamiana*

Agrobacterium tumefaciens strain GV3101 pMP90 transformed with binary vector pFK containing recombinant Arabidopsis PLCP expression cassette was grown overnight at 28 °C in 10 ml LB medium containing 50 μg/ml kanamycin and 50 μg/ml rifampicin in a 50 ml Falcon tube. The culture was centrifuged at 3000 g for 10 min, and the bacterial pellet was resuspended in 10 mM MES (pH 5), 10 mM $MgCl_2$ and 0.2 μM acetosyringone to a final OD_{600} of 2. Agrobacterium suspensions containing binary PLCP expression vectors were mixed with Agrobacterium suspensions containing binary expression vector for RNA silencing inhibitor p19 at the ratio of 1:1 (Voinnet *et al.*, 2003). The mixtures were kept at room temperature for 3 hr. The fully expanded leaves of 5-week-old *N. benthamiana* plants were poked with a needle (BD), and the mixed Agrobacterium suspensions were vacuum-infiltrated into the leaves through the needle-holes using a 1-ml syringe (Plastipak, BD) without a needle. Leaves were harvested after 3 days, and the proteins were extracted by homogenization in H_2O plus 1 mM DTT (Roche) with ice-cold mortar and pestle, and cleared by centrifugation at 16000 g for 1 min with a tabletop centrifuge (5415D, Eppendorf).

4.2.4   Recombinant EPI1a expression in *E. coli* and affinity purification

E. coli strain XL1-blue transformed with plasmid pFLAG-EPI1 containing rEPI1 expression cassette (Tian *et al.*, 2005) was grown overnight at 37 °C in 20 ml LB medium containing 100 μg/ml ampicillin. The bacterial culture was diluted to OD_{600} of 0.1 in 800 ml LB medium containing 100 μg/ml ampicillin and 1 mM IPTG, and incubated at 37 °C for 5 hr with vigorous agitation at 200 rpm on a shaker (Infos). Then the bacterial culture was centrifugated at 6000 g for 30 min with Sorvall RC-5B

centrifuge (Du Pont Instruments), and the supernatant containing secreted rEPI1 was filtered through 0.22 μm filters (Steritop, Millipore) and mixed with 2 volumes of -20 °C acetone. Secreted proteins in the supernatant were pelleted by centrifugation at 12210 g for 30 min at 4 °C and resolved in TBS buffer by gentle agitation on a roller mixer (SRT2, Stuart). rEPI1a recovered from the culture supernatant was captured and purified by immunoaffinity using a Poly-prep C-column (Bio-Rad) packed with 500 μl anti-FLAG M2 affinity gel (Sigma) at 4 °C. The column was washed 3 times with 2 ml TBS buffer, and the bound proteins were eluted with 0.1 M glycine (pH 3.5) and immediately equilibrated in 20 mM Tris buffer (pH 8.0).

4.2.5   Tomato apoplastic fluid isolation

Mature leaves from 6-week-old tomato plants were picked and submerged into 200 ml H_2O in a 500 ml beaker underneath a grid and a moderate weight to avoid up-floating of the leaves. Then H_2O was vacuum-infiltrated into tomato leaf apoplast by pumping out of the air for 5 min and releasing the vacuum slowly in an exicator. H_2O-infiltrated leaves were dried on surface using tissue paper and centrifuged at 1600 g for 10 min at 4 °C in a tube with holes (diameter = 1 mm) in the bottom (generic "AF-isolation device"). The AF was collected below in a larger collection tube.

4.2.6   Nuclear fractionation

Arabidopsis leaves of 2 g fresh-weight were homogenized with mortar and pestle in 4 ml Honda buffer containing 2.5% Ficoll 400, 5% Dextran T40, 0.4 M sucrose, 10 mM $mgCl_2$ and 5 mM DTT in 25 mM Tris buffer (pH 7.4), and filtered through a 64 μm nylon mesh. Triton X-100 was added into the leaf extracts to a final concentration of 0.5%, and the sample for total protein was taken. The extracts were then incubated on ice for 15 min and centrifuged at 1500 g for 15 min at 4 °C, and the supernatant was the nucleus-depleted fraction. Protein pellet was washed with Honda buffer plus 0.1% Triton X-100 once and with Honda buffer once. After two washes, starch and cell debris were spun down by centrifugation at 100 g for 5 min at 4 °C, and nuclei in the supernatant were then spun down by centrifugation at 2000 g for 5 min at 4 °C in a new Eppendorf tube.

4.2.7 Protein concentration quantification

Protein concentration quantification was done with Bio-Rad protein assay. In brief, serial dilutions of BSA standard (Promega) of 0.1-0.5 mg/ml were prepared, and the protein samples were diluted to a concentration of 0.1-0.5 mg/ml. 10 μl of each concentration standard and each protein sample were loaded into wells of a 96-well microtiter plate (Microtest, Falcon), and mixed with 200 μl of 1: 4-diluted dye reagent concentrate (Bio-Rad). The absorbance at 595 nm was measured with 680 Microplate reader (Bio-Rad), and the concentrations of the protein samples were deduced from the standard curve made from the concentration standards. Protein solutions were assayed in duplo.

4.2.8 Activity-based labeling

Arabidopsis leaf extracts

Proteins were extracted by grinding one rosette leaf from a 4-6-week-old Arabidopsis plant in H_2O in a 1.5 mL Eppendorf tube with a plastic "blue stick" homogenizer. The extract was mixed with 0.5 ml of H_2O and cleared by centrifugation at 16000 g for 1 min with a tabletop centrifuge. Protein concentration was quantified with Bio-Rad protein assay (see 4.2.7). FPBio, FPpBio or FPpRh labeling was usually done by incubating ~100 μg protein in 0.5 ml containing 50 mM Tris buffer (pH 8) and 0.4 μM FPBio, FPpBio or FPpRh for 2 hours (in the dark for FPpRh). DCG-04 labeling was usually done by incubating ~20 μg protein in 0.5 ml containing 50 mM sodium acetate buffer (pH 6) with 1 mM DTT and 2 μM DCG-04 for 5 hours. MV151 or BioVS labeling was usually done by incubating ~100 μg protein in 0.5 ml containing 50 mM Tris buffer (pH 7.4) and 0.4 μM MV151 or 2 μM BioVS for 3-4 hours (in the dark for the MV151). IS4 labeling was usually done by incubating ~20 μg protein in 0.5 ml containing 50 mM Tris buffer (pH 8) with 1 mM DTT and 2 μM IS4 for 2 hours. All labeling reactions were performed at room temperature under gentle agitation on a rotator (STR4, Stuart). Equal volumes of DMSO were added to the no-probe controls. Proteins were precipitated after labeling by adding 1 ml -20 °C acetone and subsequent centrifugation at 16000g for 1 min. The protein pellet was dissolved in 2x SDS-PAGE loading buffer containing β-mercaptoethanol, and the proteins were separated on 12% SDS PAGE gels at 200 V using Novex Minicell

system (Invitrogen), with ~10 μg protein per lane for FP or MV151/BioVS labeling, or ~4 μg protein per lane for DCG-04 or IS4 labeling.

Tomato apoplastic fluids

FPpBio or FPpRh labeling was usually done for 1D analysis by incubating 200-300 μl tomato AFs in 0.5 ml containing 50 mM sodium acetate buffer (pH 6) and 0.4 μM FPpBio or FPpRh for 2 hours (in the dark for FPpRh). Proteins from 40-60 μl AFs were loaded to each lane in SDS PAGE. FPpRh labeling was done for 2D analysis by incubating 617.5 μl tomato AFs in 650 μl containing 50 mM sodium acetate buffer (pH 6) and 0.4 μM FPpRh for 2 hours in the dark. Proteins from 560 μl AFs were used to soak IEF stripe (see 4.2.11). DCG-04 labeling was usually done for 1D analysis by incubating 200-300 μl tomato AFs in 0.5 ml containing 50 mM sodium acetate buffer (pH 5) with 1 mM DTT and 2 μM DCG-04 for 3 hr for C14 profiling or 5 hr for PIP1 profiling. Proteins from 40-60 μl AFs were loaded to each lane in SDS PAGE. TMR-DCG-04 labeling was done for 2D analysis by incubating 565 μl tomato AFs in 650 μl containing 50 mM sodium acetate buffer (pH 5) with 1 mM DTT and 3 μM TMR-DCG-04 for 5 hours in the dark. Proteins from 460 μl AFs were used to soak IEF stripe (see 4.2.11). All labeling reactions were performed at room temperature under gentle agitation on a rotator (STR4, Stuart).

Profiling at various pH values was done using 50 mM sodium acetate (pH 4-6.5) or Tris (pH 7-11) buffers. Competition or inhibition assays were done by preincubating the protein extracts with competitor or inhibitor molecules for 30 minutes before labeling with activity-based probes.

4.2.9   In-gel fluorescence scanning

SDS-PAGE gel containing fluorescent probe-labeled proteins was washed 3 times with ddH$_2$O and labeled proteins were visualized by in-gel fluorescence scanning using a Typhoon 8600 scanner (Molecular Dynamics) with excitation and emission at 532 and 580 nm, respectively. Fluorescent signals were quantified with ImageQuant 5.2 software (Molecular Dynamics).

4.2.10 Western blotting

After SDS PAGE, proteins were transferred onto polyvinylidene fluoride membrane (Immobilon-P, Millipore) at 200 mA for 60-70 min using X-Cell II Blot Module system (Invitrogen). After the transfer, the membrane was moved into a 50 ml Falcon tube and blocked with 5 ml of 3% BSA (biomol) solution for 5 min with gentle agitation on a roller mixer (SRT2, Stuart). In the detection of biotinylated proteins, the membrane was incubated with streptavidin-HRP (Ultrasensitive, Sigma) at 1:3000 in the presence of 2% Tween-20 for 1 hr, and then washed 5 times with TBS buffer plus 0.1% Tween-20 for 5 min each time. In the detection of nonbiotinylated proteins, the membrane was incubated with the protein-specific first antibody (see 4.1.2) at 1:5000 in the presence of 2% Tween-20 for 1 hr, and then washed 5 times with TBS buffer plus 0.1% Tween-20 for 5 min each time. Next, the membrane was incubated with HRP-conjugated anti-rabbit secondary antibodies (Amersham) at 1:5000 in the presence of 2% Tween-20 for 1 hr, and then washed 5 times with TBS buffer plus 0.1% Tween-20 for 5 min each time. At the end, the membrane was covered with chemiluminescent substrates of HRP (SuperSignal West Pico/Femto, Pierce) underneath a piece of overhead-projection transparency, and exposed to X-ray films (BioMax MR, Kodak) in the darkroom. The exposed film was developed by automatic X-ray film processor (Optimax, Protec).

4.2.11 2-dimentional electrophoresis

Two volumes of acetone containing 10% trichloroacetic acid were mixed with the labeled protein extracts, and the resulting mixture is stored at -20 °C for at least 24 hr. Proteins were precipitated by centrifugation at 27000 g for 10 min at 4 °C, washed with -20 °C acetone twice, and solved in 160 μl of IEF buffer containing 9 M urea, 2% CHAPS, 0.5% v/v ampholytes (ZOOM Carrier pH 3-10, Invitrogen), 0.002% bromophenol blue and 20 mM DTT. The protein sample was impregnated overnight into an IPG strip (ReadyStrip pH 3-6 for DCG-04 profiling or pH 3-10 for FPpRh profiling, Bio-Rad). Isoelectric focusing (IEF) was done in ZOOM IPGRunner cassettes (Invitrogen) attached to a ZOOM IPGRunner Core (Invitrogen) with a voltage program (175 V for 15 min; 175 to 2000 V ramp for 45 min; 2000 V for 30 min) of a voltage ramp-compatible power supply (EPS 3501XL, GE). After IEF,

strips were incubated in 5 ml of equilibrium buffer containing 35% glycerol, 0.4% SDS, 7 M Urea, 50 mM DTT and 0.1% bromophenol blue in 60 mM Tris buffer (pH 6.8) for 15 min, and then loaded to a 12% SDS PAGE gel. The proteins were further separated by the 2nd dimension electrophoresis at 200 V using Novex Minicell system (Invitrogen).

4.2.12 Affinity purification and target identification

For large-scale labeling of Arabidopsis leaf extracts, rosette leaves of 4-8-week-old Arabidopsis plants were homogenized in H_2O with ice-cold mortar and pestle, and the leaf extracts were cleared by centrifugation at 16000 g for 1 min with a tabletop centrifuge. Then 2.5 ml leaf extracts at a concentration of ~4 mg/ml were labeled with 20 μM BioVS in 50 mM Tris buffer (pH 9) with 1 mM DTT for 4 hr, or with 40 μM IS4 in 50 mM Tris buffer (pH 8) with 1 mM DTT for 2 hr. For large-scale labeling of tomato apoplastic fluids, 2.5 ml AFs were isolated from 6-week-old tomato plants (see 4.2.5), and labeled with 3 μM FPpBio in 50 mM Tris buffer (pH 8) for 2 hr. All labeling reactions were performed at room temperature in a 15 ml Falcon tube under gentle agitation on a rotator (STR4, Stuart). The labeled protein extracts were applied to PD-10 size exclusion columns (Econo-Pac 10-DG, Bio-Rad) to remove the unlabeled probes. Desalted protein samples were eluted with 3.5 ml of new 50 mM Tris buffer (pH 8) from the columns, and then incubated with 100 μl of streptavidin agarose beads (Pierce) for BioVS or FPpBio labeling, or 100 μl magnetic streptavidin beads (Promega) and protease inhibitor cocktail (Complete tablet, Roche) for IS4 labeling, for 1 hour at room temperature under gentle agitation. After the incubation, streptavidin agarose beads were collected by centrifuging at 3000 g for 10 min; washed twice with 0.1% SDS, twice with 6 M urea, once with 50 mM Tris buffer (pH 8) containing 1% Triton X-100, once with 1% Triton X-100 and once with H_2O; and boiled in 30 μl of 2x SDS-PAGE gel loading buffer containing β-mercaptoethanol. Affinity-purified proteins were separated on 12% 1D SDS PAGE gel and stained with coomassie blue (Imperial Protein Stain, Pierce). The specific bands were excised from the coomassie-stained gel and subjected to in-gel tryptic digestion and subsequent MS analysis.

REFERENCES

Adam, G.C., Cravatt, B.F. and Sorensen, E.J. (2001) Profiling the specific reactivity of the proteome with non-directed activity-based probes. *Chem. Biol.* **8**(1), 81-95.

Adam, G.C., Sorensen, E.J. and Cravatt, B.F. (2002a) Chemical strategies for functional proteomics. *Mol. Cell. Proteomics,* **1**(10), 781-790.

Adam, G.C., Sorensen, E.J. and Cravatt, B.F. (2002b) Trifunctional chemical probes for the consolidated detection and identification of enzyme activities from complex proteomes. *Mol. Cell. Proteomics,* **1**(10), 828-835.

Avrova, A.O., Stewart, H.E., De Jong, W., Heilbronn, J., Lyon, G.D. and Birch, P.R.J. (1999) A cysteine protease gene is expressed early in resistant potato interactions with *Phytophthora infestans*. *Mol. Plant-Microbe Interact.,* **12**(12), 1114-1119.

Avrova, A.O., Taleb, N., Rokka, V., Heilbronn, J., Campbell, E., Hein, I., Gilroy, E.M., Cardle, L., Bradshaw, J.E., Stewart, H.E., Fakim, Y.J., Loake, G. and Birch, P.R.J. (2004) Potato oxysterol binding protein and cathepsin B are rapidly up-regulated in independent defence pathways that distinguish *R* gene-mediated and field resistances to *Phytophthora infestans*. *Mol. Plant Pathol.,* **5**(1), 45-56.

Barglow, K.T. and Cravatt, B.F. (2004) Discovering disease-associated enzymes by proteome reactivity profiling. *Chem. Biol.* **11**(11), 1523-1531.

Baruch, A., Jeffery, D.A. and Bogyo, M. (2004) Enzyme activity - it's all about image. *Trends Cell Biol.,* **14**(1), 29-35.

Basset, G., Raymond, P., Malek, L. and Brouquisse, R. (2002) Changes in the expression and the enzymic properties of the 20S proteasome in sugar-starved maize roots. Evidence for an in vivo oxidation of the proteasome. *Plant Physiol.,* **128**(3), 1149.

Bateman, A. and Bennett, H. (1998) Granulins: The structure and function of an emerging family of growth factors. *J. Endocrinol.,* **158**(2), 145-151.

Beers, E.P., Jones, A. M. and Dickerman, A.W. (2004) The S8 serine, C1A cysteine and A1 aspartic protease families in Arabidopsis. *Phytochemistry,* **65**(1), 43-58.

Berger, D. and Altmann, T. (2000) A subtilisin-like serine protease involved in the regulation of stomatal density and distribution in *Arabidopsis thaliana*. *Genes Dev.,* **14**(9), 1119-1131.

Boller, T. (2005) Peptide signalling in plant development and self/non-self perception. *Curr. Opin. Cell Biol.,* **17**(2), 116-122.

Böttcher, T. and Sieber, S.A. (2008) Beta-lactones as privileged structures for the active-site labeling of versatile bacterial enzyme Classes13. *Angewandte Chemie,* **47**(24), 4600-4603.

Bowles, D.J. (1990) Defense-related proteins in higher plants. *Annu. Rev. Biochem.,* **59**(1), 873-907.

Cao, H., Bowling, S.A., Gordon, A.S. and Dong, X. (1994) Characterization of an arabidopsis mutant that is nonresponsive to inducers of systemic acquired resistance. *Plant Cell,* **6**(11), 1583-1592.

Carter, C., Pan, S., Zouhar, J., Avila, E.L., Girke, T. and Raikhel, N.V. (2004) The vegetative vacuole proteome of *Arabidopsis thaliana* reveals predicted and unexpected proteins. *Plant Cell,* **16**(12), 3285-3303.

Chang, T.K., Jackson, D.Y., Burnier, J.P. and Wells, J.A. (1994) Subtiligase: A tool for semisynthesis of proteins. *Proc. Natl. Acad. Sci. USA,* **91**(26), 12544-12548.

Cheng, F., Zamski, E., Guo, W., Pharr, D. and Williamson, J. (2009) Salicylic acid stimulates secretion of the normally symplastic enzyme mannitol dehydrogenase: A possible defense against mannitol-secreting fungal pathogens. *Planta, in press*.

Cheng, Y.T., Germain, H., Wiermer, M., Bi, D., Xu, F., Garcia, A.V., Wirthmueller, L., Despres, C., Parker, J.E., Zhang, Y. and Li, X. (2009) Nuclear pore complex component MOS7/Nup88 is required for innate immunity and nuclear accumulation of defense regulators in Arabidopsis. *Plant Cell, in press*.

Chiang, K.P., Niessen, S., Saghatelian, A. and Cravatt, B.F. (2006) An enzyme that regulates ether lipid signaling pathways in cancer annotated by multidimensional profiling. *Chem. Biol.* **13**(10), 1041-1050.

Clemens, S. (2006) Evolution and function of phytochelatin synthases. *J. Plant Physiol.,* **163**(3), 319-332.

Cobbett, C. and Goldsbrough, P. (2002) Phytochelatins and metallothioneins: Roles in heavy metal detoxification and homeostasis. *Annu. Rev. Plant Biol.,* **53**(1), 159-182.

Cong, Y., Zhang, Q., Woolford, D., Schweikardt, T., Khant, H., Dougherty, M., Ludtke, S.J., Chiu, W. and Decker, H. (2009) Structural mechanism of SDS-induced enzyme activity of scorpion hemocyanin revealed by electron cryomicroscopy. *Structure,* **17**(5), 749-758.

Cravatt, B.F., Wright, A.T. and Kozarich, J.W. (2008) Activity-based protein profiling: From enzyme chemistry to proteomic chemistry. *Annu. Rev. Biochem.,* **77**(1), 383-414.

Dangl, J.L. and Jones, J.D.G. (2001) Plant pathogens and integrated defence responses to infection. *Nature,* **411**(6839), 826-833.

De Wit, Pierre J. G. M. and Spikman, G. (1982) Evidence for the occurrence of race- and cultivar-specific elicitors of necrosis in intercellular fluids of compatible interactions between *Cladosporium fulvum* and tomato. *Physiol. Plant Pathol.,* **21**(1), 1-11.

Dick, L.R., Cruikshank, A.A., Destree, A.T., Grenier, L., McCormack, T.A., Melandri, F.D., Nunes, S.L., Palombella, V.J., Parent, L.A., Plamondon, L. and Stein, R.L. (1997) Mechanistic studies on the inactivation of the proteasome by lactacystin in cultured cells. *J. Biol. Chem.,* **272**(1), 182-188.

Diethich, R., Ploß, K. and Heil, M. (2004) Constitutive and induced resistance to pathogens in *Arabidopsis thaliana* depends on nitrogen supply. *Plant, Cell Environ.,* **27**(7), 896-906.

Dijkstra, H.P., Sprong, H., Aerts, B.N.H., Kruithof, C.A., Egmond, M.R. and Gebbink, R.J.M.K. (2008) Selective and diagnostic labelling of serine hydrolases with reactive phosphonate inhibitors. *Organic & Biomolecular Chemistry,* **6**(3), 523-531.

Djordjevic, M.A., Oakes, M., Li, D.X., Hwang, C.H., Hocart, C.H. and Gresshoff, P.M. (2007) The glycine max xylem sap and apoplast proteome. *J. Proteome Res.,* **6**(9), 3771-3779.

Dong, X., Mindrinos, M., Davis, K. R. and Ausubel, F.M. (1991) Induction of Arabidopsis defense genes by virulent and avirulent pseudomonas syringae strains and by a cloned avirulence gene. *Plant Cell,* **3**(1), 61-72.

Drahl, C., Cravatt, B.F. and Sorensen, E.J. (2005) Protein-reactive natural products. *Angewandte Chemie,* **44**(36), 5788-5809.

Drake, R., John, I., Farrell, A., Cooper, W., Schuch, W. and Grierson, D. (1996) Isolation and analysis of cDNAs encoding tomato cysteine proteases expressed during leaf senescence. *Plant Mol. Biol.,* **30**(4), 755-767.

Drews, O., Wildgruber, R., Zong, C., Sukop, U., Nissum, M., Weber, G., Gomes, A.V. and Ping, P. (2007) Mammalian proteasome subpopulations with distinct molecular compositions and proteolytic activities. *Mol. Cell. Proteomics,* **6**(11), 2021-2031.

Evans, M.J., Saghatelian, A., Sorensen, E.J. and Cravatt, B.F. (2005) Target discovery in small-molecule cell-based screens by in situ proteome reactivity profiling. *Nat. Biotech.,* **23**(10), 1303-1307.

Evans, M.J. and Cravatt, B.F. (2006) Mechanism-based profiling of enzyme families. *Chem. Rev.,* **106**(8), 3279-3301.

Ferrari, S., Plotnikova, J.M., Lorenzo, G.D. and Ausubel, F.M. (2003) *Arabidopsis* local resistance to *Botrytis cinerea* involves salicylic acid and camalexin and requires *EDS4* and *PAD2*, but not *SID2*, *EDS5* or *PAD4*. *Plant J.,* **35**(2), 193-205.

Ferreira, R.B., Monteiro, S., Freitas, R., Santos, C.N., Chen, Z., Batista, L.M., Duarte, J., Borges, A. and Teixeira, A.R. (2007) The role of plant defence proteins in fungal pathogenesis. *Mol. Plant Pathol.,* **8**(5), 677-700.

Fu, N., Drinnenberg, I., Kelso, J., Wu, J., Pääbo, S., Zeng, R. and Khaitovich, P. (2007) Comparison of protein and mRNA expression evolution in humans and chimpanzees. *PLoS ONE,* **2**(2), e216.

Gershater, M.C., Cummins, I. and Edwards, R. (2007) Role of a carboxylesterase in herbicide bioactivation in *Arabidopsis thaliana*. *J. Biol. Chem.,* **282**(29), 21460-21466.

Gilroy, E.M., Hein, I., Van der Hoorn, R., Boevink, P.C., Venter, E., McLellan, H., Kaffarnik, F., Hrubikova, K., Shaw, J., Holeva, M., López, E.C., Borras-Hidalgo, O., Pritchard, L., Loake, G.J., Lacomme, C. and Birch, P.R.J. (2007) Involvement of cathepsin B in the plant disease resistance hypersensitive response. *Plant J.,* **52**(1), 1-13.

Glazebrook, J. and Ausubel, F.M. (1994) Isolation of phytoalexin-deficient mutants of *Arabidopsis thaliana* and characterization of their interactions with bacterial pathogens. *Proc. Natl. Acad. Sci. USA,* **91**(19), 8955-8959.

Goldberg, A.L., Cascio, P., Saric, T. and Rock, K.L. (2002) The importance of the proteasome and subsequent proteolytic steps in the generation of antigenic peptides. *Mol. Immunol.,* **39**(3-4), 147-164.

Goulet, M., Dallaire, C., Vaillancourt, L., Khalf, M., Badri, A.M., Preradov, A., Duceppe, M., Goulet, C., Cloutier, C. and Michaud, D. (2008) Tailoring the specificity of a plant cystatin toward herbivorous insect digestive cysteine proteases by single mutations at positively selected amino acid sites. *Plant Physiol.,* **146**(3), 1010-1019.

Greenbaum, D., Medzihradszky, K.F., Burlingame, A. and Bogyo, M. (2000) Epoxide electrophiles as activity-dependent cysteine protease profiling and discovery tools. *Chem. Biol.* **7**(8), 569-581.

Greenbaum, D.C., Arnold, W. D., Lu, F., Hayrapetian, L., Baruch, A., Krumrine, J., Toba, S., Chehade, K., Brömme, D., Kuntz, I. D. and Bogyo, M. (2002a) Small molecule affinity fingerprinting: A tool for enzyme family subclassification, target identification, and inhibitor design. *Chem., Biol.* **9**(10), 1085-1094.

Greenbaum, D., Baruch, A., Hayrapetian, L., Darula, Z., Burlingame, A., Medzihradszky, K. F. and Bogyo, M. (2002b) Chemical approaches for functionally probing the proteome. *Mol. Cell. Proteomics,* **1**(1), 60-68.

Greenbaum, D.C., Baruch, A., Grainger, M., Bozdech, Z., Medzihradszky, K.F., Engel, J., DeRisi, J., Holder, A.A. and Bogyo, M. (2002c) A role for the protease falcipain 1 in host cell invasion by the human malaria parasite. *Science,* **298**(5600), 2002-2006.

Groll, M., Ditzel, L., Lowe, J., Stock, D., Bochtler, M., Bartunik, H.D. and Huber, R. (1997) Structure of 20S proteasome from yeast at 2.4A resolution. *Nature,* **386**(6624), 463-471.

Groll, M., Schellenberg, B., Bachmann, A.S., Archer, C.R., Huber, R., Powell, T.K., Lindow, S., Kaiser, M. and Dudler, R. (2008) A plant pathogen virulence factor inhibits the eukaryotic proteasome by a novel mechanism. *Nature,* **452**(7188), 755-758.

Gygi, S.P., Rist, B. and Aebersold, R. (2000) Measuring gene expression by quantitative proteome analysis. *Curr. Opin. Biotechnol.,* **11**(4), 396-401.

Harrak, H., Azelmat, S., Baker, E.N. and Tabaeizadeh, Z. (2001) Isolation and characterization of a gene encoding a drought-induced cysteine protease in tomato (*Lycopersicon esculentum*). *Genome,* **44**(3), 368-374.

Harris, J.L., Backes, B.J., Leonetti, F., Mahrus, S., Ellman, J.A. and Craik, C.S. (2000) Rapid and general profiling of protease specificity by using combinatorial fluorogenic substrate libraries. *Proc. Natl. Acad. Sci. USA,* **97**(14), 7754-7759.

Hatsugai, N., Kuroyanagi, M., Yamada, K., Meshi, T., Tsuda, S., Kondo, M., Nishimura, M. and Hara-Nishimura, I. (2004) A plant vacuolar protease, VPE, mediates virus-induced hypersensitive cell death. *Science,* **305**(5685), 855-858.

Hatsugai, N., Iwasaki, S., Tamura, K., Kondo, M., Fuji, K., Ogasawara, K., Nishimura, M. and Hara-Nishimura, I. (2009) A novel membrane-fusion-mediated plant immunity against bacterial pathogens. *Genes Dev., in press*.

Hayashi, Y., Yamada, K., Shimada, T., Matsushima, R., Nishizawa, N. K., Nishimura, M. and Hara-Nishimura, I. (2001) A proteinase-storing body that prepares for cell death or stresses in the epidermal cells of arabidopsis. *Plant Cell Physiol.,* **42**(9), 894-899.

Heinemeyer, W., Fischer, M., Krimmer, T., Stachon, U. and Wolf, D.H. (1997) The active sites of the eukaryotic 20 S proteasome and their involvement in subunit precursor processing. *J. Biol. Chem.,* **272**(40), 25200-25209.

Hogenhout, S.A., Van der Hoorn, R., Terauchi, R. and Kamoun, S. (2009) Emerging concepts in effector biology of plant-associated organisms. *Mol. Plant-Microbe Interact.,* **22**(2), 115-122.

Jeffery, D.A. and Bogyo, M. (2003) Chemical proteomics and its application to drug discovery. *Curr. Opin. Biotechnol.,* **14**(1), 87-95.

Jessani, N. and Cravatt, B.F. (2004) The development and application of methods for activity-based protein profiling. *Curr. Opin. Chem. Biol.,* **8**(1), 54-59.

Jessani, N., Niessen, S., Wei, B.Q., Nicolau, M., Humphrey, M., Ji, Y., Han, W., Noh, D., Yates, J.R., Jeffrey, S.S. and Cravatt, B.F. (2005a) A streamlined platform for high-content functional proteomics of primary human specimens. *Nat. Meth.,* **2**(9), 691-697.

Jessani, N., Young, J.A., Diaz, S.L., Patricelli, M.P., Varki, A. and Cravatt, B.F. (2005b) Class assignment of sequence-unrelated members of enzyme superfamilies by activity-based protein Profiling. *Angewandte Chemie,* **44**(16), 2400-2403.

Jones, J.D.G. and Dangl, J.L. (2006) The plant immune system. *Nature,* **444**(7117), 323-329.

Joosten, M.H.A.J. and De Wit, P.J.G.M. (1989) Identification of several pathogenesis-related proteins in tomato leaves inoculated with *Cladosporium fulvum* (syn. fulvia fulva) as 1,3-{beta}-glucanases and chitinases. *Plant Physiol.,* **89**(3), 945-951.

Jordá, L., Coego, A., Conejero, V. and Vera, P. (1999) A genomic cluster containing four differentially regulated subtilisin-like processing protease genes is in tomato plants. *J. Biol. Chem.,* **274**(4), 2360-2365.

Jorda, L., Conejero, V. and Vera, P. (2000) Characterization of P69E and P69F, two differentially regulated genes encoding new members of the subtilisin-like proteinase family from tomato plants. *Plant Physiol.,* **122**(1), 67-74.

Jorda, L. and Vera, P. (2000) Local and systemic induction of two defense-related subtilisin-like protease promoters in transgenic Arabidopsis plants. Luciferin induction of PR gene expression. *Plant Physiol.,* **124**(3), 1049-1058.

Kamoun, S. and Smart, C. D. (2005) Late blight of potato and tomato in the genomics era. *Plant Dis.,* **89**(7), 692-699.

Kaschani, F., Verhelst, S.H.L., Swieten, P.F.v., Verdoes, M., Wong, C., Wang, Z., Kaiser, M., Overkleeft, H. S., Bogyo, M. and Van der Hoorn, R.A.L. (2009a) Minitags for small molecules: Detecting targets of reactive small molecules in living plant tissues using 'click chemistry'. *Plant J.,* **57**(2), 373-385.

Kaschani, F., Gu, C., Niessen, S., Hoover, H., Cravatt, B.F. and Van der Hoorn, R.A.L. (2009b) Diversity of serine hydrolase activities of unchallenged and *Botrytis*-infected *Arabidopsis thaliana. Mol Cell Proteomics,* **8**(5), 1082-1093.

Kessler, B.M., Tortorella, D., Altun, M., Kisselev, A.F., Fiebiger, E., Hekking, B.G., Ploegh, H.L. and Overkleeft, H.S. (2001) Extended peptide-based inhibitors efficiently target the proteasome and reveal overlapping specificities of the catalytic β-subunits. *Chem. Biol.* **8**(9), 913-929.

Kidd, D., Liu, Y. and Cravatt, B.F. (2001) Profiling serine hydrolase activities in complex proteomes. *Biochemistry (N.Y.),* **40**(13), 4005-4015.

Kobe, B. and Kemp, B.E. (1999) Active site-directed protein regulation. *Nature,* **402**(6760), 373-376.

Kohler, A., Schwindling, S. and Conrath, U. (2002) Benzothiadiazole-induced priming for potentiated responses to pathogen infection, wounding, and infiltration of water into leaves requires the NPR1/NIM1 gene in Arabidopsis. *Plant Physiol.,* **128**(3), 1046-1056.

Kombrink, E., Schröder, M. and Hahlbrock, K. (1988) Several "pathogenesis-related" proteins in potato are 1,3-β-glucanases and chitinases. *Proc. Natl. Acad. Sci. USA,* **85**(3), 782-786.

Krüger, J., Thomas, C.M., Golstein, C., Dixon, M.S., Smoker, M., Tang, S., Mulder, L. and Jones, J.D.G. (2002) A tomato cysteine protease required for *cf-2*-dependent disease resistance and suppression of autonecrosis. *Science,* **296**(5568), 744-747.

Kurepa, J. and Smalle, J.A. (2008) Structure, function and regulation of plant proteasomes. *Biochimie,* **90**(2), 324-335.

Kusumawati, L., Imin, N. and Djordjevic, M.A. (2008) Characterization of the secretome of suspension cultures of medicago species reveals proteins important for defense and development. *J. Proteome Res.,* **7**(10), 4508-4520.

Lall, M.S., Karvellas, C. and Vederas, J.C. (1999) β-lactones as a new class of cysteine proteinase inhibitors: inhibition of hepatitis A virus 3C proteinase by N-Cbz-serine β-lactone. *Org. Lett.,* **1**(5), 803-806.

Lawton, K.A., Friedrich, L., Hunt, M., Weymann, K., Delaney, T., Kessmann, H., Staub, T. and Ryals, J. (1996) Benzothiadiazole induces disease resistance in *arabidopsis* by activation of the systemic acquired resistance signal transduction pathway. *Plant J.,* **10**(1), 71-82.

Lee, S., Saravanan, R.S., Damasceno, C.M.B., Yamane, H., Kim, B. and Rose, J.K.C. (2004) Digging deeper into the plant cell wall proteome. *Plant Physiol. Biochem.,* **42**(12), 979-988.

Lehfeldt, C., Shirley, A.M., Meyer, K., Ruegger, M.O., Cusumano, J.C., Viitanen, P.V., Strack, D. and Chapple, C. (2000) Cloning of the SNG1 gene of Arabidopsis reveals a role for a serine carboxypeptidase-like protein as an acyltransferase in secondary metabolism. *Plant Cell,* **12**(8), 1295-1306.

Leung, D., Hardouin, C., Boger, D.L. and Cravatt, B.F. (2003) Discovering potent and selective reversible inhibitors of enzymes in complex proteomes. *Nat. Biotech.,* **21**(6), 687-691.

Liu, Y., Patricelli, M.P. and Cravatt, B.F. (1999) Activity-based protein profiling: The serine hydrolases. *Proc. Natl. Acad. Sci. USA,* **96**(26), 14694-14699.

Loake, G. and Grant, M. (2007) Salicylic acid in plant defence-the players and protagonists. *Curr. Opin. Plant Biol.,* **10**(5), 466-472.

Lombard, C., Saulnier, J. and Wallach, J.M. (2005) Recent trends in protease-catalyzed peptide synthesis. *Protein & Peptide Letters,* **12**(7), 621-629.

Martinez, D.E., Bartoli, C.G., Grbic, V. and Guiamet, J.J. (2007) Vacuolar cysteine proteases of wheat (*Triticum aestivum L.*) are common to leaf senescence induced by different factors. *J. Exp. Bot.,* **58**(5), 1099-1107.

May, M.J. and Leaver, C.J. (1993) Oxidative stimulation of glutathione synthesis in *Arabidopsis thaliana* suspension cultures. *Plant Physiol.,* **103**(2), 621-627.

Meng, L., Mohan, R., Kwok, B.H.B., Elofsson, M., Sin, N. and Crews, C.M. (1999) Epoxomicin, a potent and selective proteasome inhibitor, exhibits in vivo antiinflammatory activity. *Proc. Natl. Acad. Sci. USA,* **96**(18), 10403-10408.

Misas-Villamil, J.C. and Van der Hoorn, R.A.L. (2008) Enzyme-inhibitor interactions at the plant-pathogen interface. *Curr. Opin. Plant Biol.,* **11**(4), 380-388.

Nawrath, C. and Metraux, J. (1999) Salicylic acid Induction-Deficient mutants of Arabidopsis express PR-2 and PR-5 and accumulate high levels of camalexin after pathogen inoculation. *Plant Cell,* **11**(8), 1393-1404.

Noel, L.D., Cagna, G., Stuttmann, J., Wirthmuller, L., Betsuyaku, S., Witte, C., Bhat, R., Pochon, N., Colby, T. and Parker, J. E. (2007) Interaction between SGT1 and Cytosolic/Nuclear HSC70 chaperones regulates Arabidopsis immune responses. *Plant Cell,* **19**(12), 4061-4076.

Oh, I.S., Park, A.R., Bae, M.S., Kwon, S.J., Kim, Y.S., Lee, J.E., Kang, N.Y., Lee, S., Cheong, H. and Park, O.K. (2005) Secretome analysis reveals an Arabidopsis lipase involved in defense against *Alternaria brassicicola*. *Plant Cell,* **17**(10), 2832-2847.

Patricelli, M.P., Giang, D.K., Stamp, L.M. and Burbaum, J.J. (2001) Direct visualization of serine hydrolase activities in complex proteomes using fluorescent active site-directed probes. *Proteomics,* **1**(9), 1067-1071.

Paungfoo-Lonhienne, C., Lonhienne, T.G.A., Rentsch, D., Robinson, N., Christie, M., Webb, R.I., Gamage, H.K., Carroll, B.J., Schenk, P.M. and Schmidt, S. (2008) Plants can use protein as a nitrogen source without assistance from other organisms. *Proc. Natl. Acad. Sci. USA,* **105**(11), 4524-4529.

Phillips, C.I. and Bogyo, M. (2005) Proteomics meets microbiology: Technical advances in the global mapping of protein expression and function. *Cell. Microbiol.,* **7**(8), 1061-1076.

Popp, M.W., Antos, J.M., Grotenbreg, G.M., Spooner, E. and Ploegh, H.L. (2007) Sortagging: A versatile method for protein labeling. *Nat. Chem. Biol.,* **3**(11), 707-708.

Powers, J.C., Asgian, J.L., Ekici, O.D. and James, K.E. (2002) Irreversible inhibitors of serine, cysteine, and threonine proteases. *Chem. Rev.,* **102**(12), 4639-4750.

Puri, N., Jenner, C., Bennett, M., Stewart, R., Mansfield, J., Lyons, N. and Taylor, J. (1997) Expression of avrPphB, an avirulence gene from *Pseudomonas syringae* pv. *phaseolicola*, and the delivery of signals causing the hypersensitive reaction in bean. *Mol. Plant-Microbe Interact.,* **10**(2), 247-256.

Rautengarten, C., Usadel, B., Neumetzler, L., Hartmann, J., Büssis, D. and Altmann, T. (2008) A subtilisin-like serine protease essential for mucilage release from Arabidopsis seed coats. *Plant J.,* **54**(3), 466-480.

Read, R.J., Fujinaga, M., Sielecki, A.R. and James, M.N.G. (1983) Structure of the complex of *Streptomyces griseus* protease B and the third domain of the turkey ovomucoid inhibitor at 1.8-A resolution. *Biochemistry (N.Y.),* **22**(19), 4420-4433.

Reis, H., Pfiffi, S. and Hahn, M. (2005) Molecular and functional characterization of a secreted lipase from *Botrytis cinerea*. *Mol. Plant Pathol.,* **6**(3), 257-267.

Rock, K.L., Gramm, C., Rothstein, L., Clark, K., Stein, R., Dick, L., Hwang, D. and Goldberg, A.L. (1994) Inhibitors of the proteasome block the degradation of most cell proteins and the generation of peptides presented on MHC class I molecules. *Cell,* **78**(5), 761-771.

Rooney, H.C.E., Van't Klooster, J.W., Van der Hoorn, R.A.L., Joosten, M.H.A.J., Jones, J.D.G. and de Wit, P.J.G.M. (2005) Cladosporium Avr2 inhibits tomato Rcr3 protease required for *cf-2*-dependent disease resistance. *Science,* **308**(5729), 1783-1786.

Rose, J.K.C., Ham, K., Darvill, A.G. and Albersheim, P. (2002) Molecular cloning and characterization of glucanase inhibitor proteins: Coevolution of a counterdefense mechanism by plant pathogens. *Plant Cell,* **14**(6), 1329-1345.

Saghatelian, A., Jessani, N., Joseph, A., Humphrey, M. and Cravatt, B.F. (2004) Activity-based probes for the proteomic profiling of metalloproteases. *Proc. Natl. Acad. Sci. USA,* **101**(27), 10000-10005.

Salisbury, C.M. and Cravatt, B.F. (2007) Activity-based probes for proteomic profiling of histone deacetylase complexes. *Proc. Natl. Acad. Sci. USA,* **104**(4), 1171-1176.

Sanz-Alférez, S., Mateos, B., Alvarado, R. and Sánchez, M. (2008) SAR induction in tomato plants is not effective against root-knot nematode infection. *Eur. J. Plant Pathol.,* **120**(4), 417-425.

Saska, I., Gillon, A.D., Hatsugai, N., Dietzgen, R.G., Hara-Nishimura, I., Anderson, M.A. and Craik, D.J. (2007) An asparaginyl endopeptidase mediates in vivo protein backbone cyclization. *J. Biol. Chem.,* **282**(40), 29721-29728.

Schaffer, M.A. and Fischer, R.L. (1988) Analysis of mRNAs that accumulate in response to low temperature identifies a thiol protease gene in tomato. *Plant Physiol.,* **87**(2), 431-436.

Schaffer, M.A. and Fischer, R.L. (1990) Transcriptional activation by heat and cold of a thiol protease gene in tomato. *Plant Physiol.,* **93**(4), 1486-1491.

Schuhegger, R., Nafisi, M., Mansourova, M., Petersen, B.L., Olsen, C.E., Svatos, A., Halkier, B.A. and Glawischnig, E. (2006) CYP71B15 (PAD3) catalyzes the final step in camalexin biosynthesis. *Plant Physiol.,* **141**(4), 1248-1254.

Shabab, M., Shindo, T., Gu, C., Kaschani, F., Pansuriya, T., Chintha, R., Harzen, A., Colby, T., Kamoun, S. and Van der Hoorn, R.A.L. (2008) Fungal effector protein AVR2 targets diversifying defense-related Cys proteases of tomato. *Plant Cell,* **20**(4), 1169-1183.

Shah, J. (2003) The salicylic acid loop in plant defense. *Curr. Opin. Plant Biol.,* **6**(4), 365-371.

Shao, F., Merritt, P. M., Bao, Z., Innes, R. W. and Dixon, J.E. (2002) A yersinia effector and a pseudomonas avirulence protein define a family of cysteine proteases functioning in bacterial pathogenesis. *Cell*, **109**(5), 575-588.

Sieber, S.A. and Cravatt, B.F. (2006) Analytical platforms for activity-based protein profiling - exploiting the versatility of chemistry for functional proteomics. *Chem. Comm.,* (22), 2311-2319.

Sieber, S.A., Niessen, S., Hoover, H.S. and Cravatt, B.F. (2006) Proteomic profiling of metalloprotease activities with cocktails of active-site probes. *Nat. Chem. Biol.,* **2**(5), 274-281.

Solinas, G. and Motto, M. (1999) Nonradioactive multi-sample protein-protein interaction assay using an epitope tagging technique. *Biotech.,* **26**(2), 246-249.

Song, J., Win, J., Tian, M., Schornack, S., Kaschani, F., Ilyas, M., Van der Hoorn, R.A.L. and Kamoun, S. (2009) Apoplastic effectors secreted by two unrelated eukaryotic plant pathogens target the tomato defense protease Rcr3. *Proc. Natl. Acad. Sci. USA,* **106**(5), 1654-1659.

Speers, A.E., Adam, G.C. and Cravatt, B.F. (2003) Activity-based protein profiling in vivo using a copper(I)-catalyzed azide-alkyne [3 + 2] cycloaddition. *J. Am. Chem. Soc.,* **125**(16), 4686-4687.

Speers, A.E. and Cravatt, B.F. (2004) Chemical strategies for activity-based proteomics. *ChemBioChem,* **5**(1), 41-47.

Spoel, S.H., Mou, Z., Tada, Y., Spivey, N.W., Genschik, P. and Dong, X. (2009) Proteasome-mediated turnover of the transcription coactivator NPR1 plays dual roles in regulating plant immunity. *Cell*, **137**(5), 860-872.

Springman, E.B., Angleton, E.L., Birkedal-Hansen, H. and Van Wart, H.E. (1990) Multiple modes of activation of latent human fibroblast collagenase: Evidence for the role of a Cys73 active-site zinc complex in latency and a "cysteine switch" mechanism for activation. *Proc. Natl. Acad. Sci. USA,* **87**(1), 364-368.

Sullivan, J.A., Shirasu, K. and Deng, X.W. (2003) The diverse roles of ubiquitin and the 26S proteasome in the life of plants. *Nat. Rev. Genet.,* **4**(12), 948-958.

Sudhindra Rao, K. and Prakash, V. (1993) Interaction of sodium dodecyl sulfate with multi-subunit proteins. A case study with carmin. *J. Biol. Chem.,* **268**(20), 14769-14775.

Suty, L., Lequeu, J., Lançon, A., Etienne, P., Petitot, A. and Blein, J. (2003) Preferential induction of 20S proteasome subunits during elicitation of plant defense reactions: Towards the characterization of "plant defense proteasomes". *Int. J. Biochem. Cell Biol.,* **35**(5), 637-650.

Tabaeizadeh, Z., Chamberland, H., Chen, R.D., Yu, L.X., Bellemare, G. and Lafontaine, J.G. (1995) Identification and immunolocalization of a 65 kDa drought induced protein in cultivated tomato *Lycopersicon esculentum*. *Protoplasma,* **186**(3), 208-219.

Tan, X., Zhang, X., Yang, R. and Liu, C. (2008) A simple method for preparing peptide C-terminal thioacids and their application in sequential chemoenzymatic ligation. *ChemBioChem,* **9**(7), 1052-1056.

Tanaka, K., Yoshimura, T. and Ichihara, A. (1989) Role of substrate in reversible activation of proteasomes (multi-protease complexes) by sodium dodecyl sulfate. *J Biochem.,* **106**(3), 495-500.

Tanaka, T., Yamamoto, T., Tsukiji, S. and Nagamune, T. (2008) Site-specific protein modification on living cells catalyzed by sortase. *ChemBioChem,* **9**(5), 802-807.

Taşgın, E., Atıcı, Ö., Nalbantoğlu, B. and Popova, L. P. (2006) Effects of salicylic acid and cold treatments on protein levels and on the activities of antioxidant enzymes in the apoplast of winter wheat leaves. *Phytochem.,* **67**(7), 710-715.

The Arabidopsis Genome Initiative (2000) Analysis of the genome sequence of the flowering plant arabidopsis thaliana. *Nature,* **408**(6814), 796-815.

Thornberry, N.A., Peterson, E.P., Zhao, J.J., Howard, A.D., Griffin, P.R. and Chapman, K.T. (1994) Inactivation of interleukin-1 beta converting enzyme by peptide (acyloxy)methyl ketones. *Biochemistry (N.Y.),* **33**(13), 3934-3940.

Tian, M., Huitema, E., Da Cunha, L., Torto-Alalibo, T. and Kamoun, S. (2004) A Kazal-like extracellular serine protease inhibitor from *Phytophthora infestans* targets the tomato pathogenesis-related protease P69B. *J. Biol. Chem.,* **279**(25), 26370-26377.

Tian, M. and Kamoun, S. (2005) A two disulfide bridge Kazal domain from Phytophthora exhibits stable inhibitory activity against serine proteases of the subtilisin family. *BMC Biochem.,* **6**(1), 15.

Tian, M., Win, J., Song, J., Van der Hoorn, R., Van der Knaap, E. and Kamoun, S. (2007) A *Phytophthora infestans* cystatin-like protein targets a novel tomato papain-like apoplastic protease. *Plant Physiol.,* **143**(1), 364-377.

Tornero, P., Conejero, V. and Vera, P. (1996) Primary structure and expression of a pathogen-induced protease (PR-P69) in tomato plants: Similarity of functional domains to subtilisin-like endoproteases. *Proc. Natl. Acad. Sci. USA,* **93**(13), 6332-6337.

Tornero, P., Conejero, V. and Vera, P. (1997) Identification of a new pathogen-induced member of the subtilisin-like processing protease family from plants. *J. Biol. Chem.,* **272**(22), 14412-14419.

Tóth, M., Kukor, Z. and Sahin-Tóth, M. (1998) Differential response of basal and tetrahydrobiopterin-stimulated activities of placental type III nitric oxide synthase to sodium dodecyl sulphate: Relation to dimeric structure. *Mol. Hum. Reprod.,* **4**(12), 1165-1172.

Tran, H.T. and Plaxton, W.C. (2008) Proteomic analysis of alterations in the secretome of *Arabidopsis thaliana* suspension cells subjected to nutritional phosphate deficiency. *Proteomics,* 8(20), 4317-4326.

Van der Burg, H.A., Harrison, S.J., Joosten, M.H.A.J., Vervoort, J. and De Wit, P.J.G.M. (2006) *Cladosporium fulvum* Avr4 protects fungal cell walls against hydrolysis by plant chitinases accumulating during infection. *Mol. Plant-Microbe Interact.,* **19**(12), 1420-1430.

Van der Hoorn, R.A.L., Laurent, F., Roth, R. and De Wit, P.J.G.M. (2000) Agroinfiltration is a versatile tool that facilitates comparative analyses of Avr9/Cf-9-induced and Avr4/Cf-4-induced necrosis. *Mol. Plant-Microbe Interact.,* **13**(4), 439-446.

Van der Hoorn, R.A.L., De Wit, P.J.G.M. and Joosten, M.H.A.J. (2002) Balancing selection favors guarding resistance proteins. *Trends Plant Sci.,* **7**(2), 67-71.

Van der Hoorn, R.A.L., Leeuwenburgh, M.A., Bogyo, M., Joosten, M.H.A.J. and Peck, S.C. (2004) Activity profiling of papain-like cysteine proteases in plants. *Plant Physiol.,* **135**(3), 1170-1178.

Van der Hoorn, R.A.L. (2008) Plant proteases: From phenotypes to molecular mechanisms. *Annu. Rev. Plant Biol.,* **59**(1), 191-223.

Van der Hoorn, R.A.L. and Jones, J.D. (2004) The plant proteolytic machinery and its role in defence. *Curr. Opin. Plant Biol.,* **7**(4), 400-407.

Van Esse, H.P., Bolton, M.D., Stergiopoulos, I., De Wit, P.J.G.M. and Thomma, B.P.H.J. (2007) The chitin-binding *Cladosporium fulvum* effector protein Avr4 is a virulence factor. *Mol. Plant-Microbe Interact.,* **20**(9), 1092-1101.

Van Esse, H.P., Van't Klooster, J.W., Bolton, M.D., Yadeta, K.A., van Baarlen, P., Boeren, S., Vervoort, J., De Wit, P.J.G.M. and Thomma, B.P.H.J. (2008) The *Cladosporium fulvum* virulence protein Avr2 inhibits host proteases required for basal defense. *Plant Cell,* **20**(7), 1948-1963.

Van Kan, J.A.L., Van 't Klooster, J.W., Wagemakers, C.A.M., Dees, D.C.T. and Van der Vlugt-Bergmans, C.J.B. (1997) Cutinase A of botrytis cinerea is expressed, but not essential, during penetration of gerbera and tomato. *Mol. Plant-Microbe Interact.,* 10(1), 30-38.

Van Kan, J.A.L. (2006) Licensed to kill: The lifestyle of a necrotrophic plant pathogen. *Trends Plant Sci.,* **11**(5), 247-253.

Van Loon, L.C., Rep, M. and Pieterse, C.M.J. (2006) Significance of inducible defense-related proteins in infected plants. *Annu. Rev. Phytopathol.,* **44**(1), 135-162.

Vera, P. and Conejero, V. (1988) Pathogenesis-related proteins of tomato: P-69 as an alkaline endoproteinase. *Plant Physiol.,* **87**(1), 58-63.

Vera, P. and Conejero, V. (1989) The induction and accumulation of the pathogenesis-related P69 proteinase in tomato during citrus exocortis viroid infection and in response to chemical treatments. *Physiol. Mol. Plant Pathol.,* **34**(4), 323-334.

Verdoes, M., Florea, B.I., Menendez-Benito, V., Maynard, C.J., Witte, M.D., Van der Linden, W.A., Van den Nieuwendijk, A.M.C.H., Hofmann, T., Berkers, C.R., Van Leeuwen, F.W.B., Groothuis, T.A., Leeuwenburgh, M.A., Ovaa, H., Neefjes, J.J., Filippov, D.V., Van der Marel, G.A., Dantuma, N.P. and Overkleeft, H.S. (2006) A fluorescent broad-spectrum proteasome inhibitor for labeling proteasomes in vitro and in vivo. *Chem. Biol.,* **13**(11), 1217-1226.

Vincents, B., Vindebro, R., Abrahamson, M. and von Pawel-Rammingen, U. (2008) The human protease inhibitor cystatin C is an activating cofactor for the streptococcal cysteine protease IdeS. *Chem. Biol.* **15**(9), 960-968.

Voinnet, O., Rivas, S., Mestre, P. and Baulcombe, D. (2003) An enhanced transient expression system in plants based on suppression of gene silencing by the p19 protein of tomato bushy stunt virus. *Plant J.,* **33**(5), 949-956.

Von Rad, U., Mueller, M.J. and Durner, J. (2005) Evaluation of natural and synthetic stimulants of plant immunity by microarray technology. *New Phytol.,* **165**(1), 191-202.

Walling, L.L. (2006) Recycling or regulation? The role of amino-terminal modifying enzymes. *Curr. Opin. Plant Biol.,* **9**(3), 227-233.

Walsh, C.T., Garneau-Tsodikova, S. and Jr., G.J.G. (2005) Protein posttranslational modifications: The chemistry of proteome diversifications. *Angewandte Chemie,* **44**(45), 7342-7372.

Wang, Z., Gu, C., Colby, T., Shindo, T., Balamurugan, R., Waldmann, H., Kaiser, M. and Van der Hoorn, R.A.L. (2008) β-lactone probes identify a papain-like peptide ligase in *Arabidopsis thaliana*. *Nat. Chem. Biol.,* **4**(9), 557-563.

Weerapana, E., Speers, A.E. and Cravatt, B.F. (2007) Tandem orthogonal proteolysis-activity-based protein profiling (TOP-ABPP) - a general method for mapping sites of probe modification in proteomes. *Nat. Protocols,* **2**(6), 1414-1425.

Whalen, M.C., Innes, R.W., Bent, A.F. and Staskawicz, B.J. (1991) Identification of *Pseudomonas syringae* pathogens of Arabidopsis and a bacterial locus determining avirulence on both Arabidopsis and soybean. *Plant Cell,* **3**(1), 49-59.

Wilk, S. and Orlowski, M. (1980) Cation-sensitive neutral endopeptidase: Isolation and specificity of the bovine pituitary enzyme. *J. Neurochem.,* **35**(5), 1172-1182.

Yamada, K., Matsushima, R., Nishimura, M. and Hara-Nishimura, I. (2001) A slow maturation of a cysteine protease with a granulin domain in the vacuoles of senescing Arabidopsis leaves. *Plant Physiol.,* **127**(4), 1626-1634.

Yamada, T., Ohta, H.,Masuda, T., Ikeda, M., Tomita, N., Ozawa, A., Shioi, Y. and Takamiya, K. (1998) Purification of a novel type of SDS-dependent protease in maize using a monoclonal antibody. *Plant Cell Physiol.,* **39**, 106-114.

Yang, P., Fu, H., Walker, J., Papa, C. M., Smalle, J., Ju, Y. and Vierstra, R.D. (2004) Purification of the Arabidopsis 26 S proteasome. *J. Biol. Chem.,* **279**(8), 6401-6413.

Yi, X., Hargett, S.R., Liu, H., Frankel, L.K. and Bricker, T.M. (2007) The PsbP protein is required for photosystem II complex assembly/stability and photoautotrophy in *Arabidopsis thaliana*. *J. Biol. Chem.,* **282**(34), 24833-24841.

Zhao, Y., Thilmony, R., Bender, C.L., Schaller, A., He, S.Y. and Howe, G.A. (2003) Virulence systems of *pseudomonas syringae* pv. *tomato* promote bacterial speck disease in tomato by targeting the jasmonate signaling pathway. *Plant J.,* **36**(4), 485-499.

Zhou, N., Tootle, T.L. and Glazebrook, J. (1999) Arabidopsis PAD3, a gene required for camalexin biosynthesis, encodes a putative cytochrome P450 monooxygenase. *Plant Cell,* **11**(12), 2419-2428.

Zimmermann, P., Hirsch-Hoffmann, M., Hennig, L. and Gruissem, W. (2004) GENEVESTIGATOR. Arabidopsis microarray database and analysis toolbox. *Plant Physiol.,* **136**(1), 2621-2632.

ERKLÄRUNG

Ich versichere, dass ich die von mir vorgelegte Dissertation selbständig angefertigt, die benutzten Quellen und Hilfsmittel vollständig angegeben und die Stellen der Arbeit - einschließlich Tabellen, Karten und Abbildungen -, die anderen Werken im Wortlaut oder dem Sinn nach entnommen sind, in jedem Einzelfall als Entlehnung kenntlich gemacht habe; dass diese Dissertation noch keiner anderen Fakultät oder Universität zur Prüfung vorgelegen hat; dass sie - abgesehen von unten angegebenen Teilpublikationen - noch nicht veröffentlicht worden ist sowie, dass ich eine solche Veröffentlichung vor Abschluss des Promotionsverfahrens nicht vornehmen werde. Die Bestimmungen dieser Promotionsordnung sind mir bekannt. Die von mir vorgelegte Dissertation ist von Prof. Dr. Paul Schulze-Lefert betreut worden.

Max-Planck-Institut für Züchtungsforschung,
Köln, 28/09/2009,

Christian Gu

Teilpublikationen:

Gu, C., Kolodziejek*, I., Misas-Villamil*, J., Shindo, T., Colby, T., Verdoes, M., Richau, K., Schmidt, J., Overkleeft, H., and Van der Hoorn, R. A. L. (2010) Proteasome activity profiling: a simple, robust and versatile method revealing subunit-selective inhibitors and cytoplasmic, defense-induced proteasome activities. (*The Plant Journal*; in press)

Kaschani*, F., **Gu*, C.**, Niessen, S., Hoover, H., Cravatt, B. F., and Van der Hoorn, R. A. L. (2009) Diversity of serine hydrolase activities of unchallenged and *Botrytis*-infected *Arabidopsis thaliana*. *Molecular & Cellular Proteomics* 8, 1082-1093.

Wang*, Z., **Gu*, C.**, Colby, T., Shindo, T., Balamurugan, R., Waldmann, H., Kaiser, M., and Van der Hoorn, R. A. L. (2008) Beta-lactone probes identify a papain-like peptide ligase in *Arabidopsis thaliana*. *Nature Chemical Biology* 4, 557-563.

Shabab*, M., Shindo*, T., **Gu, C.**, Kaschani, F., Pansuriya, T., Chintha, R., Harzen A., Colby, T., Kamoun, S., and Van der Hoorn, R. A. L. (2008) Fungal effector protein AVR2 targets diversifying defense-related Cys proteases of tomato. *The Plant Cell* 20, 1169-1183.

(*, equal contributions)
*, Zu gleichen Teilen; Die Autoren trugen zu gleichen Teilen zur Veröffentlichung bei.